N78-28816

N78-(5515)

J85 Nonaxisymmetric Nozzle
Design and Cooling Study

General Electric Co.
Cincinnati, OH

Prepared for

National Aeronautics and Space Administration
Cleveland, OH

Jun 78

U.S. Department of Commerce
National Technical Information Service
NTIS

NASA CR-135289

June 1978

J85 NONAXISYMMETRIC NOZZLE DESIGN AND COOLING STUDY

General Electric Company

Prepared for

National Aeronautics and Space Administration

NASA-Lewis Research Center

NAS3-20617

1. Report No. NASA CR-135283	2. Government Accession No.	3. Recipient's Catalog No.
4. Title and Subtitle J85 NONAXISYMMETRIC NOZZLE DESIGN AND COOLING STUDY		5. Report Date [illegible] 6. Performing Organization Code
7. Author(s) M. Konarski, T. [illegible]		8. Performing Organization Report No. [illegible] 10. Work Unit No.
9. Performing Organization Name and Address General Electric Company Interstate 75/Neumann Way Cincinnati, Ohio 45215		11. Contract or Grant No. NAS3-20617
12. Sponsoring Agency Name and Address National Aeronautics and Space Administration Washington, D.C. 2[illegible]		13. Type of Report and Period Covered 14. Sponsoring Agency Code
15. Supplementary Notes Project Manager, Rudy Grey NASA-Lewis Research Center Cleveland, Ohio		

16. Abstract

A variety of nonaxisymmetric exhaust nozzles applicable to highly maneuverable advanced aircraft applications were reviewed and the gimbaled [illegible] nozzle was selected for subsequent cooling evaluation and preliminary design studies. A trade study of various exhaust nozzle cooling methods including effects on nozzle performance, cooling efficiency, mechanical simplicity, and cost effectiveness resulted in conventional film cooling being used for the final design. Preliminary conceptual design layouts and detailed cooling analyses were completed for three gimbaled 2D-CD exhaust systems having aspect ratios of [illegible] and [illegible].

17. Key Words (Suggested by Author(s)) Nonaxisymmetric Nozzle Cooling System Jet Vectoring Thrust Reversing	18. Distribution Statement Unclassified

19. Security Classif. (of this report) Unclassified	20. Security Classif. (of this page) Unclassified	21. No. of Pages 84	22. Price*

* For sale by the National Technical Information Service, Springfield, Virginia 22151

NASA-C-168 (Rev. 6-71)

TABLE OF CONTENTS

TABLE OF CONTENTS (Concluded)

LIST OF ILLUSTRATIONS

LIST OF ILLUSTRATIONS (Concluded)

LIST OF TABLES

1.0 SUMMARY

This study program was conducted in three technical phases (tasks). Task I consisted of a review of nonaxisymmetric exhaust systems applicable to highly maneuverable advanced aircraft applications. Available exhaust system designs were categorized as three basic concepts for ranking evaluation: the two-dimensional convergent-divergent (2D-CD), two-dimensional asymmetric (2DA), and two-dimensional wedge (2DW). The 2D-CD and 2DW were selected for further investigation and preliminary design.

Flowpaths were established for the two selected concepts for application to the J85-21 engine and a typical advanced fighter mission. A 2D-CD and 2DW concept with an aspect ratio (dry throat width to throat height) of four and an additional 2D-CD concept with an aspect ratio of eight yielded a total of three preliminary flowpaths.

A cooling system trade study was conducted in Task II for each of the three preliminary flowpath designs. The trade study consisted of applying various cooling methods to the internal exhaust system components and evaluating them on a relative basis. For each flowpath, a total of four different cooling schemes was derived by applying film cooling or film impingement cooling to the internal nozzle parts either individually or in various combinations. Preliminary cooling estimates were empirically determined for each cooling scheme on each of the three flowpath designs. The cooling efficiencies, performance effects, mechanical simplicity, and costs were compared and ranked in order to select the cooling scheme for each concept's final design. The trade study resulted in the selection of conventional film cooling schemes for all study concepts.

The Task III design studies were initiated on the 2D-CD 4AR exhaust systems utilizing the selected film cooling approach and assuming the coolant was supplied at typical fan air discharge conditions. Detailed cooling analyses were conducted on this configuration and a conceptual design was completed.

At this point in the program, the 2DW 4AR exhaust system was deleted from further study to allow a study of cooling the 2D-CD 8AR and a second 2D-CD 4AR exhaust system utilizing only cooling sources available from the J85-21 engine; i.e., turbine discharge air and compressor bleed.

The Task III technical effort was completed by defining preliminary conceptual layouts and supporting cooling analyses for the following three vectorable and thrust reversing exhaust systems:

- 2D-CD 4AR (Turbofan Cooled)
- 2D-CD 4AR (Turbine Discharge and Compressor Bleed Cooled)
- 2D-CD 8AR (Turbine Discharge and Compressor Bleed Cooled)

2.0 INTRODUCTION

Available data (e.g., References 1 through 9) indicate that nonaxisymmetric exhaust systems have potential for improving advanced fighter aircraft in three important areas.

- The two-dimensional geometry of nonaxisymmetric nozzles permits better integration with aircraft and, therefore, provides more efficient aerodynamics resulting in improved cruise performance.
- Maneuverability is enhanced by more readily accommodated thrust vectoring and reversing hardware. Vectored thrust of a properly integrated system produces a supercirculation effect that augments wing lift, particularly at high angle of attack conditions for maneuvering.
- Nonaxisymmetric jet and nozzle geometry can reduce infrared radiation (IR) signatures and radar cross section (RCS) relative to conventional axisymmetric exhaust systems, thus improving survivability against missile threats.

Only full-scale tests of nonaxisymmetric hardware in aircraft will establish to what degree these benefits can be realized. However, prior to such a demonstration, a design technology base must be developed to lessen the risks associated with operating vectorable nonaxisymmetric nozzles.

One critical area requiring attention is in cooling exhaust system components. Departures from circular afterburning ducts, complex nozzle vectoring and area control motions, as well as the imposition of widely varying pressures on nozzle components, can result in increased cooling requirements and corresponding performance losses for these exhaust systems. Accordingly, cooling methods must be developed which minimize or eliminate these losses if nonaxisymmetric nozzles are to remain of interest for application on advanced aircraft.

The program reported herein is an initial step in the formulation of an appropriate cooling technology data base. As its principal objective, preliminary design layouts were prepared for three nonaxisymmetric nozzles installed on the J85-21 engine. These designs define the hardware requirements for conducting future design programs and generating cooling data on full-scale engine components.

Program objectives were achieved in three parts as described in the following sections. Section 3.0 defines the selection process by which two exhaust system study concepts were identified and flowpaths prepared for further study. Section 4.0 presents an evaluation of cooling schemes resulting in a selection of one for each study concept. Section 5.0 describes the procedures used to complete conceptual design layouts and the technology risks associated for each of the study nozzles. The report concludes with a Summary of Results, Section 6.0, and an outline of cooling methodology that was applied to the designs in the Appendix, Section 7.0.

The International System of Units (SI) has been used as the primary system for weights and measures throughout this report. U.S. Customary Units have been included (in parentheses) beside the SI units to enhance communication and utility of the report.

3.0 CONCEPT SELECTION

The selection process was initiated by assembling available nonaxisymmetric nozzle designs and associated data. A broad set of design considerations applicable to advanced fighter aircraft installations was established for these exhaust systems. They were compared on a relative basis to form rankings and identify two generic types that best satisfy program requirements. More specific concept definition was then obtained by preparing preliminary flowpath designs meeting installation requirements for the J85-21 engine and the mission points listed in Table 1 below.

Table 1. Nozzle Operating Requirements.

Operating Condition	Setting	Altitude km (ft)	Mach No.	P_{T8}/P_o	Area Ratio
Cruise	Dry	3.048 (10 000)	0.9	3.8	1.14
Acceleration	A/B	10.668 (35 000)	0.8→1.6	4.2→7.2	1.24→1.72
Cruise	A/B	6.096 (20 000)	1.50	6.5	1.59
Vector	A/B	10.663 (35 000)	0.9	4.4	1.31

3.1 GENERAL CLASSIFICATION OF EXHAUST SYSTEMS

An initial review of available designs produced a total of 31 possible nonaxisymmetric nozzle candidates for study in this program, as shown in Table 2. To simplify the selection process, these nozzle designs were classified as belonging to one of three generic groups: (1) 2D-CD (convergent divergent), (2) 2DA (asymmetric), and (3) 2DW (wedge or twin throat).

The principal differences between categories are whether there are one or two expanding flows and/or planes of symmetry (Figure 1). In general, some available designs listed in Table 2 were judged similar, differing slightly in flowpath geometry or flap size. Accordingly, the initial total of 31 designs was reduced to eleven 2D-CD, five 2DA, and seven 2DW concepts for a total of 23 study candidates; thus, providing a broad coverage of flap arrangements, reverser configurations, and vectoring methods (Figures 2, 3, and 4).

Table 2. J85 Nonaxisymmetric Nozzle Cooling Study Concept Candidates.

Applicable Program	Available Designs 2D-CD	2DA	2DW
Navy V/STOL		1	
GE Nonaxisymmetric Nozzle Study	9	2	5
GE/McAir	1	1	
HIMAT	1	1	1
GE/CALAC		1	
AFTI		1	
B-1		1	
GE TFCD	1		
TBC/NASA			1
McAir/AFFDL	1		2
GD OTW		1	

3.2 SELECTION CRITERIA

To provide a quantitative basis for concept selection, criteria were established which have an impact on nozzle static performance, nozzle mechanical design, or aircraft survivability (Table 3). The forward thrust coefficient (C_{fg}) was determined by assuming that max C_{fg} was obtained at the subsonic cruise point (0.9 at 10,000 ft alt). Expansion losses were then charged if the nozzle was not fully variable and could not provide the required exit-to-throat area ratio (A_9/A_g) for the average acceleration point (1.2 M at 35,000 ft alt) and the supersonic cruise point (1.5 M at 20,000 ft). The C_{fg} for these three points was averaged to give one representative value for forward thrust C_{fg}. Maximum lift C_{fg} is an assessment of the lift thrust vector magnitude, while the maximum vector angle is an assessment of the resultant thrust direction as constrained by the nozzle's mechanical and/or flowpath arrangements. All of these estimated performance characteristics are based on the latest available model test results and are ranked with values of one to five corresponding from highest through lowest performance, respectively.

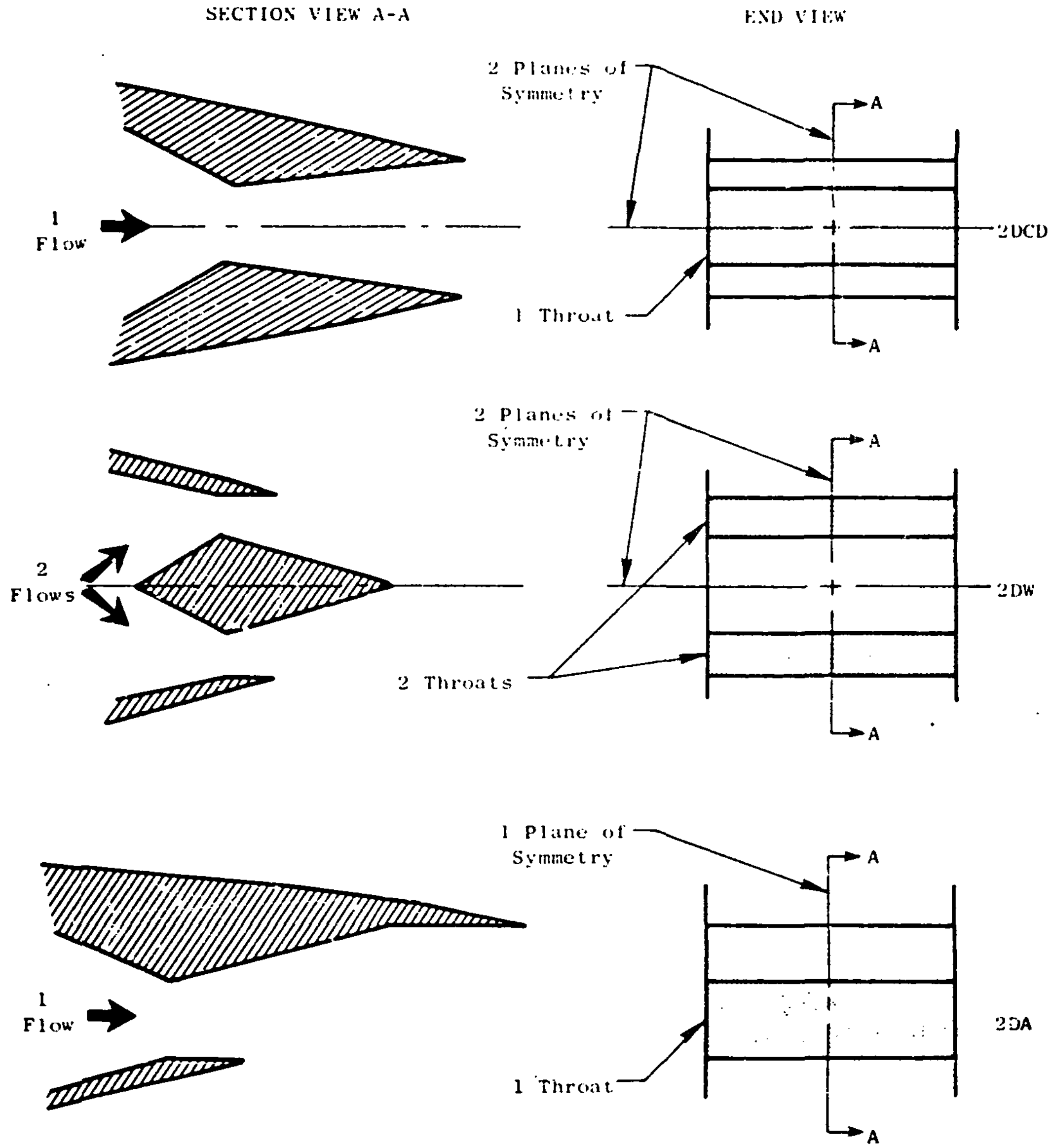

Figure 1. Nonaxisymmetric Nozzle Categories.

-962 Vector

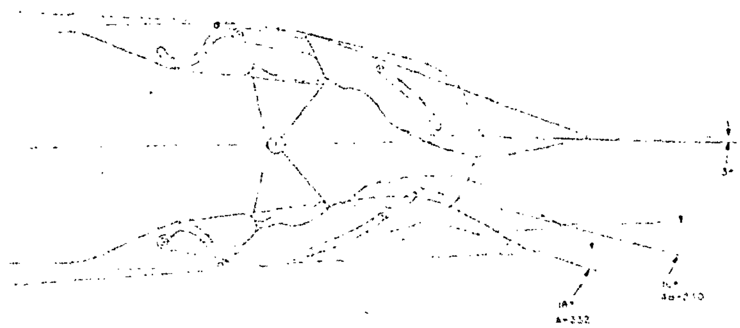

-974 Vector

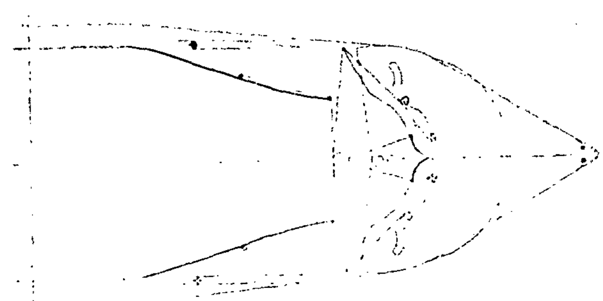

-976 Reverse

*NASA CR-135252.

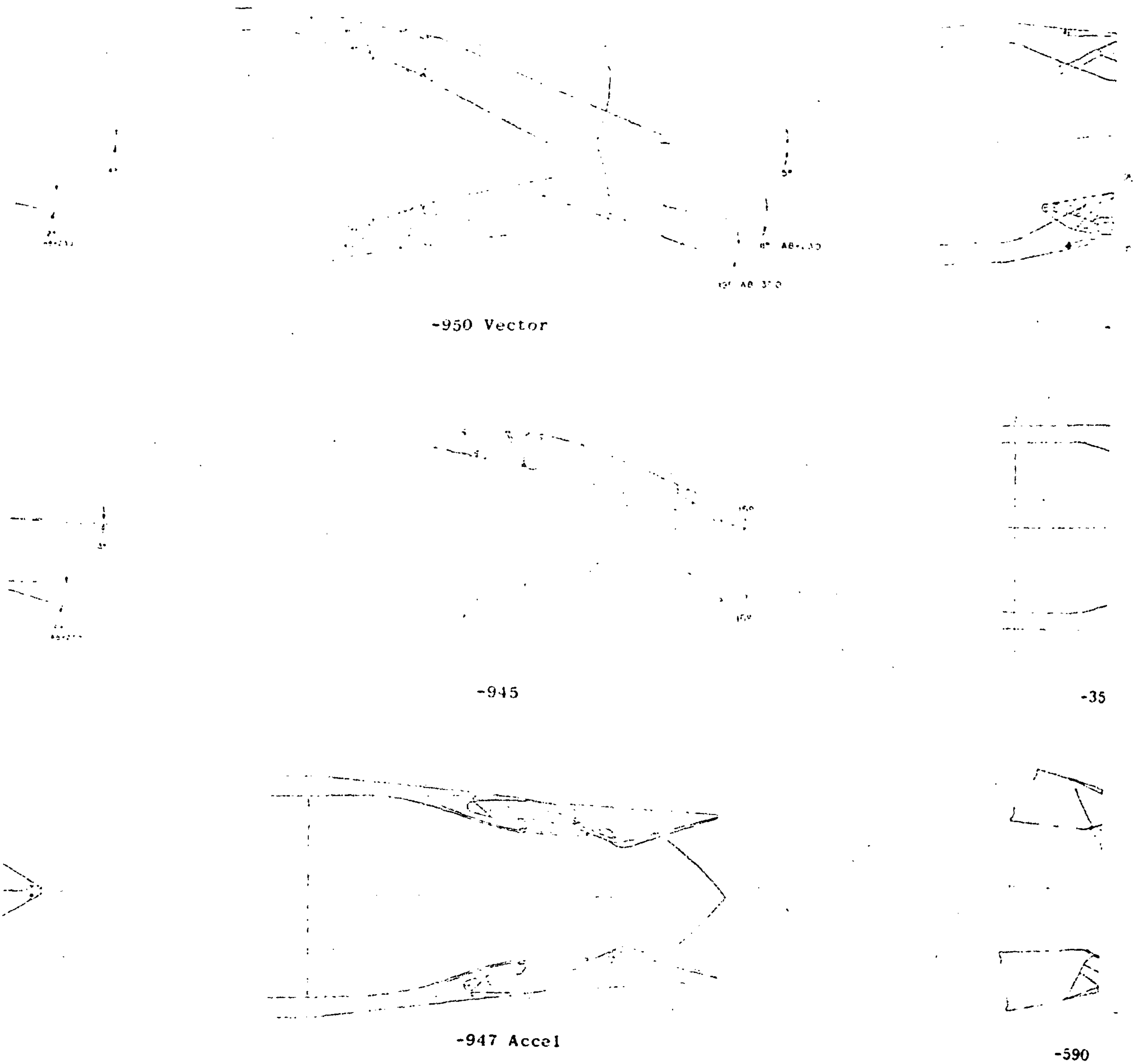

-950 Vector

-945

-35

-947 Accel

-590

Figure 2. 2D-CD Study Candidates.

-051 Vector

Translating Flap

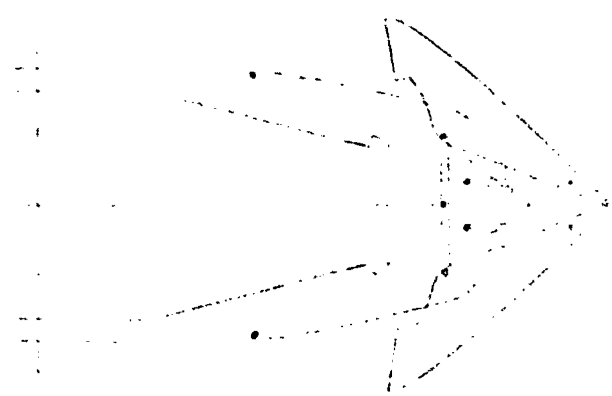

-352 Reverse

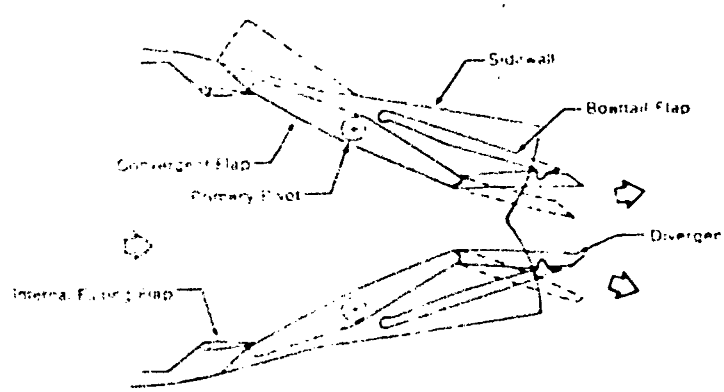

Flap Cruise Vectored Mode

-590 Vectored Mode

lates.

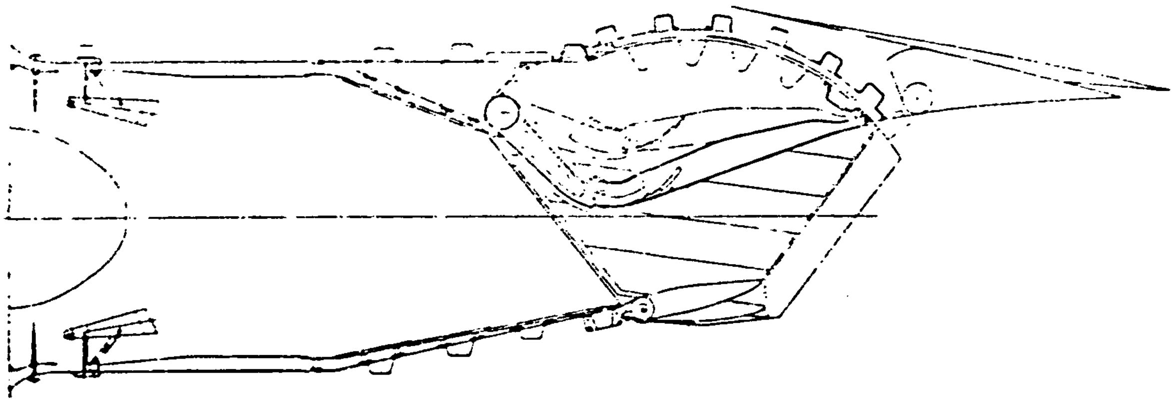

ADEN Cruise Mode

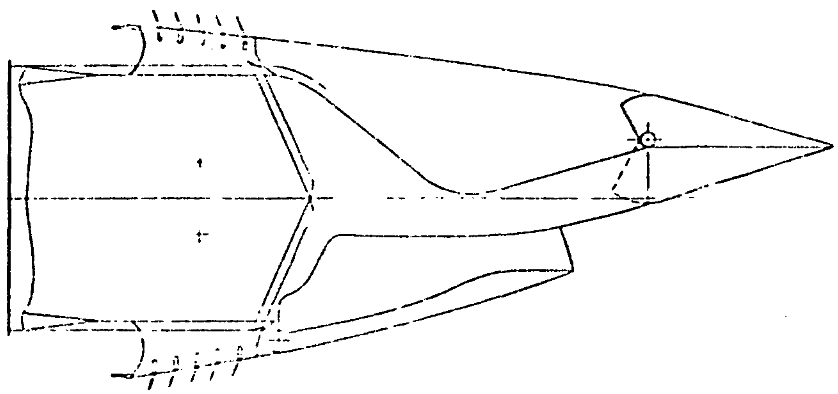

-965 Reverse

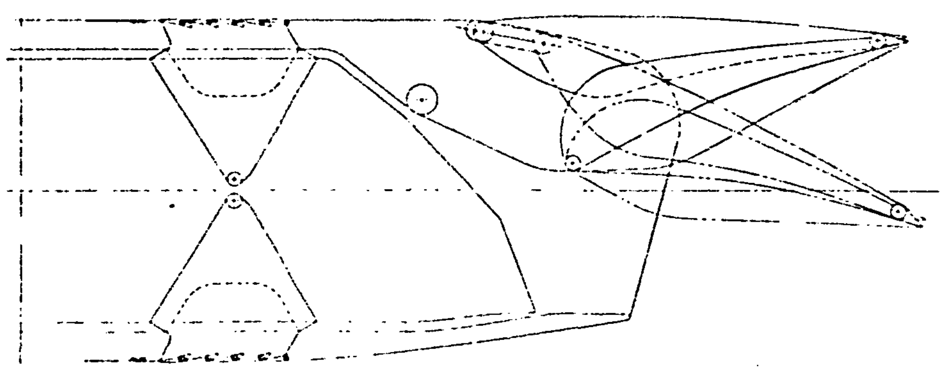

-994 Vectored

Figure 3. 2DA Stuc

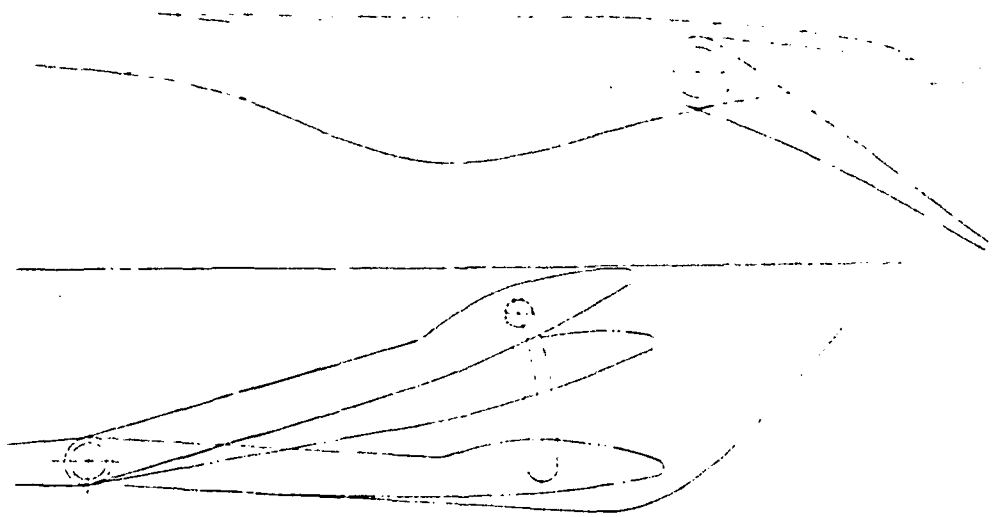

-591

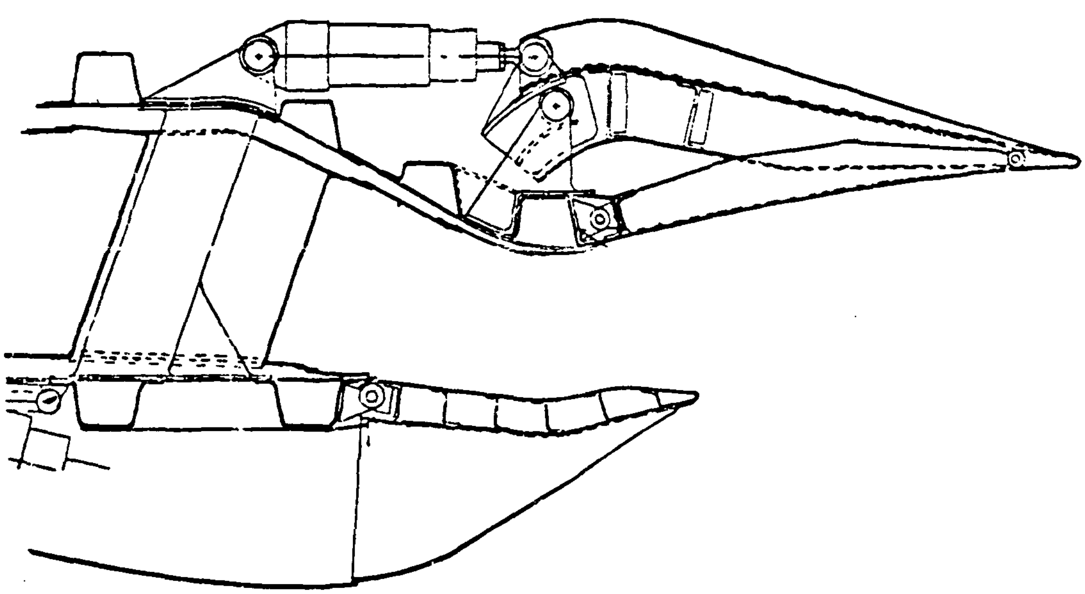

Jet Flap

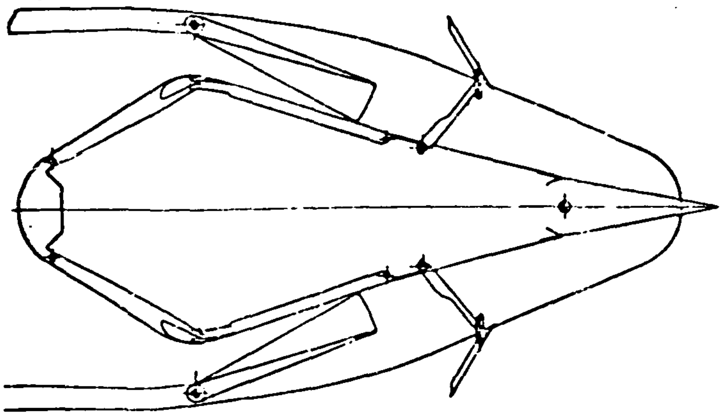

-961 Reverse

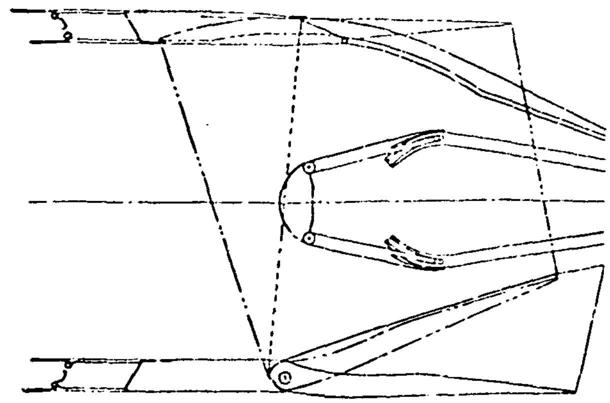

-996 Vectored

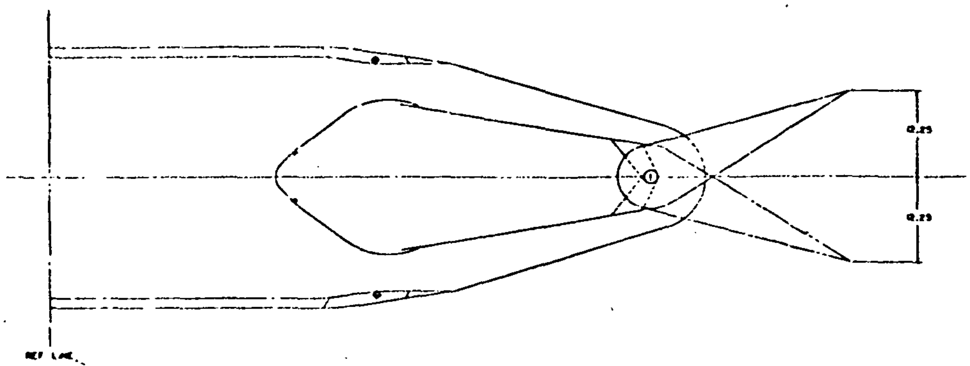

-376 Vectored

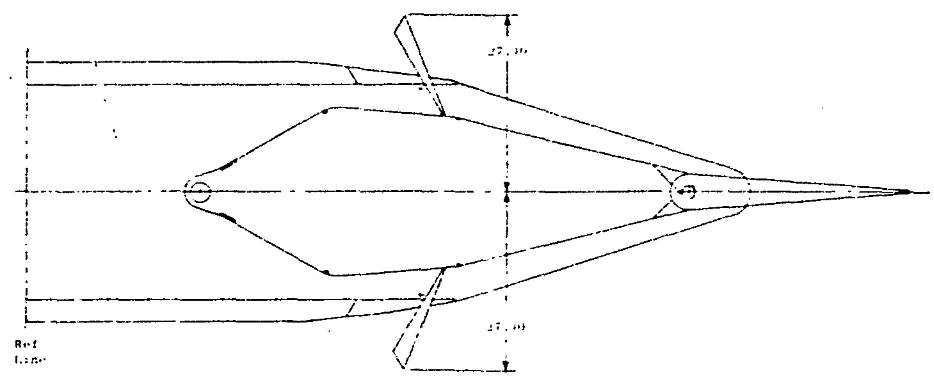

-375 Reverse

Figure 4. 2DW Study Candidate.

'ASA CR-135252.

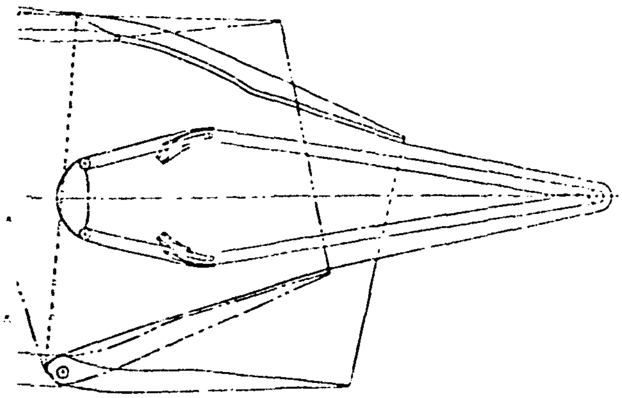

-996 Vectored

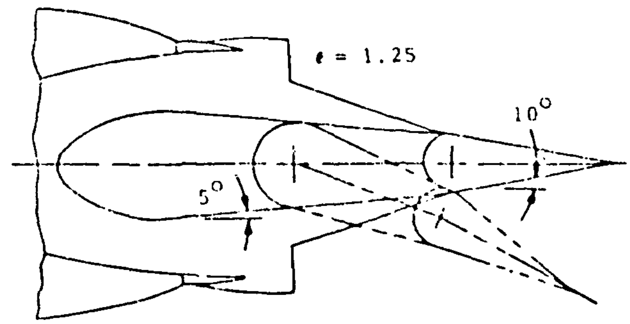

NASA Wedge* Dry Power

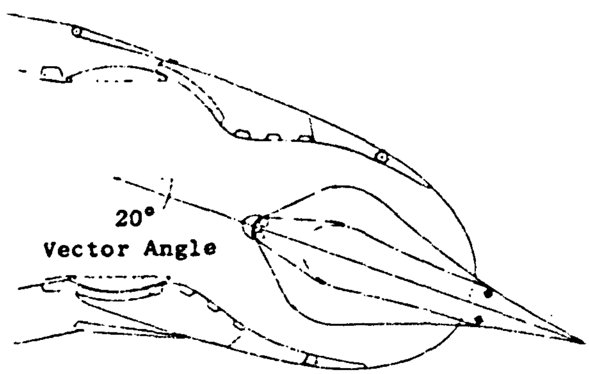

-592 Vectored

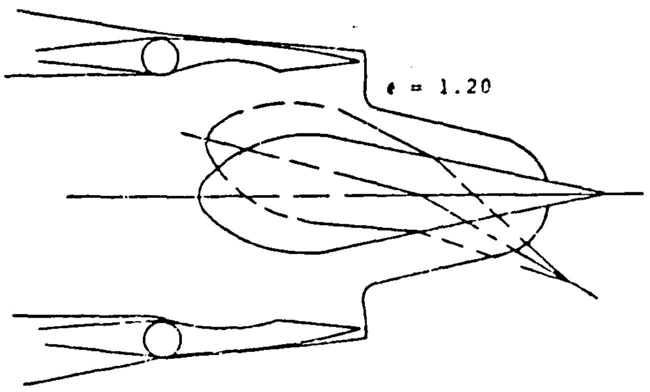

VIP Low Mach A/B

* 2DW Study Candidate.

Table 3. Selection Criteria and Ranking Assignments.

Ranked Criteria	1	2	3	4	5
Forward Thrust C_{FG}	0.98	0.97	0.96	0.95	
Maximum Lift C_{FG}	0.48-0.36	0.35-0.26	0.25-0.16	0.15-0.06	
Max. Vector Angle, Rad (Deg)	0.52-0.44 30-25	0.42-0.35 24-20	0.33-0.26 19-15	0.24-0.17 14-10	0.16-0.09 9-5
Relative Weight	0.76-0.84	0.85-0.92	0.93-1.01	1.02-1.09	1.10-1.18
Drag $(L/H)_p$	5.9-5.0	4.9-4.0	3.9-3.0	2.9-2.0	
Trim Requirement	None	Some			
Cooling* W_c/W_8, Percent	10-12	13-15	16-18		
Reverser Adaptability Actuation Systems Control/Structural Complexity Leakage Control	Best——————Worst (based on Design and Test Experience)				
IR Signature	Low Level——————High Level				

*Includes A/B Cooling

Preceding page blank

The relative weight was established using actual weight estimates for each design and using the fully variable 2D-CD hinged flap exhaust system, -945, Figure 2, as the baseline weight. While some concepts are long and relatively heavy, they tend to install better with lower boattail angles and, therefore, have a lower drag. The drag impacting parameter (L/H_B) was included in the selection criteria to reflect this aspect of a nozzle's design on installed performance. It is a ratio of exhaust system plus nominal aircraft section length to projected boattail height, and is a indicator of boattail drag area.

Asymmetric nozzles tend to produce an unbalanced load and moment in the exhaust system in comparison to the loading of symmetrical concepts. Consequently, an aircraft with an asymmetric exhaust system requires trimming during cruise by the aircraft which, in effect, produces additional drag. The trim requirement was, therefore, included as a selection criterion.

The cooling requirements for the various exhaust systems which include all parts aft of the engine turbine exit, are an initial approximation based on wetted surface areas and generalized heat transfer data.

The next four items (reverser adaptability, actuation systems, control/structural complexity, and leakage control) are all mechanical design criteria. They are of importance in this program since the final products are design layouts. These criteria were assigned qualitative rankings of one to three based on past experience with nonaxisymmetric exhaust system designs.

Finally, the IR signature was included to provide a measure of relative survivability levels between concepts. It is an overall assessment of IR signature taking into account unsuppressed signature shape, plume radiation, and the concept's suppression potential. Concepts were ranked 1, 2, or 3, depending on relative values of these criteria.

3.3 Ranking and Evaluation

Criteria rankings for 2D-CD, 2DA, and 2DW concepts are given in Tables 4 and 5 for all the study candidates. The rankings were totalled to provide an overall ranking for each concept. If it is assumed that all criteria are of equal importance, the total ranking represents a concept's status for this broad range of considerations. On this basis, the lowest totals (best concept) appear for the 2D-CD (total rankings 21, 22) and the 2DA (total rankings 20, 21). In comparison, the lowest 2DW total rankings are 26 and 27.

A large number of 2D-CD designs, although low in weight, cannot vector the required 30°, as shown in Table 4 by the cross hatched sections. As a result, the 2D-CD concepts have a broad distribution of total rankings overlapping the rankings for the 2DA and 2DW exhaust systems (Table 5). This is shown more clearly by the bargraph in Figure 5. If the study concepts were restricted to vector angles greater than 15°, this eliminates all but three 2D-CD (-945, -590, and SF in Table 4) and one 2DW (VIP) from further consideration. This is also reflected in Figure 5, where the 2D-CD surviving

Table 4. Ranked Data Matrix - 2D-CD.

Nozzle Designs	Performance Criteria: Cruise Thrust C_{FG}	Maximum Lift C_{FG}	Maximum Vector Angle	Relative Weight	Drag	Trim Requirement	Cooling	Design Criteria: Thrust Reverser Adaptation	Actuation System	Controls and Structures	Leak Control	IR	Total Ranking
-962	*2	4	5	2	5		1	1	3	2	1	2	37
-974	1	3	4	2	3			1		3	1		24
-976	2	4	6	3	4			3		3	3		34
-950	2	3	5	1	4			2		2	1		38
-945	2	1	1	3	4			1		2	1		22
-947	3	4	6	2	4			3		3	3		53
-951	1	4	5	2	5			3		3	5		91
-952	1	3	4	2	4			2		2	2		27
-590	2	2	2	1	4			1		1	1		21
-960	3	3	4	2	3			3		2	3		28
Short Flap (SF)	2	1	2	2	4			2		3	2		25

* Assigned Rankings: Low Value → High Value

Best → Worst

Concepts with ℓ < 0.26 Rad (15°)

Table 5. Ranked Data Matrix - 2DA and 2DW.

Nozzle Designs		Cruise Thrust C_{FG}	Maximum Lift C_{FG}	Maximum Vector Angle	Relative Weight	Drag	Trim Requirement	Cooling	Thrust Reverser Adaptation	Actuation System	Controls and Structures	Leak Control	IR	Total Ranking
		Performance Criteria							Design Criteria					
ADEN	2DA	*2	1	1	4	2	2	2	2	3	1	1	1	22
-965	2DA	2			2	3		1						20
-994	2DA	1			4	3		1						21
-591	2DA	2			2	2		2						20
JF	2DA	2			3	3		2						22
-961	2DW	2	2	3	4	2	1	2	3	3	1	1	3	27
-376	2DW	3	2	3	5	2		1	1		1	1		26
-375	2DW	3	2	3	6	1		3	1		1	1		28
-996	2DW	3	4	5	3	3		2	1		2	2		32
-592	2DW	3	2	3	3	3		2	3		2	1		29
VIP	2DW	3	1	1	4	3		1	1		3	2		26
Short Flap (SF)	2DW	3	2	3	4	2		2	3		3	2		31

* Assigned Rankings: Low Value → High Value

Best → Worst

Concepts with $\delta < 0.26$ Rad (15°)

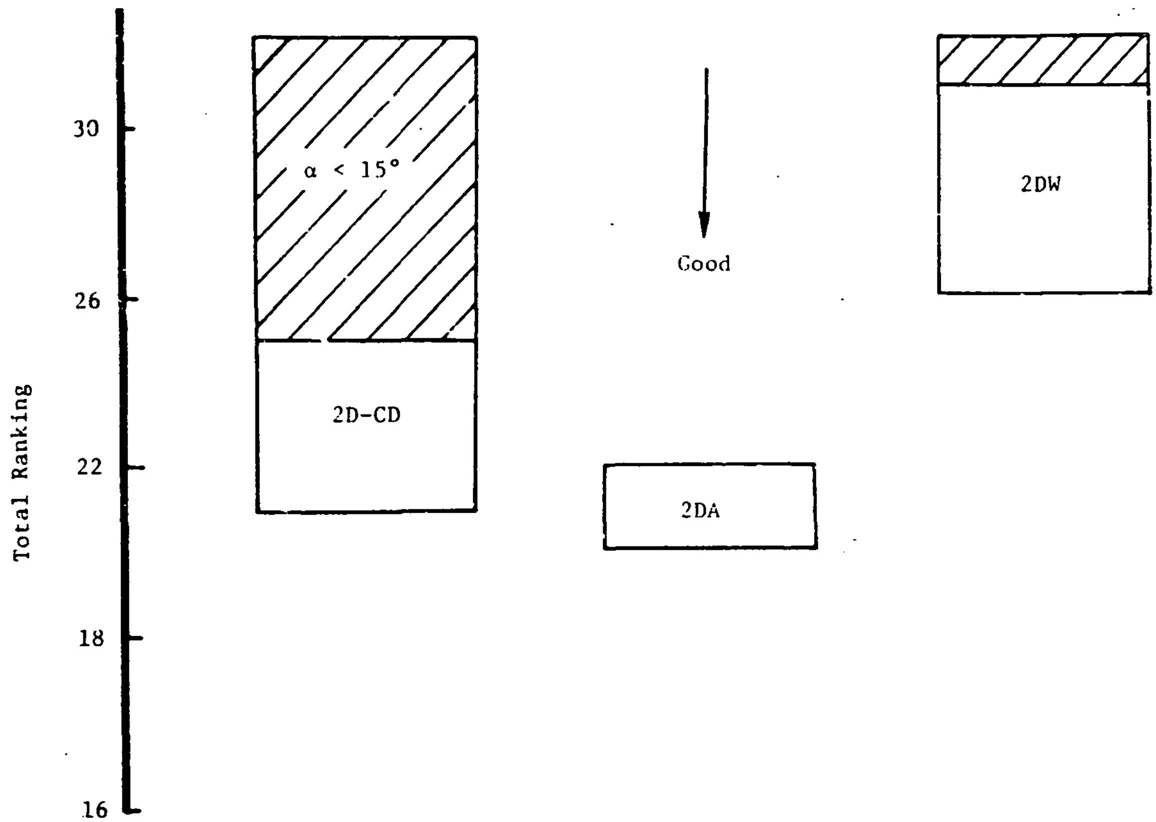

Figure 5. Summary of Overall Considerations.

designs do not overlap the 2DW design. The 2DA were unchanged because they all vector to angles greater than 15°. Thus, even with the vector angle restriction, the 2D-CD and 2DA concepts continue to produce better rankings than the 2DW.

For the final evaluative approach, criteria under consideration were limited to exhaust system internal performance and weight, thus eliminating any influence of the qualitative drag, mechanical design, and survivability criteria. Cruise and vectored static thrust-to-weight ratios were eliminated for a J85 size exhaust system. The ratios were prepared for all surviving concepts achieving more than a 15° maximum vector angle and are compared in Figure 6. The uppermost values represent the best vectoring and the concepts to the far right represent the best cruise concepts. Each concept is also described by its characteristic design feature. The -590 hinge gimbal 2D-CD (Figure 2) concept has both the best vectoring and best forward thrust attributes of all surviving concepts. Two other 2D-CD concepts are also hinged flap but at lower cruise thrust/weight (T/W) than the gimbal. The 2DA also has high vectoring potential equivalent to that of the 2D-CD but at lower forward thrust due to their relatively high weight. In comparison, with one exception, the 2DW has lower vector thrust potential because the flow on either the top or bottom is limited to a vector angle set by the wedge surface angles and because of high weight. Thus, the limited T/W criteria support the overall criteria trends demonstrated in Tables 4 and 5 and in Figure 5. The lone exception is the variable incidence plug which utilizes subsonic turning upstream of the throat. As a result, the VIP 2DW concept T/W shown in Figure 6 is grouped with the 2DA and approaches the hinged flap 2D-CD concepts.

On the basis of the Figure 6 results, the hinge gimbal 2D-CD was recommended for further study as an aspect ratio 4 and 8 exhaust system.

Considerable development of asymmetric nozzle cooling technology had already been accomplished at General Electric at the inception of the present program. These efforts culminated in a full-scale demonstrator 2DA nozzle (ADEN) that was successfully tested in 1976, Reference 10. Cooling technology for the 2DA nozzle, therefore, had been demonstrated and was available for use in future designs. In contrast, 2DW cooling technology has not been developed to the same degree and is complicated by the differing characteristics of two separate deflected flows for vectored wedge nozzles and stagnation areas requiring special cooling treatment. For this reason it was concluded that selection of the 2DW as the second study concept would best satisfy the objectives of this program.

3.4 PRELIMINARY FLOWPATH DESIGN

As described above, the 2D-CD and 2DW exhaust systems were identified as best satisfying study concept objectives. This section outlines how more specific cruise, vectored, and reverse thrust internal flowpaths were devel-

$$\text{Cruise T/W} = \frac{C_{FGR\,0.9M}\, F_{Gi\,0.9M} + C_{FGR\,1.2M}\, F_{Gi\,1.2M} + C_{FGR\,1.6M}\, F_{Gi\,1.6M}}{3W}$$

$$\text{Vector T/W} = \frac{C_{FGR\,0.9M}\, F_{Gi\,0.9M}\, \text{SIN}\delta\ \text{Maximum}}{W}$$

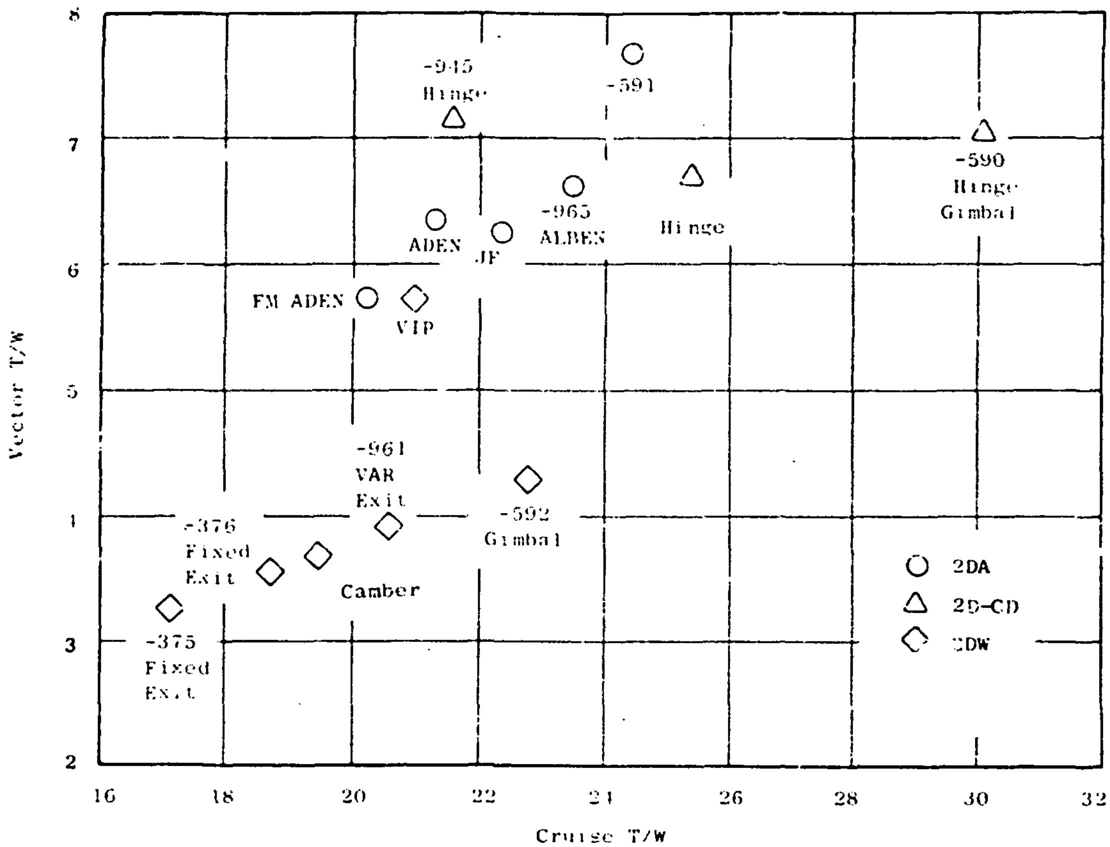

Note: W includes augmentor casing, liner, nozzle flaps, actuators, and links

Figure 6. Thrust-to-Weight Comparison.

oped to provide a basis for evaluating cooling schemes. For the 2D-CD, the specification of gimbal vectoring provides the guidelines necessary to establish flowpaths. However, the vectoring approach to be used for the 2DW was only generally defined. Therefore, three different 2DW mechanical approaches were given consideration and one selected for further study. The resulting 2DW flowpaths and final study concept selection are also described in this section.

The aspect ratio 4 (dry throat width-to-height ratio) 2D-CD flowpath was designed as shown in the top half of Figure 7. Nozzle internal and external flaps are actuated symmetrically about the nozzle's horizontal centerplane for both cruise and vectored modes to produce a simple schedule of A_9 as a function of A_8, Figure 8. Scheduling A_9 as a function of A_8 eliminates the weight and complexity of the actuation system that would be required for A_9. In accordance with this schedule, the subsonic cruise expansion ratio requirements are met exactly while the supersonic cruise and acceleration expansion ratios are slightly compromised. The gimbal section just upstream of the nozzle provides a seal surface at all operating positions. To obtain this seal a circular shaped subsonic convergnet section is necessary on the rotating nozzle with a displaced angle equal to the maximum vector angle. This displaced angle is governed by the difference between the transition duct height and the flowpath height at the primary flap hinge point. Since both dimensions are set by the nozzle aspect ratio and the engine's afterburner and cycle requirements, the maximum possible vector angle is also fixed for this exhaust system at 24°. Larger vector angles are possible if:

- a step can be tolerated between the primary flap hinge point and gimbal with an associated performance penalty (dash flaps in Figure 7), or

- the afterburner duct is allowed to diverge producing an internal diffusion loss and a steeper external boattail angle.

However, such compromises should be weight against the importance of achieving greater thrust angles. Aircraft manufacturer inquiries to date indicate that a practical maximum for in-flight vectoring is about 15°. On this basis, the present 2D-CD design maximum vector angle of 24° adequately covers a realistic range of interest.

The transition duct for this nozzle was tailored to hold a constant area from the maximum available circular afterburner cross section to the nozzle's rectangular gimbal section. The transition duct will require attachment at a point downstream of the J85-21 flameholder station to maintain the required afterburning length of 132 cm from the flameholders to the afterburning nozzle throat.

The aspect ratio 8 exhaust system is basically the same as the aspect ratio 4 except for the relative size of components, as shown in the lower schematic of Figure 7. While the nozzle section has a larger span, its throat and exit height are smaller resulting in shorter flaps and actuation stroke requirements. Its transition duct is longer to maintain low divergent

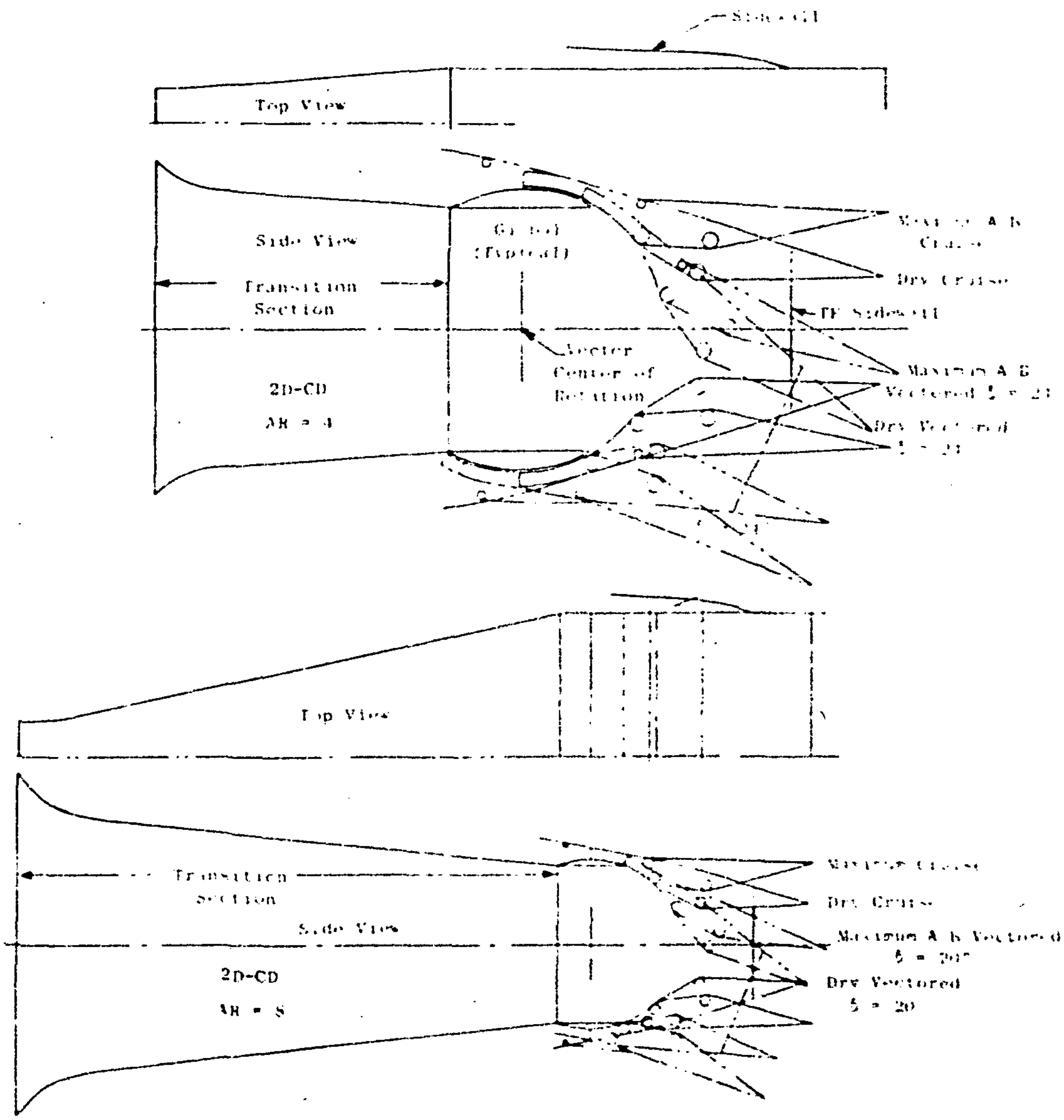

Figure 7. 2D–CD Flowpath Designs.

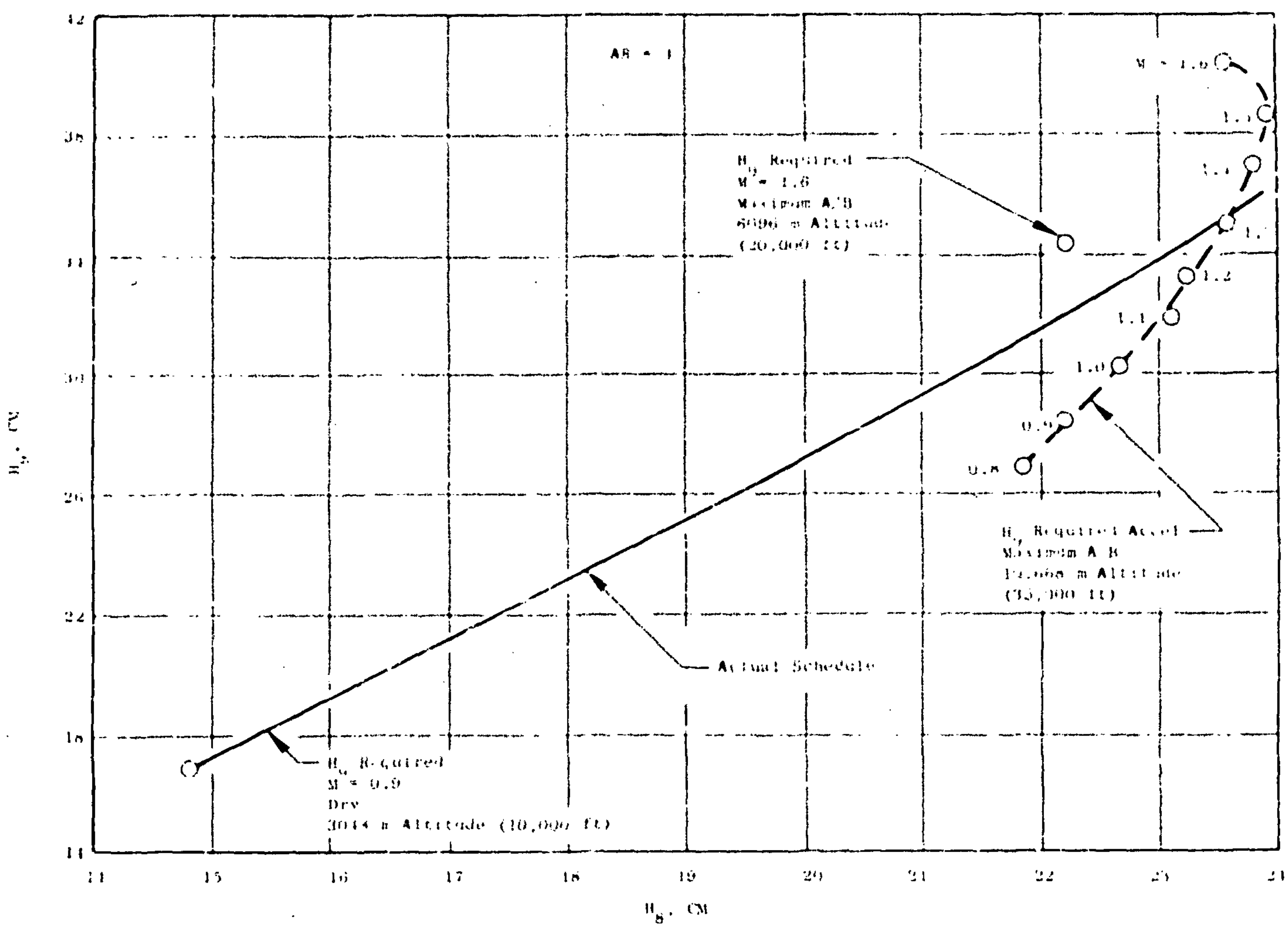

Figure 8. J85 Nonaxisymmetric Nozzle Design.

corner and sidewall angles to keep the internal flow from separating during transition. If the throat position 132 cm downstream of the flameholders is maintained, the aspect ratio 8 exhaust system is shorter than the aspect ratio 4 because the divergent flaps are shorter. The present aspect ratio 8 flowpath has a smaller maximum vector angle, $\delta = 20°$. Larger vector angles can be obtained by increasing the size of the gimbal and nozzle convergent sections. This would result in a longer transition plus nozzle section than the one shown in Figure 7.

The test results summarized in Figure 9 and Reference 11 show that supersonically deflected jets (ALBEN, NASA wedge) produce a significant loss in thrust coefficient. Conversely, subsonically or sonically turned flows (e.g., VIP wedge) have a lower performance loss. Therefore, three different wedge nozzle flowpaths were designed to represent a realistic range of possibilities with the ground rule that the flow would be vectored subsonically or sonically and thereby maintain high internal performance. The designs, as well as some of their important performance characteristics, are compared in Figure 10.

Design 20617-2 is a gimbaled 2DW flowpath. In this approach, A_8 control is obtained by a pair of upper and lower wedge flaps. The fixed geometry cowl has a low boattail angle for low drag installed cruise performance. For vectoring, the entire nozzle rotates about a gimbal section that is similar to the 2D-CD concept. The present 2DW design is limited to a vector angle of 20° due to the compromise that must be made between the nozzle's circular seal surface and maintenance of flowpath convergence to the nozzle's throat at maximum reheat power. This type of 2DW flowpath features a simple actuation system with separately controllable A_8 and vectoring functions. The main disadvantage of this design is the introduction of relatively large top and bottom external flap projected areas into the external stream while vectored. Thus, on an installed basis, it may yield higher drags in the vectored mode, although this has not been confirmed.

In a second 2DW approach (20617-3 in Figure 10), relatively long cowl flaps are converged or diverged to obtain A_9 control. The flaps are also actuated parallel with each other during vectored modes to produce subsonic flow turning. Externally, the flaps provide a gentle boattail to promote an unseparated flow expansion and maximize supercirculation. The rotating fixed geometry wedge completes the jet flow turning in the desired direction. This concept requires a more complex control system for its double functioning area control and vectoring flaps. In addition, A_8 would need different schedules for cruise and vectoring. Its main advantage is a gradual flow turning outer surface contour while vectored.

The third 2DW flowpath, 20617-4, uses short cowl flaps for A_9 control during cruise and for aiding flow turning while vectored. Vectoring is primarily controlled by the rotating wedge. Its center of rotation is located downstream of the nozzle's exit to direct most of the exhaust stream into a position for positive (as opposed to Coanda) vectoring. A_8 is controlled by a pair of wedge flaps similar to the gimbal 2DW, 20617-2. This concept

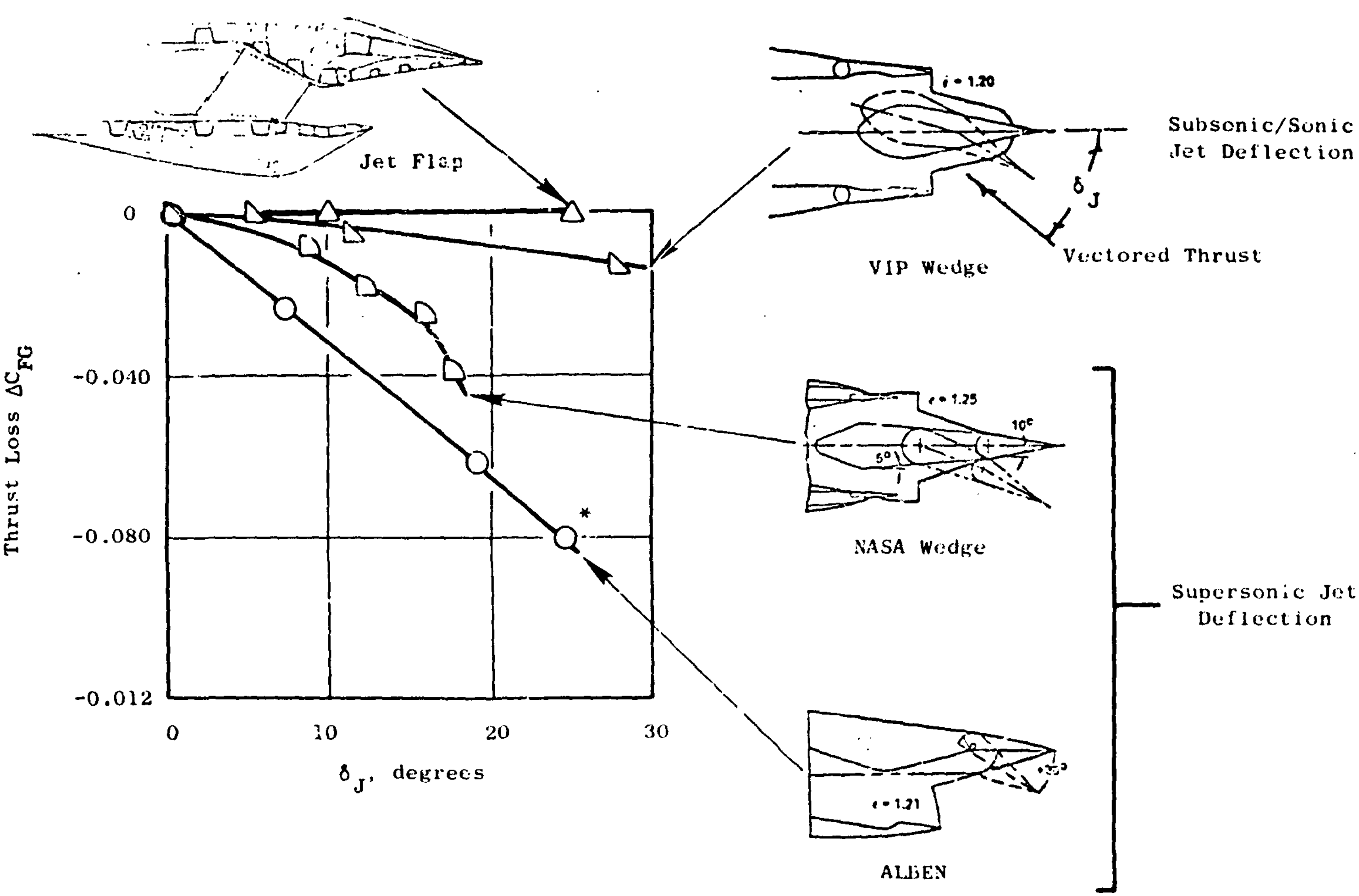

Figure 9. Effect of Jet Mach Number on Deflection Thrust Loss.

* Static Performance, External Flow Effects Reduce This Loss.

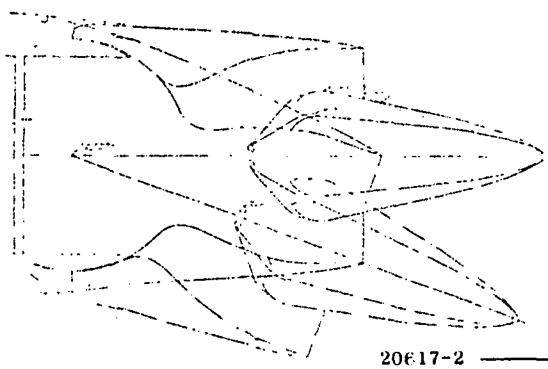

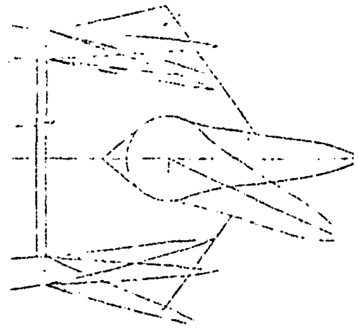

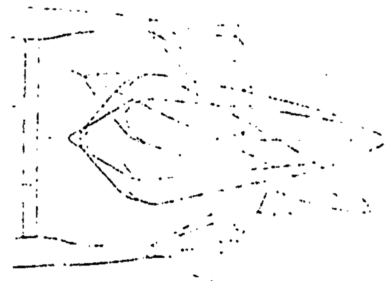

	Flight Mode	M_o	Power	δ, degrees	20617-2	20617-3	20617-4
Internal Performance C_{FG}	Subsonic Cruise	0.9	Dry	0	0.972	0.974	0.972
	Accel	1.2	A/B	0	0.983	0.978	0.987
	Supersonic Cruise	1.6	A/B	0	0.980	0.974	0.985
	Combat	0.9	A/B	15	0.984	0.976	0.982
Design Criteria	Controls and Structure				Simple	Complex	Very Complex
	Weight				3*	4	4

* Rankings as Defined in Table 3

Figure 10. Wedge Nozzle Concepts - Performance and Design Characteristics.

has cruise performance benefits due to its independent A_8 and A_9 controls. In addition, it produces the least projected drag area while vectored, thus maximizing supercirculation benefits. Its principle disadvantage is its relatively complex actuation system.

As shown by the table on Figure 10, the performance for all concepts is approximately equivalent (i.e., within one percent). Consequently, it is only in the controls, structural, and weight areas in which any selective judgment can be made.

The 20617-4 exhaust system has both cowl and wedge rotating flaps. In addition, the entire wedge and its flap system rotate to provide thrust vectoring. The cowl flaps must also have a capability for both convergent motion during cruise modes and move parallel with each other during vectored modes. This convergent and parallel motion double function of the cowl flaps for cruise and vectored modes is considered very complicated and entails high development risk. In comparison the -2's concept control system and structure is simpler. This is because it requires only two independent control systems (one for A_8 control and the other for vectoring). Furthermore, it has a fixed outer structure that is less difficult to seal than the -3 and -4 concepts with rotating cowl flaps. The -3 concept control system and structure ranking falls between the -2 and -4 concepts because its outer flaps are still double functioning, but the fixed geometry rotating wedge is less complicated. These variations in control and structural requirements lead to the weight rankings shown in Figure 10.

Attention was also given to the drag aspects of the 2DW concepts. In general, the drag during cruise modes is approximately equivalent for the three 2DW concepts. However, there is considerable difference in external projected flap area when vectored. Whether this is necessarily bad aerodynamically depends on how much lift is generated and how much must be paid in drag for this lift. For example, while the upper and lower cowl flaps appear long for the -2 concept, the angles are shallow and the external stream is turned with little or no flow separation. Conversely, the -4 has shorter flaps with higher external flap angles tending to promote external (and probably internal) flow separation. The best vectored performance, therefore, depends on which of these situations produces the greatest lift force for the least external drag and internal performance penalty. However, there are no data available to make a good quantitative evaluation of vectored thrust minus drag for the flowpath geometries of the 2DW concepts at the present time.

Accordingly, the only significant differences between concepts remain in the controls, structural, and weight criteria, all of which indicate the gimbaled -2 concept as having the most desirable attributes. As a result, the -2 exhaust system was selected as the 2DW study concept.

To complete the exhaust system flowpaths, thrust reversing schemes were provided for the selected 2D-CD and 2DW concepts as shown in Figure 11. The 2D-CD reverser deployment is initiated by opening a pair of doors at the gimbal section, thus exposing the reverser's exit port. The gimbal sections

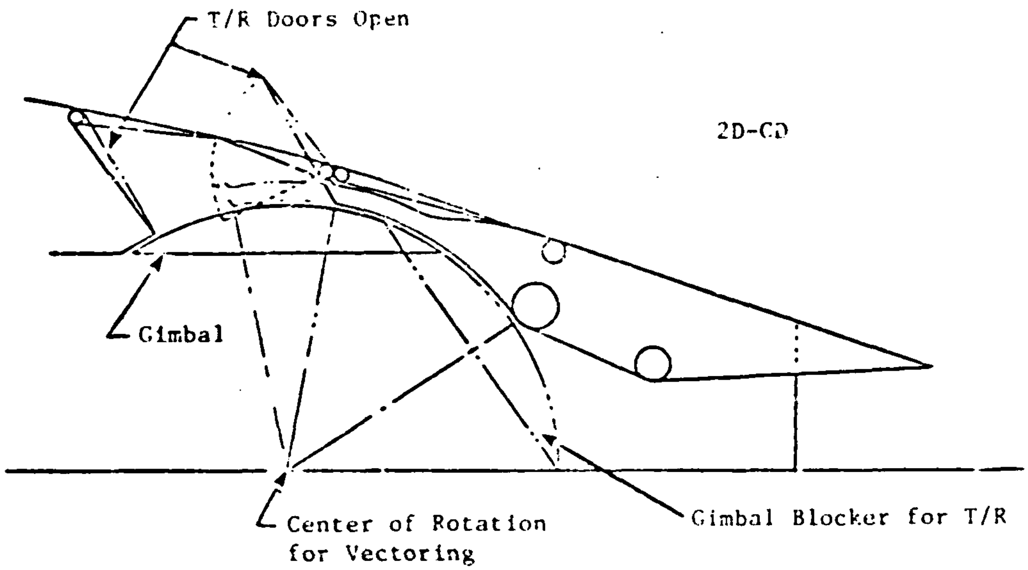

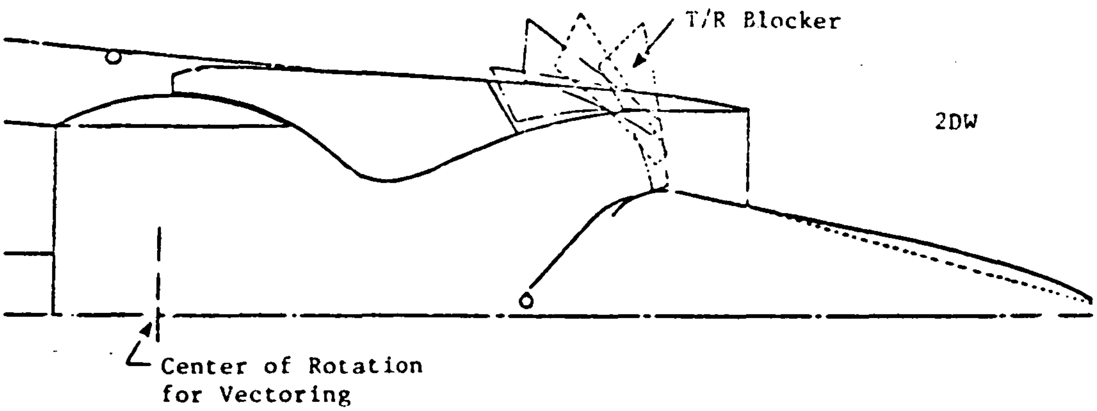

Figure 11. Selected Study Concepts.

counterrotate inwards to deflect the flow while maintaining a seal against the nozzle's convergent section. Small sidewalls are supported by the downstream reverser door to prevent side spillage and maintain good reverser efficiency.

The 2DW reverser uses a portion of the cowl as a combination blocker and flow deflector. The reversing is accomplished with a flap that is translated and rotated to maintain the proper exchange between cruise throat and reverser throat while holding total throat area constant, thus having no effect on the engine operation. The full deployment also has the added support from the fixed cowl structure when the flow is fully blocked and turned and the reverser flap is highly loaded. Although the kinematics, structural, and seal aspects may require flowpath changes, the proposed approach of using part of the fixed 2DW cowl as a deflector appears feasible.

4.0 COOLING TRADE STUDY AND CONCEPTUAL DESIGN RECOMMENDATION

4.1 STUDY OBJECTIVE

This phase of the program evaluated cooling systems for the three selected exhaust system concepts:

- 2D-CD 4AR with gimbaled vectoring and thrust reverser
- 2D-CD 8AR with gimbaled vectoring and thrust reverser
- 2DW 4AR with gimbaled vectoring and thrust reverser

The objective of this trade study was to identify various cooling methods and to determine their effects on cooling efficiency, performance, mechanical simplicity, and costs. Based on these considerations, a cooling scheme was identified for each concept and recommended for further conceptual design and analysis.

4.2 STUDY CRITERIA

In order to ensure consistency in the analytical results which would be used for subsequent ranking and selection, design criteria were established similar to that applied successfully on the augmented deflector exhaust nozzle (ADEN) full-scale demonstrator design, Reference 10. Although the ADEN was designed as a flightweight 2-D exhaust system with primary emphasis on structural efficiency for low weight, future designs should also take into account survivability considerations. Reduced dry cruise metal temperatures increase survivability by means of IR suppression. ADEN design metal temperatures were established for structural requirements during afterburner operation. While the dry operation metal temperatures were naturally below these limits, they were higher than desirable for IR suppression. Extra cooling flow must be introduced over and above that needed for structural considerations to enhance IR suppression. Therefore, in determining the design criteria for this task, two design goals were set: first, to come within structural limitations for afterburner conditions; and second, to achieve cooler metal temperatures for IR suppression during dry operation.

Table 6 lists the design metal temperatures used in this trade study.

The cooled components in Table 6 are defined as follows:

- Liner - afterburner section from flameholder plane to start of convergent section.
- Convergent Flap - convergent section to nozzle throat.
- Divergent Flap - divergent section from nozzle throat to end of nozzle.

Table 6. Cooling Scheme Trade Study Design Temperatures (T_M)

Component	Max A/B - Structural Life*	Dry IR Goal
Liners	1061 K (1450° F)	---
Convergent Flaps	1061 K (1450° F)	---
Divergent Flaps	1061 K (1450° F)	556 K (540° F)
Sidewalls	1033 K (1400° F)	556 K (540° F)
Shrouds	1033 K (1400° F)	556 K (540° F)
Wedge Nose	1200 K (1700° F)	---
*Similar to ADEN Flight Design Criteria		

- Sidewall - side surface from end of liner to end of nozzle.
- Shroud (applies to 2DW design only) - outermost convergent and divergent section surrounding wedge flaps.
- Wedge Nose (applies to 2DW design only) - stagnation region of wedge centerbody.

The first column of design temperatures in Table 6 was used in determining the cooling flows for each cooling scheme of the three nozzle concepts (2D-CD 4AR, 2D-CD 8AR, and 2DW) under maximum afterburner gas stream conditions. The IR goals in the second column were set only for primarily line of sight visible nozzle components such as the sidewalls, divergent flap, or wedge. The liners and convergent flaps due to geometry and low residual temperatures were not considered sensitive.

For calculating the cooling flows in this study, an externally supplied cooling flow was assumed simulating fan flow conditions for advanced turbofan engines. The cooling air temperatures used are shown in Table 7.

Table 7. Trade Study Heat Transfer Design Criteria.

- Assumed 450 K (350° F) fan air available for all liners.
- Assumed 478 K (400° F) fan air available to all nozzle components.
- Screech flow not included for trade study.

The 28 K (50° F) temperature difference between the liners and nozzle components accounts for heat pick up similar to that experienced during the ADEN testing. All hot gas stream cycle parameters were based on the J85-21 study engine.

4.3 COOLING METHODS

Various cooling methods were identified which would provide a good comparison for this cooling trade study phase. These methods are shown schematically in Figure 12. Current experience in turbine and exhaust system cooling technology was utilized in the cooling method identification. As seen in Figure 12, these methods represent a wide range of cooling efficiencies indicated by the relative cooling flow parameters at the specified gross effectiveness (η_G = 0.6).

Although all possible cooling techniques were not included in the trade study, the ones shown on Figure 12 were considered to generally encompass the range of cooling efficiencies obtainable with other methods.

4.4 COOLING ESTIMATIONS

In order to determine cooling efficiencies (flows) for the different cooling schemes in the trade study, correlations of in-house turbine and exhaust nozzle cooling data were used for these preliminary predictions in Figure 13. The six methods indicated correspond to the methods identified in Figure 12. It should also be noted that the relative cooling flows in Figure 12 were obtained from the curve in Figure 13 at a constant gross effectiveness (η_G) value of 0.6 by ratioing the cooling flow parameter ($W_c C_p / h_G A_G$) of each method to the cooling flow parameter value of film-impingement cooling. This preliminary method of predicting cooling flow is used in the early phase of exhaust system design for establishing initial cooling estimates and cooling flow allocations for cycle analysis. It was used successfully in the early ADEN design phase with subsequent substantiation by more detailed analysis and test in Reference 10.

The following summarizes the cooling flow estimation procedure used for each cooling scheme:

- Afterburner liner and exhaust nozzle surface areas to be cooled were determined for the major flowpath parts.

- Gross effectiveness (η_G) for each nozzle part was determined using the design criteria for metal temperatures (T_m) and coolant temperatures (T_c) while the hot gas stream temperature (T_g) assumed a sinusoidal temperature rise from the plane of the flameholder to the nozzle throat (A_8). For this Task II study, the J85-21 maximum afterburner sea level static cycle condition was used for the structural design point.

METHOD	SCHEMATIC	RELATIVE COOLING FLOW @ η_G =.6
FILM - IMPINGEMENT	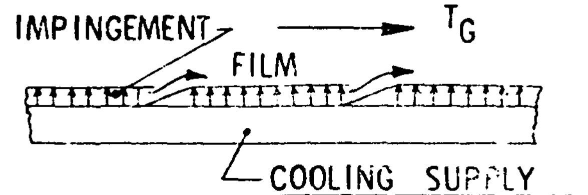	1.0
IMPINGEMENT	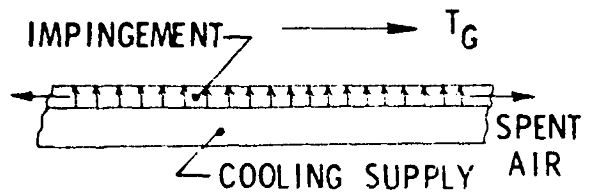	1.4
TYPICAL LINER	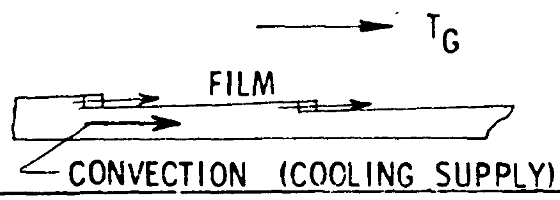	1.4
FILM	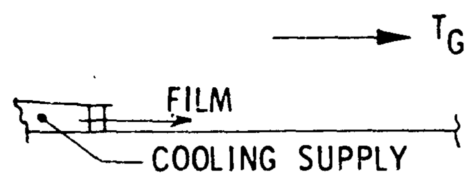	1.4
CONVECTION	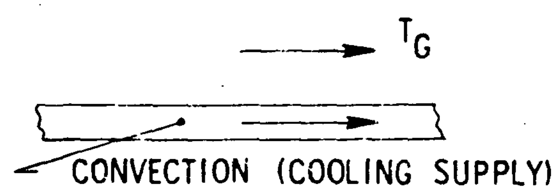	1.6
TYPICAL FLAPS	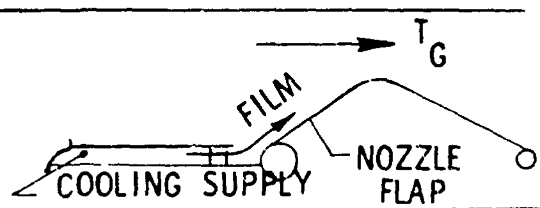	3.0

Figure 12. Typical Exhaust Nozzle Cooling Methods.

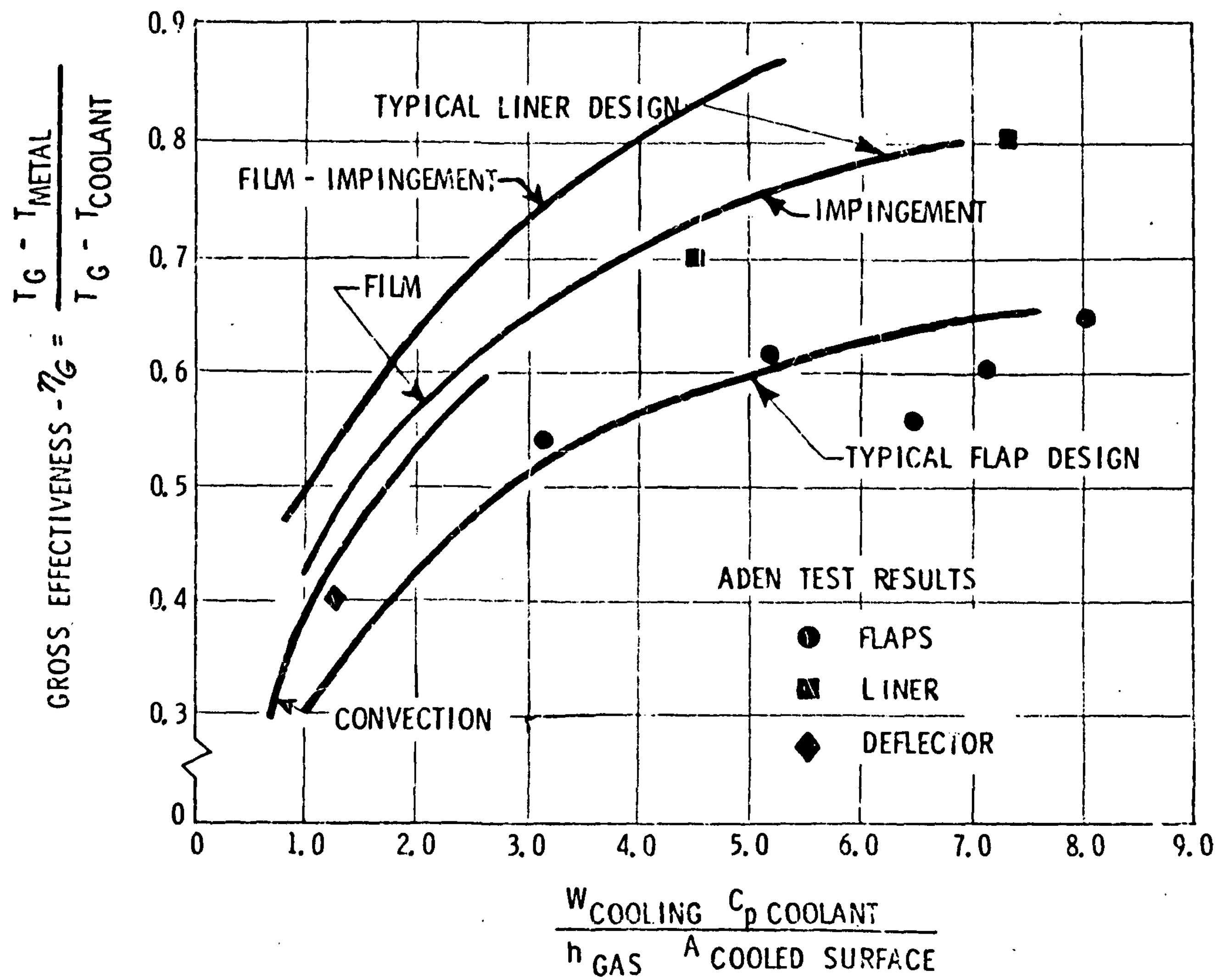

Figure 13. Exhaust Nozzle Cooling Effectiveness - Sea Level.

- Average gas side heat transfer coefficient (h_{Gas}) and cooling air specific heat (C_p Coolant) were determined consistent with the cycle conditions.

- Depending on which cooling method was used to cool a certain nozzle part, the corresponding curve of Figure 13 was used to find the required cooling flow ($W_{cooling}$).

- This procedure was used for each nozzle part and the summation of these cooling flows equaled the required total cooling flow for each cooling scheme. The total flow was ratioed to the maximum afterburner sea level static engine cycle flow to determine percent W_8 for the structural design condition.

- The cooling parameter ($W_c C_p / h_G A_c$) remains nearly constant between afterburner sea level static to dry takeoff conditions. Therefore, to determine cooling flows for meeting IR requirements, the cooling parameter determined in the procedure above for structural integrity was assumed the same for the dry condition. By using Figure 13 in reverse, a dry metal temperature T_m was determined based on the dry gas temperature T_g and the design criteria coolant temperature T_c. The metal temperature was higher than allowed for the IR goals but represents the metal temperature at dry power that could be expected for coolant flows determined at maximum afterburner. For IR goals, the lower design metal temperature was used to calculate a new and higher required gross effectiveness η_G. From this point on the curve, the corresponding higher cooling parameter was ratioed to that satisfying structural design requirements to determine the extra cooling flow required for IR design.

4.5 COOLING SCHEMES

The cooling schemes are summarized in Table 8. As shown in this matrix, four cooling schemes were studied for each of the three nozzle concepts. The subsequent ranking and selection objective was to recommend one scheme for each concept. Figures 14 through 25 schematically show the 12 cooling schemes with estimated total cooling flows (IR total cooling flows are shown in parenthesis). The two cooling schemes shown in Figures 18 and 22 used cooling methods that were unable to cool the metal to the IR goal temperatures. These are, therefore, labeled impractical for IR. In addition, screech section cooling is not included in these formulations because changing nozzle cooling schemes would not affect screech requirements.

4.6 RANKING

The cooling system ranking objective was to determine the cooling scheme for each preliminary flowpath concept which would be recommended for further detailed cooling analysis and preparation of a final conceptual design layout. Effects of cooling efficiency, performance, weight, mechanical simplicity, and costs were included in the ranking criteria. All of these parameters must be considered to define the best cooling approach.

Table 8. Task 2 - Cooling Scheme Methods Matrix.

Scheme	All Liners	Convergent Flaps	Divergent Flaps	Sidewalls	Outer Shroud	Wedge Nose
2D-CD 4AR - 1	Liner	Flap	Film	Film	N/A	N/A
- 2	Liner	Film-Imp *	Film-Imp	Film-Imp	N/A	N/A
- 3	Liner	Flap	Film	Film-Imp	N/A	N/A
- 4	Liner	Flap	Film-Imp	Film-Imp	N/A	N/A
2D-CD 8AR - 1	Liner	Flap		Film	N/A	N/A
- 2	Liner	Flap	Film	Film-Imp	N/A	N/A
- 3	Liner	Flap	Film	Film	N/A	N/A
- 4	Liner	Flap	Film-Imp	Film-Imp	N/A	N/A
2DW 4AR - 1	Liner	Flap	Film	Film	Flap	Impingement
- 2	Liner	Flap	Film	Film-Imp	Film-Imp	Impingement
- 3	Liner	Flap	Film-Imp	Film-Imp	Film-Imp	Impingement
- 4	Liner	Flap	Film-Imp	Film-Imp	Flap & Film-Imp	Impingement

Note: Methods stated above correspond to those shown on "Exhaust Nozzle Cooling Effectiveness Curve."

* Film-Imp - Film-Impingement.

$W_{Coolant} = 13.2\%\ W_8$ (23.4% for IR)

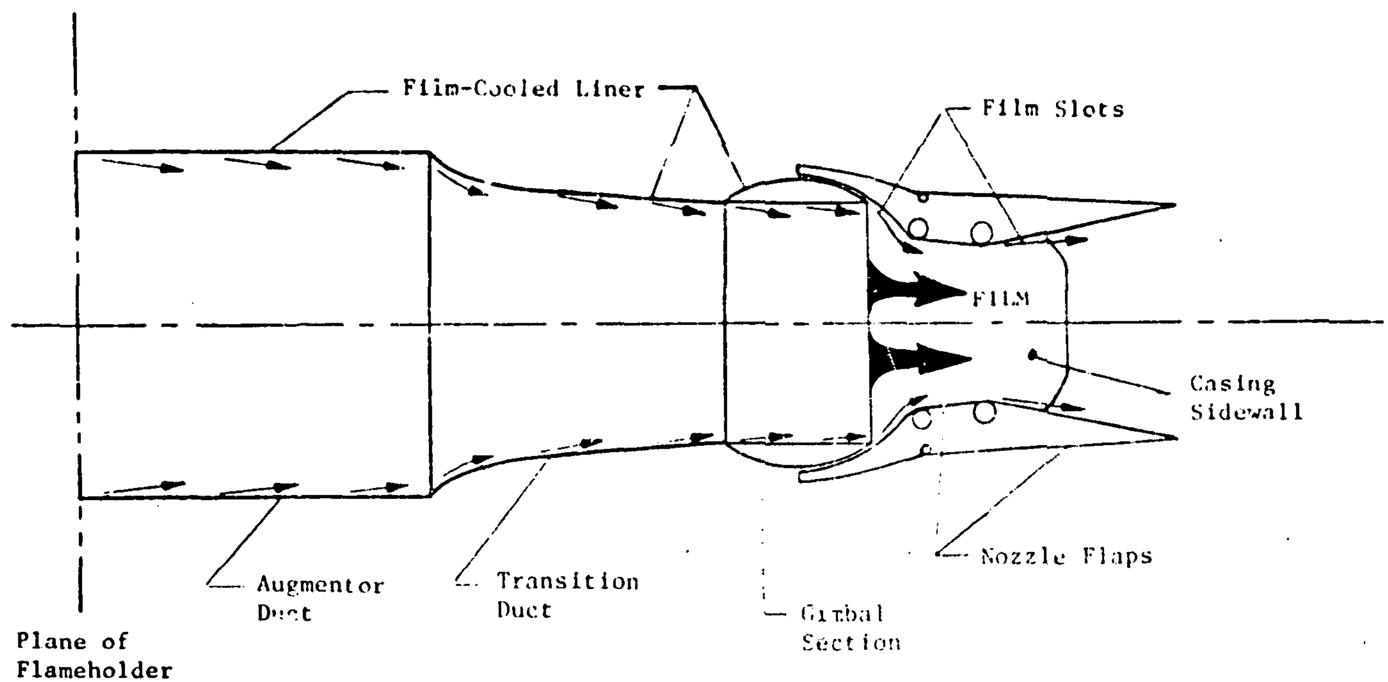

Figure 14. J85 Nonaxisymmetric Nozzle Design and Cooling Study - 2D-CD 4AR Cooling Scheme 1.

$W_{Coolant}$ = 918% w_8 (13.6% for IR)

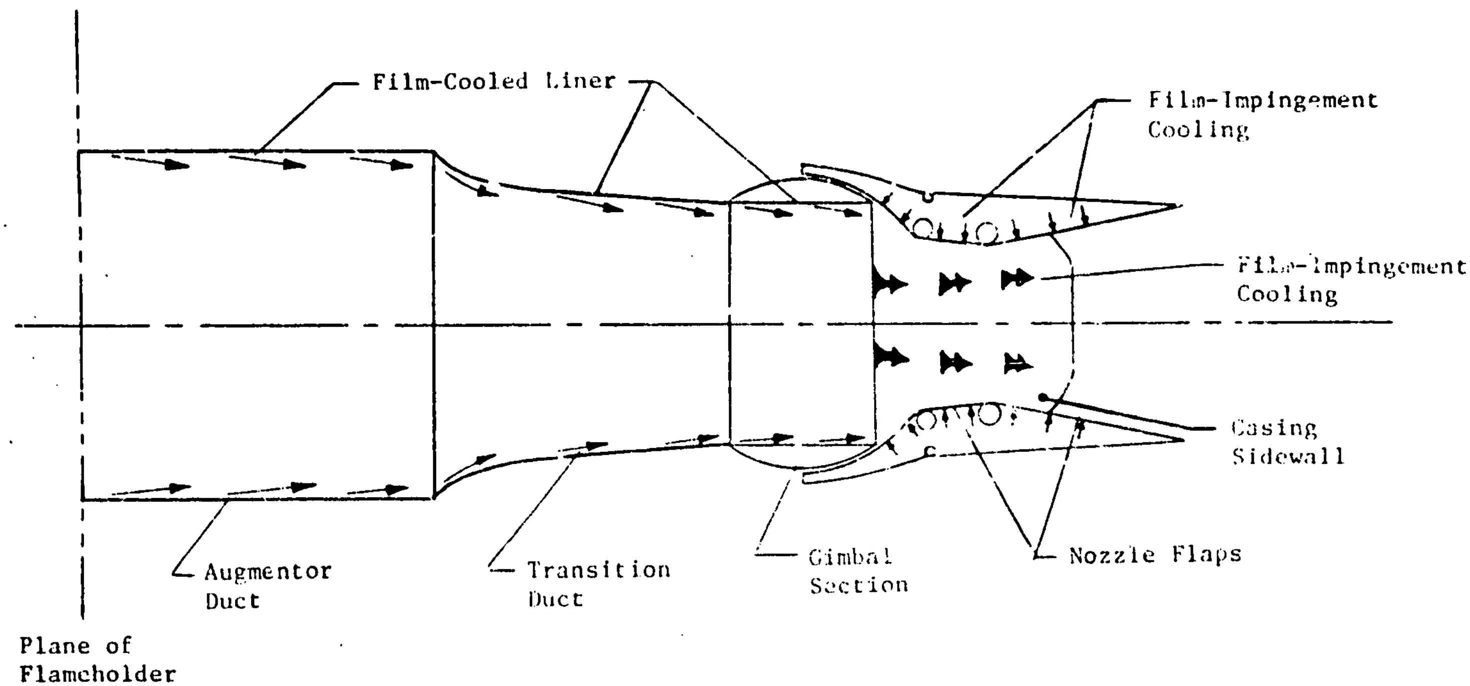

Figure 15. J85 Nonaxisymmetric Nozzle Design and Cooling Study - 2D-CD 4AR Cooling Scheme 2.

$W_{Coolant} = 12.9\% \ W_8$ (20.7% for IR)

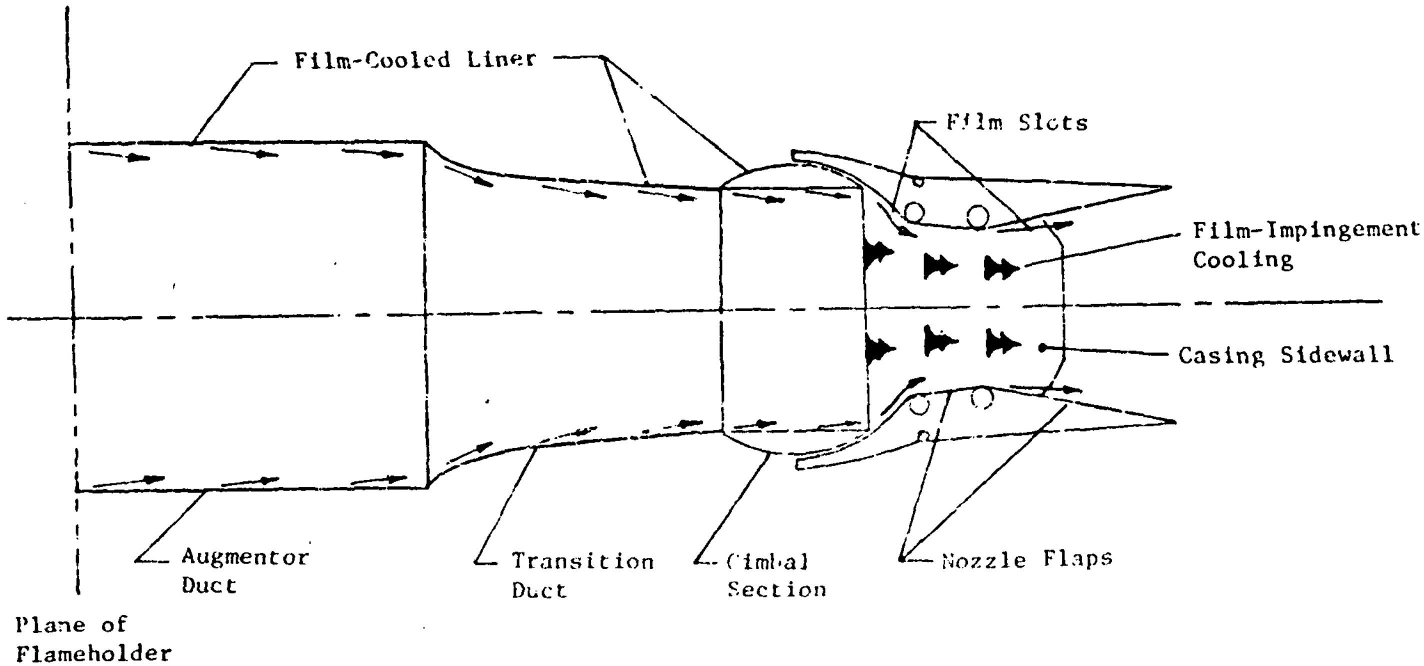

Figure 16. J85 Nonaxisymmetric Nozzle Design and Cooling Study - 2D-CD 4AR Cooling Scheme 3.

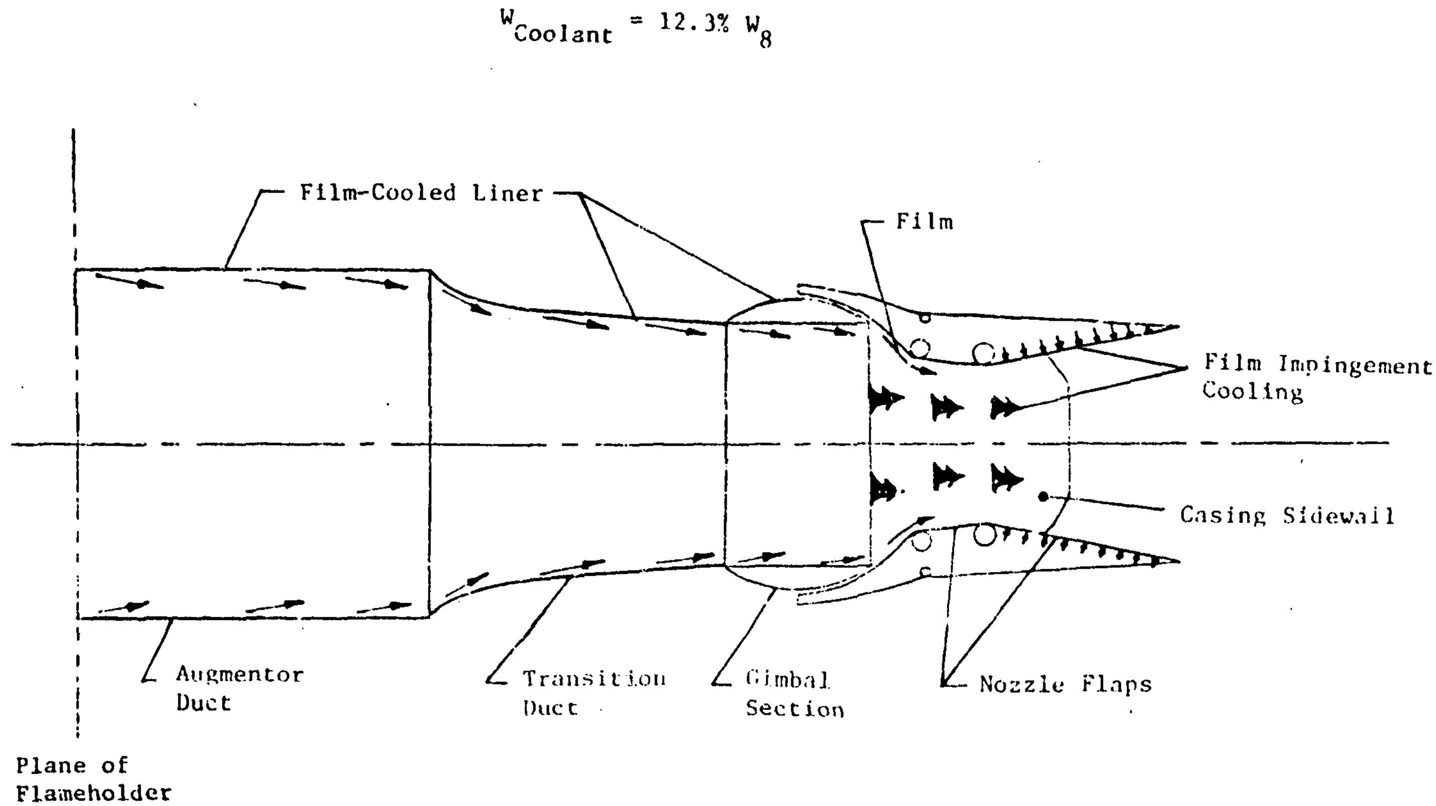

Figure 17. J85 Nonaxisymmetric Nozzle Design and Cooling Study - 2D-CD 4AR Cooling Scheme 4.

$W_{Coolant} = 16.7\% \; W_8$ (Impractical for IR)

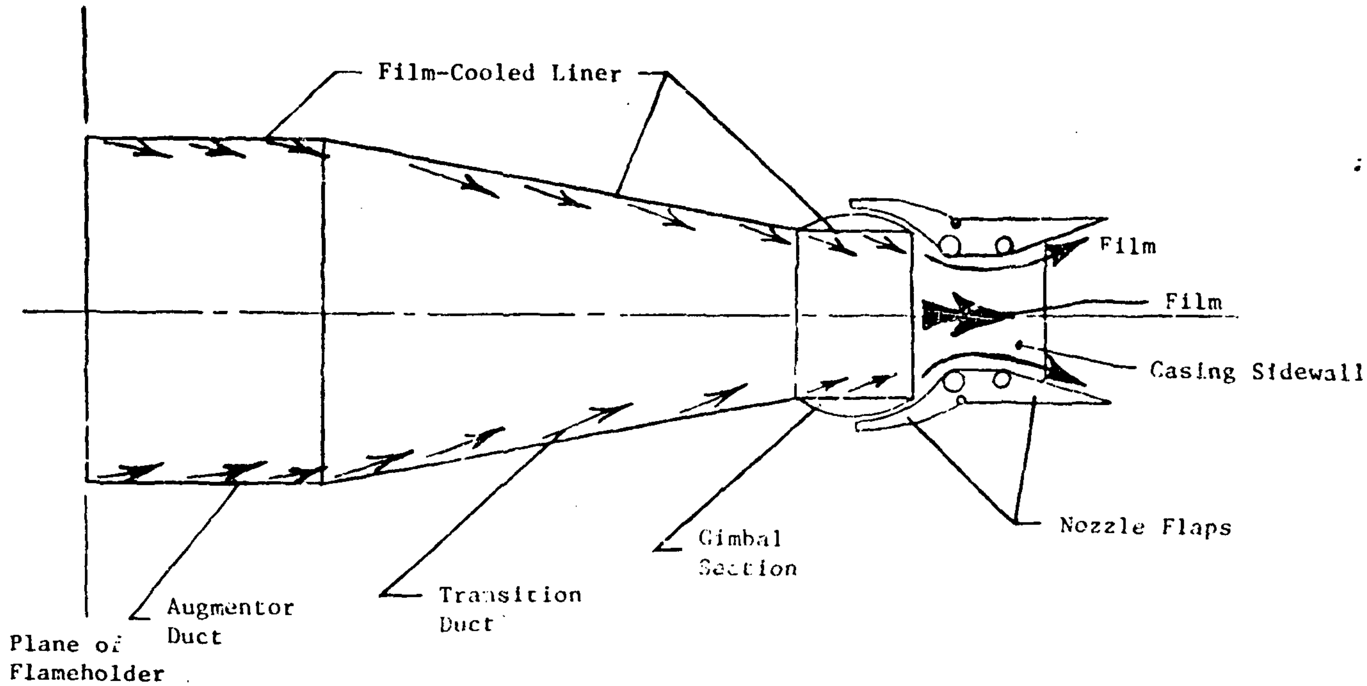

Figure 18. J85 Nonaxisymmetric Nozzle Design and Cooling Study -

2D-CD 8AR Cooling Scheme 1.

$W_{Coolant} = 14.5\% \; W_8$ (21.5% for IR)

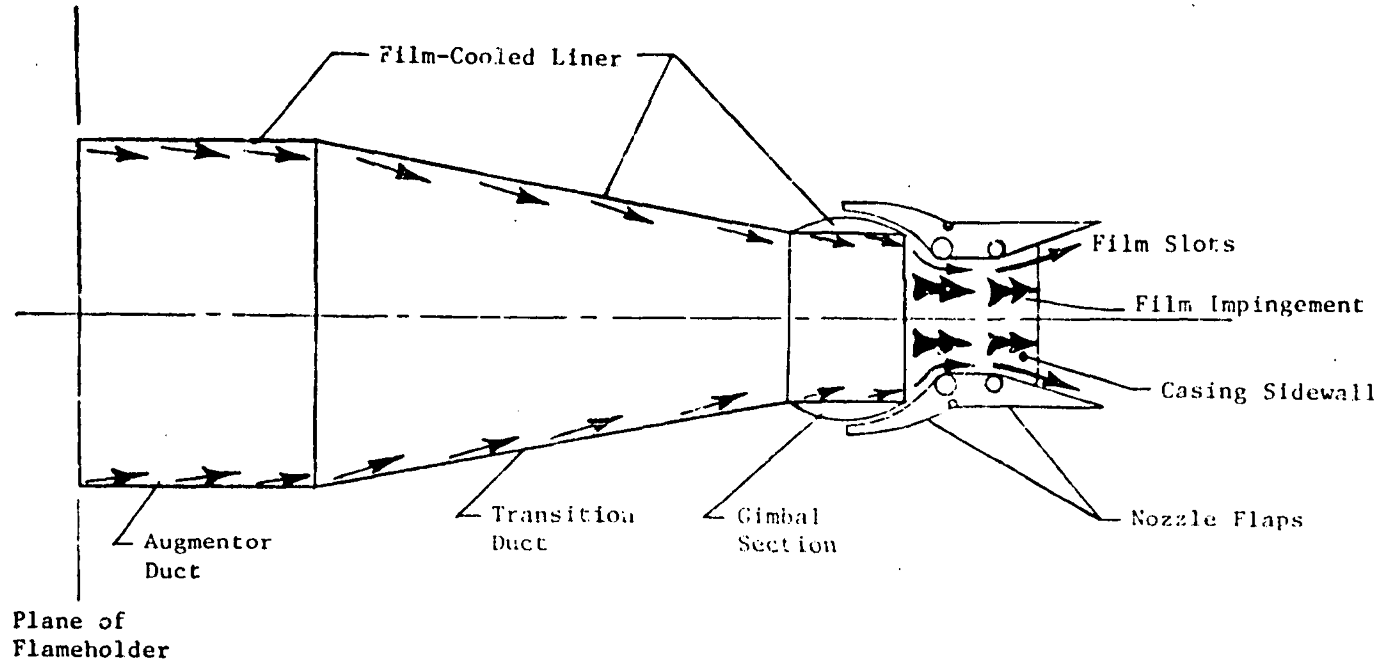

Figure 19. J85 Nonaxisymmetric Nozzle Design and Cooling Srudy - 2D-CD 8AR Cooling Scheme 2.

$W_{Coolant} = 14.6\%\ W_8$ (22.8% for IR)

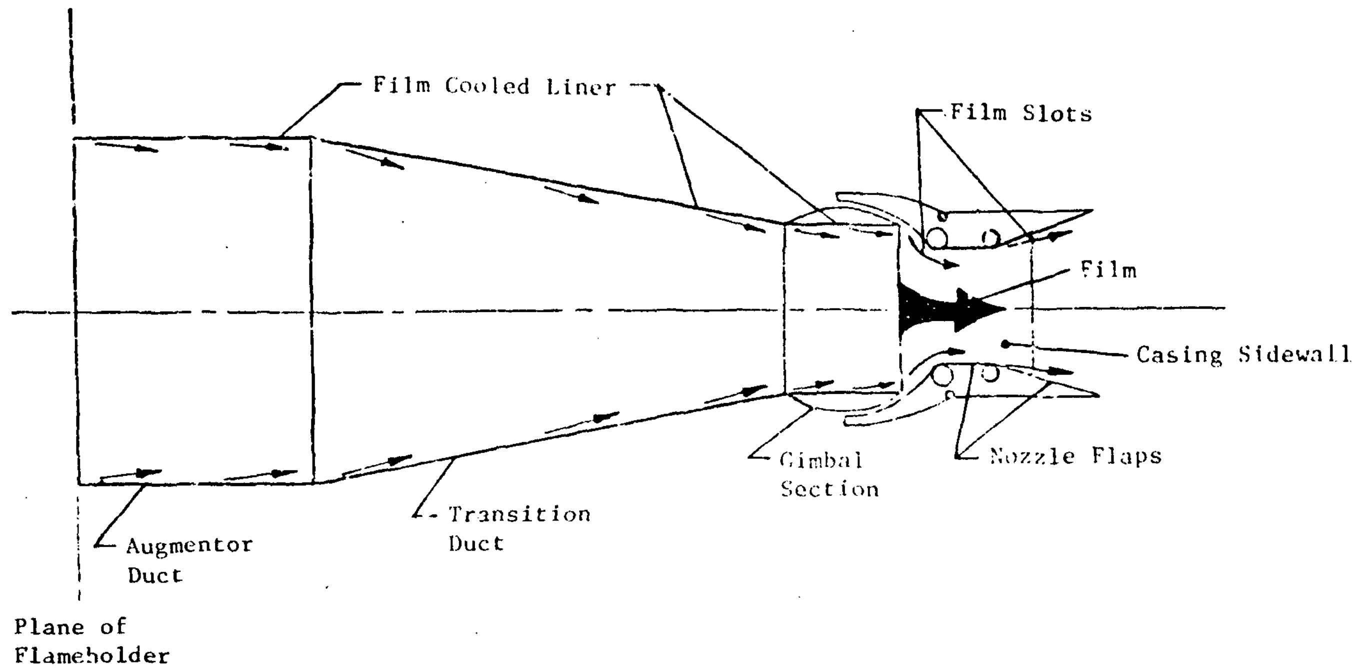

Figure 20. J85 Nonaxisymmetric Nozzle Design and Cooling Study - 2D-CD 8AR Cooling Scheme 3.

$W_{Coolant} = 13.9\% \ W_8$ (16.9% for IR)

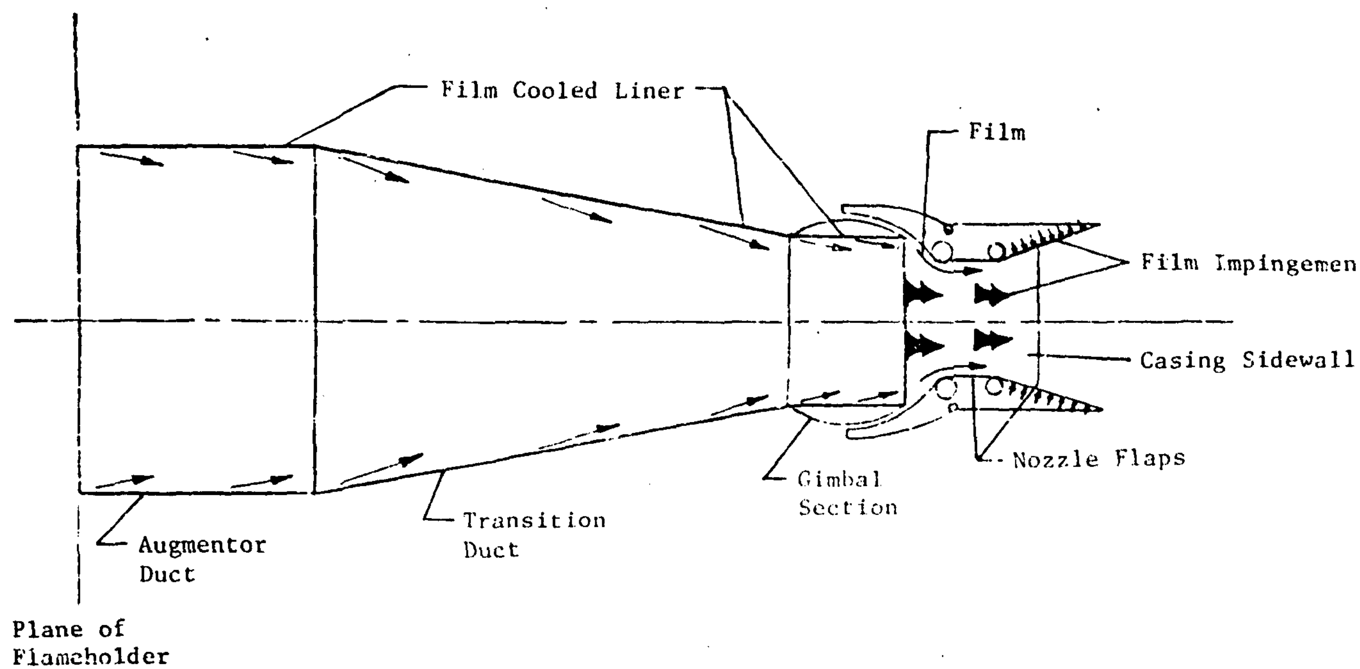

Figure 21. J85 Nonaxisymmetric Nozzle Design and Cooling Study - 2D-CD 8AR Cooling Scheme 4.

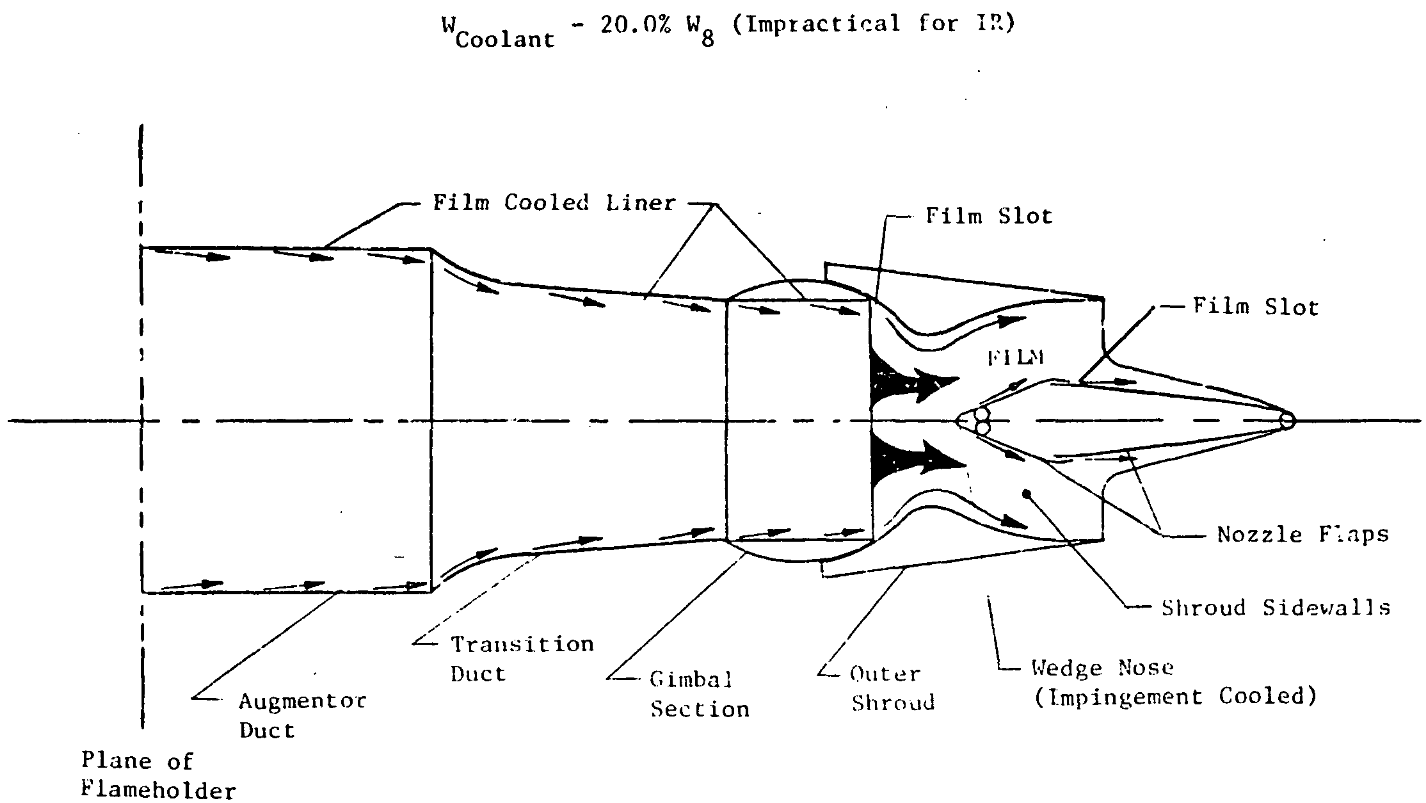

Figure 22. J85 Nonaxisymmetric Nozzle Design and Cooling Study -

2DW 4AR Cooling Scheme 1.

$$W_{Coolant} = 14.7\%\ W_8\ (27.8\%\ \text{for IR})$$

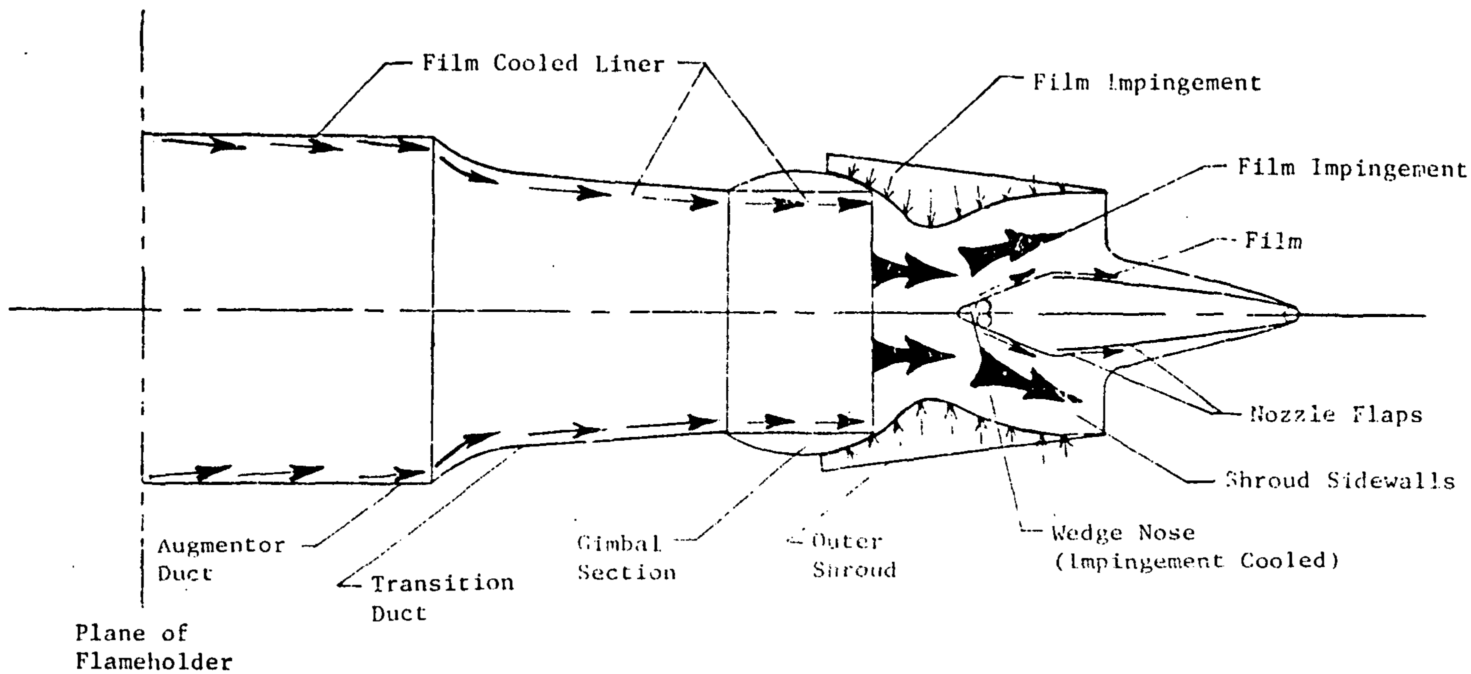

Figure 23. J85 Nonaxisymmetric Nozzle Design and Cooling Study -

2DW 4AR Cooling Scheme 2.

$W_{Coolant} = 14.0\% \; W_8$ (21.6% for IR)

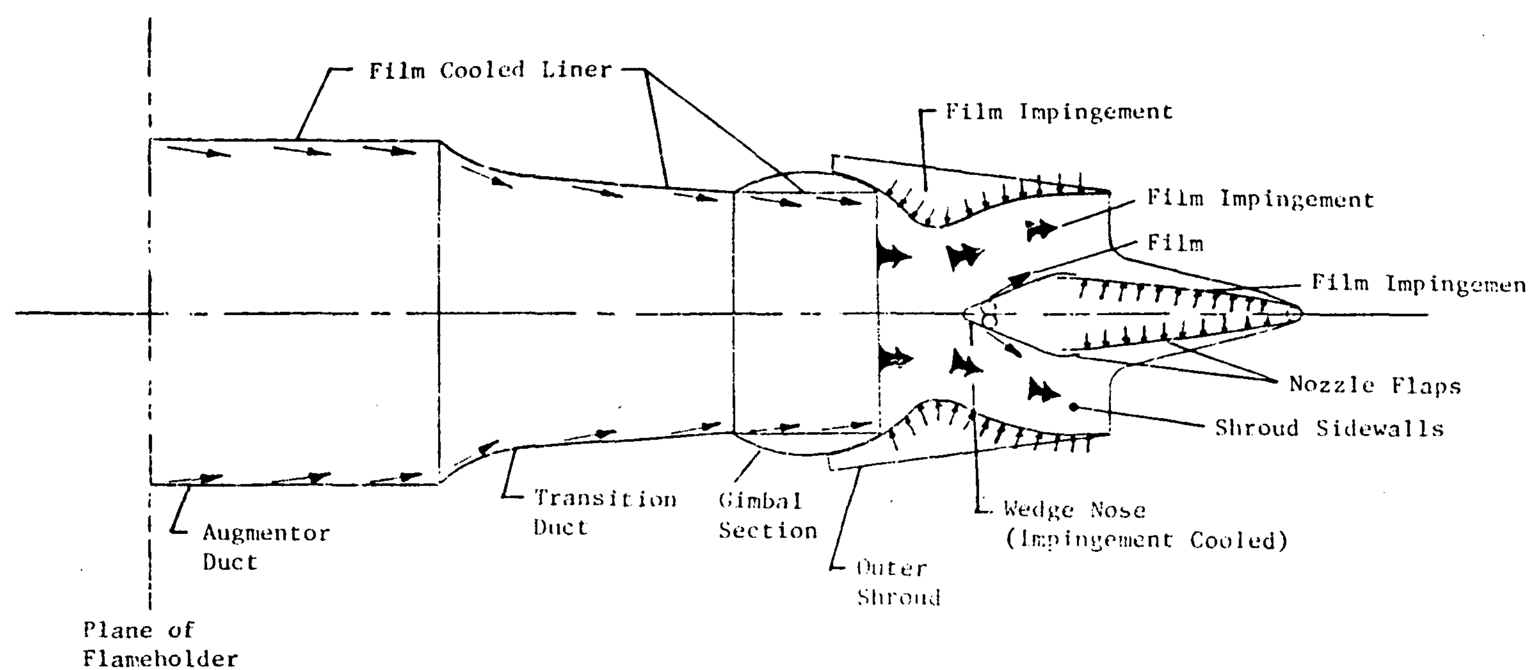

Figure 24. J85 Nonaxisymmetric Nozzle Design and Cooling Study - 2DW 4AR Cooling Scheme 3.

$W_{Coolant} = 15.2\%\ W_8$ (22.2% for IR)

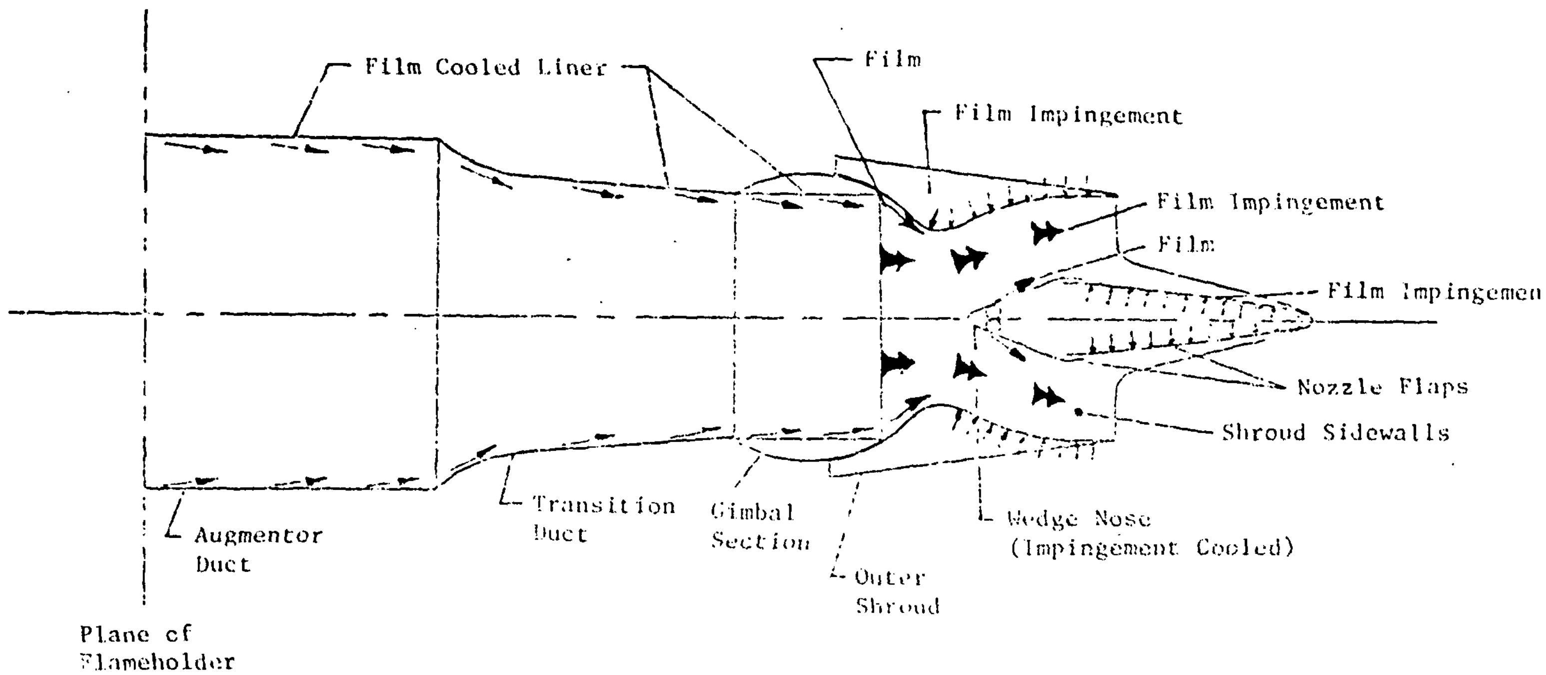

Figure 25. J85 Nonaxisymmetric Nozzle Design and Cooling Study - 2DW 4AR Cooling Scheme 4.

The ranking rationale is outlined in Figure 26. Cooling efficiency (flow), performance loss, and weight were determined for each cooling scheme. The cooling flow was estimated as outlined previously in Section 4.4. Performance losses (ΔC_{FGC}) were established by forming a difference in coolant flow thrust coefficient between the coolant thrust coefficient, C_{FGC}, assuming all the coolant was completely mixed with the main gas stream without losses, and the coolant thrust coefficient for the coolant entering the main gas stream with pressure and temperature loss. This coolant thrust coefficient loss estimating procedure is outlined in Figure 27. Performance increments were then expressed as changes in propulsion system weight using the expression in Table 9.

Table 9. Determination of Aircraft ΔTOGW.

- Determine cooling ΔCFG for pressure and temperature variations
- Determine ΔCFG effect on J85 engine weight by:

  $$\Delta W_{CFG} = [(1 + \Delta CFG)^{1.2} - 1]\, W_{J85\ \text{Engine Weight}}$$

- Determine cooling scheme added weight for film impingement over film by:

  14.65 kg/m^2 (3 lb/ft^2) for nonlined components (flap, shroud)

  4.88 kg/m^2 (1 lb/ft^2) for normally lined components (sidewalls)

  Above = ΔW_C based on ADEN experience

- Determine $\Delta\text{TOGW} = 3.0\,(\Delta W_{CFG} + \Delta W_C)$
- Determine ΔTOGW for both max A/B design point and IR design point

The performance weight increment, ΔW_{CFG}, was combined with the cooling scheme relative weight, ΔW_C, to form the total cooling system weight effect (ΔW) on propulsion system weight. Finally, the cooling scheme's impact on aircraft TOGW was established by applying a sensitivity of $\Delta\text{TOGW}/\Delta W = 3.0$, derived from previous studies as the approximate aircraft weight penalty for each pound of engine weight.

In all concepts, the augmentor duct was cooled using the "typical liner" cooling technique shown in Figure 12. Only film impingement could produce a lower cooling requirement (relative cooling flow = 1.0 vs 1.4). However, the added complexity and cost of employing this approach for augmentor cooling makes it impractical. Accordingly, film cooling was adopted for cooling the augmentor in all concepts and any differences between Schemes 1 through 4 are found only in the nozzle sections. Furthermore, as shown in Figures 14 through 25, these differences are due only to an interchange between the film impingement and film cooling in the various nozzle parts. The ranking problem,

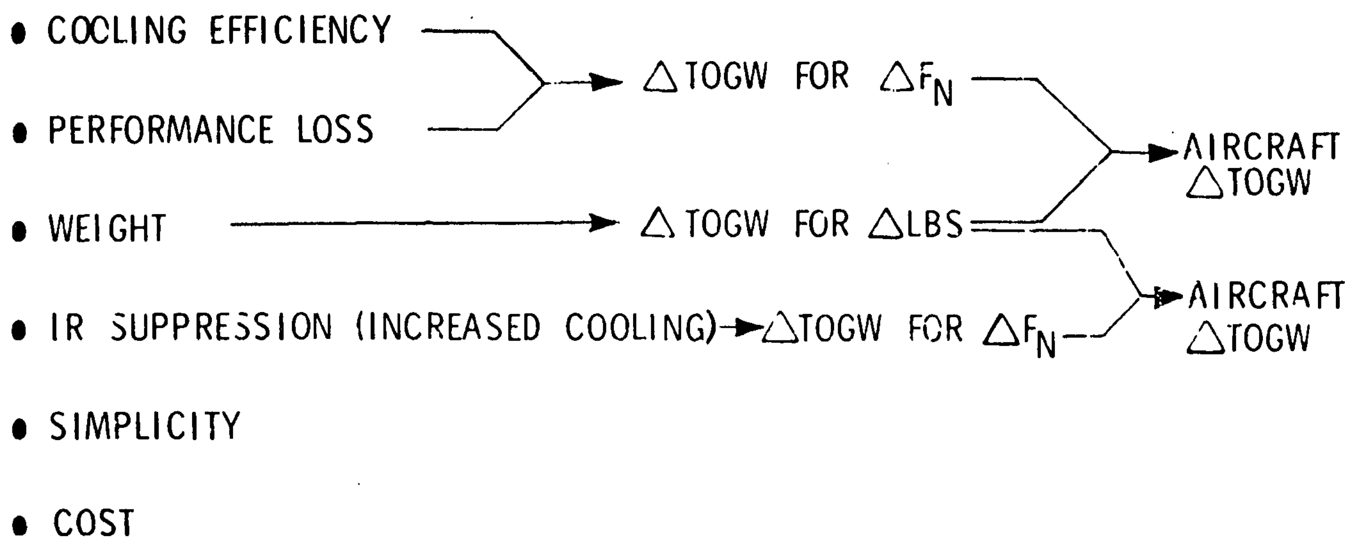

Figure 26. Task 2 - Cooling Scheme Ranking Rationale.

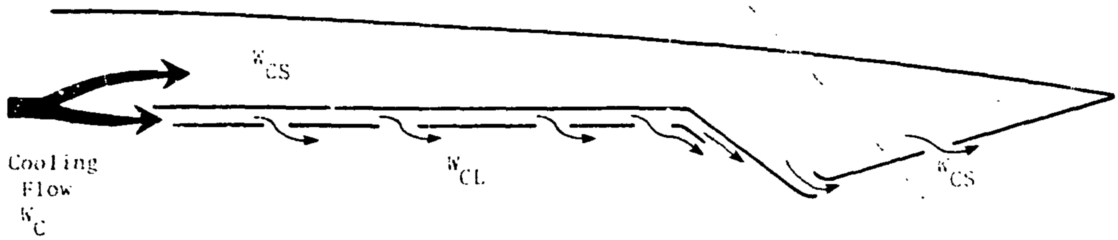

Cooling Flow Assumptions		
Slot Location	P_{TC}/P_{TS}	T_{TC}/T_{TS}
Upstream of Throat, W_{CL}	0.80	1.00
At or Downstream of Throat, W_{CS}	0.80	0.85

$$\Delta C_{FG_C} = \Delta C_{FG_{CL}} + \Delta C_{FG_{CS}}$$

$$\Delta C_{FG_{CL}} = \frac{W_{CL}}{W_S}\left[1 - \frac{F_{G_{CL}}\left(\frac{P_{T_{CL}}}{P_o}, T_{T_{CL}}\right)}{F_{G_{CL}}\left(\frac{P_{TS}}{P_o}, T_{TS}\right)}\sqrt{\frac{T_{T_{CL}}}{T_{TS}}}\right]$$

$$\Delta C_{FG_{CS}} = \frac{W_{CS}}{W_S}\left[1 - \frac{F_{G_{CS}}\left(\frac{P_{T_{CS}}}{P_o}, T_{T_{CS}}\right)}{F_{G_{CS}}\left(\frac{P_{TS}}{P_o}, T_{TS}\right)}\sqrt{\frac{T_{T_{CS}}}{T_{TS}}}\right]$$

Figure 27. Estimated Cooling Derate.

therefore, reduces to a determination of weight increments for various amounts of film-impingement cooling. Evaluation of the performance impact was outlined in the preceding paragraph. Cooling system weights were established by using ADEN data (Reference 10 and Figure 28).

The ADEN design used film-impingement cooling for the flat sidewalls at a weight of 14.65 kg/m^2 (3 lb/ft^2). This value was used to estimate weight increments for film-impingement cooling on all nozzle surface areas (flaps, etc.) except the sidewalls. It was also determined that if film-impingement cooling was not used on the sidewalls, some other wear and heat resistant material would have been applied to the sidewall structure to shield the structure and ensure a flat ware resistant surface for side seals to rub against. The weight of this surface was 9.76 kg/m^2 (2 lb/ft^2) normally film cooled. The penalty for applying film-impingement cooling on sidewalls is the difference of total film impingement minus heat shields or 4.88 kg/m^2 (1 lb/ft^2). The results of the weight study are summarized in Table 10.

The bargraph on Figure 29 shows the combined analytical results in terms of ΔTOGW for the four cooling schemes of each concept. The lower unshaded bars represent the aircraft installed ΔTOGW for the exhaust system cooling required for structural integrity design only. The upper shaded area of the bar represents the aircraft installed ΔTOGW for the exhaust system cooling required for IR requirements. The dots on selected bars indicate the lowest ΔTOGW (best cooling scheme) for the two requirements of each concept.

The ranking matrix shown in Table 11 was prepared for the structural design criteria to take into account relative values of two parameters; i.e., ΔTOGW and "simplicity and cost." Relative values for ΔTOGW were assigned from one to four with the lowest being given one. If the ΔTOGW's of two schemes were very close to being equal they were given the same value. Values for "simplicity and cost" were similarly assigned with <u>one</u> denoting the lowest cost and least complex. The two values were summed and compared to determine the scheme with the lowest total. This represented the best cooling scheme for the concept when designing for structural integrity. For IR design goals, the best scheme was determined by ΔTOGW considerations only since cost and simplicity carried highest rankings and showed no variation in this instance. As the bar chart on Figure 29 shows, the lowest relative ΔTOGW meeting IR design goals is Scheme 4 for all concepts. This approach makes maximum use of high efficiency film-impingement cooling on components contributing the most to IR signature.

4.7 COOLING SCHEME RECOMMENDATIONS

The results in the ranking matrix, Table 11, were used to develop recommended cooling schemes to be used in Task III - Conceptual Design and Cooling Analysis. Two sets of recommendations were made. The first is based on designing for structural integrity as shown in Table 12.

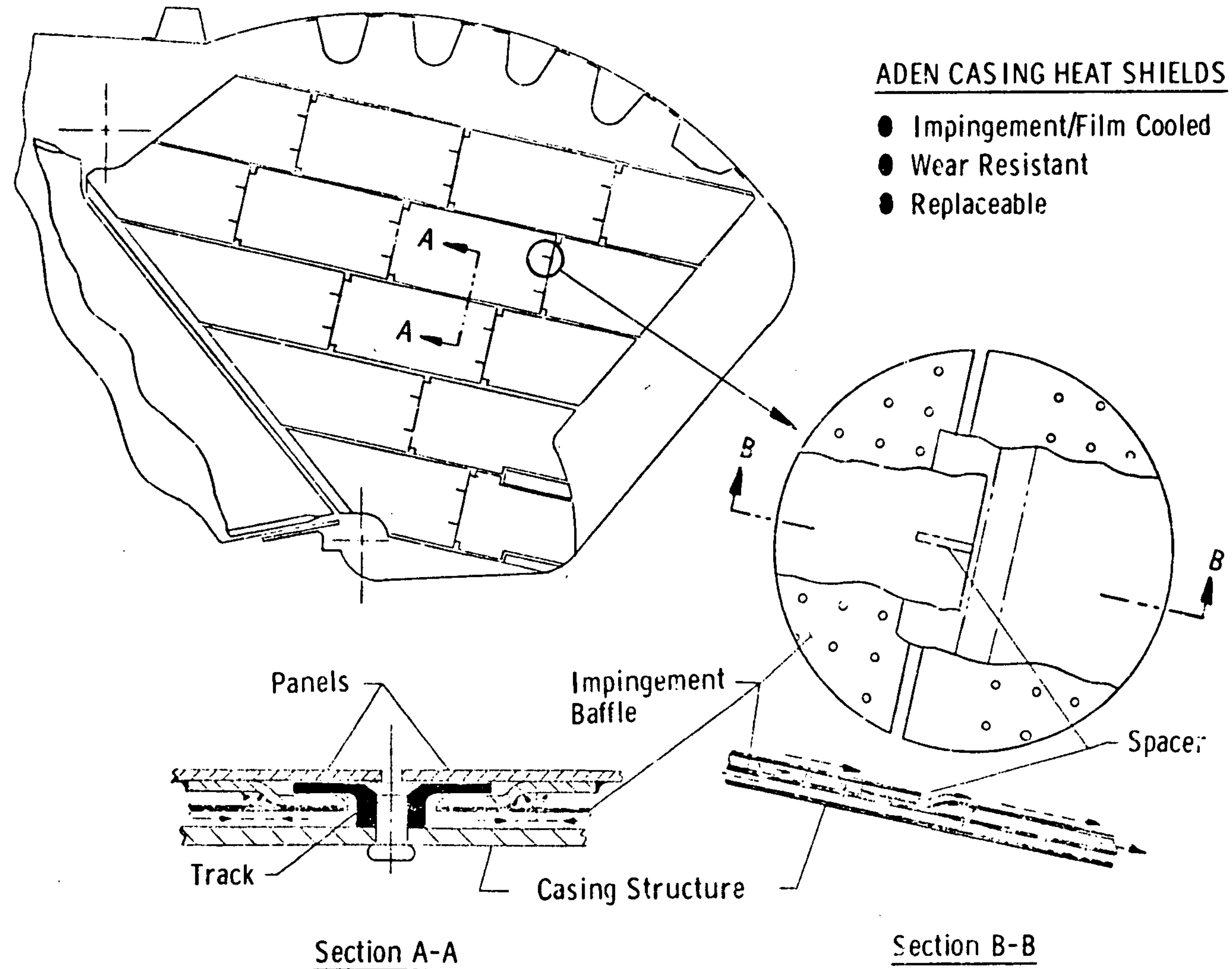

Figure 28. ADEN Casing Heat Shields.

Table 10. Task 2 - Analytical Summary.

Cooling Scheme	A_C ft^2	Maximum A/B Structural Design					IR Goal (1000° R)				
		$\%W_8$	Δ_{CFG}	ΔW_{CFG}	ΔW_{Cool}	Δ_{TOGW}	$\%W_8$	Δ_{CFG}	ΔW_{CFG}	ΔW_{Cool}	Δ_{TOGW}
2D-CD 4AR - 1	28.5	13.2	0.033	26.5	0	80	23.4	0.065	52.4	0	157
- 2	28.5	9.8	0.020	16.0	18.7	104	13.6	0.029	23.3	18.7	126
- 3	28.5	12.9	0.032	25.7	1.6	82	20.7	0.052	41.8	1.6	130
- 4	28.5	12.3	0.024	19.3	11.8	93	16.1	0.037	29.7	11.8	125
2D-CD 8AR - 1	29.8	16.7	0.036	28.9	0	87	Impractical				-
- 2	29.8	14.5	0.031	24.9	0.7	77	21.5	0.053	42.6	0.7	130
- 3	29.8	14.6	0.033	26.5	0	80	22.8	0.057	45.9	0	138
- 4	29.8	13.9	0.027	21.7	9.2	93	16.9	0.035	28.1	9.2	112
2DW 4AR - 1	32.2	20.0	0.050	40.2	0	121	Impractical				-
- 2	32.2	14.7	0.040	32.1	15.3	142	27.8	0.074	59.7	15.3	225
- 3	32.2	14.0	0.037	29.7	27.6	172	21.6	0.052	41.8	27.6	20[illegible]
- 4	32.2	15.2	0.044	35.4	24.7	180	22.[illegible]	0.049	3[illegible].4	24.7	192

ΔW_{CFG} = lb ΔW_{Cool} = lb Δ_{TOGW} = lb

1 lb = 14.54 kg

K = 5/9° R

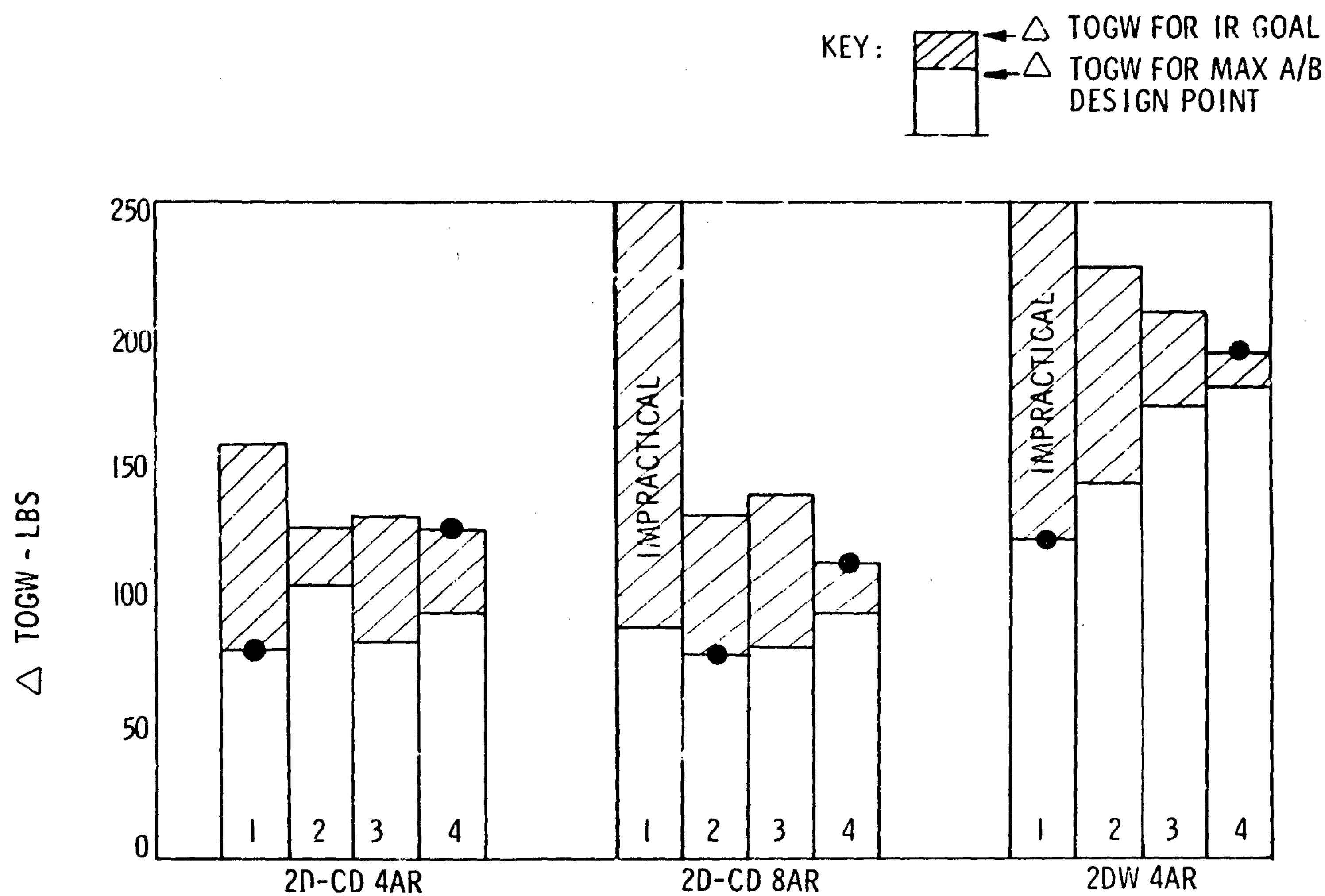

Figure 29. Effect of Cooling Scheme on Aircraft TOGW.

Table 11. Structural Design - Task 2 - Ranking.

Cooling Scheme	ΔTOGW	Simplicity and Cost	Total
2D-CD 4AR - 1	1	1	2
- 2	3	4	7
- 3	1	2	3
- 4	2	3	5
2D-CD 8AR - 1	2	1	3
- 2	1	3	4
- 3	1	2	3
- 4	3	4	7
2DW 4AR - 1	1	1	2
- 2	2	2	4
- 3	3	4	7
- 4	4	3	7

Table 12. Recommended Schemes Disregarding IR Suppression.

Schemes applying all film cooling provide the lowest combination of ΔTOGW, cost, and simplicity.
2D-CD 4AR Scheme 1.
2D-CD 8AR Scheme 1 or Scheme 3.
2DW 4 AR Scheme 1.

The second set is for exhaust systems that have advanced IR objectives (Table 13).

Table 13. Recommended Schemes for Final Design in Task 3.

IR objectives dictate efficient cooling methods.	
Cost and simplicity factors outweighed by IR (unless two schemes otherwise closely ranked).	
Resulting recommendation based on IR ΔTOGW only:	
- 2D-CD 4AR	Scheme 4
- 2D-CD 8AR	Scheme 4
- 2DW 4AR	Scheme 4

These results are summarized as follows:

- For structural design considerations including cost and simplicity, the basic film cooled designs (Scheme 1) came out best. Even disregarding cost and simplicity, these basic film cooling schemes had the lowest ΔTOGW for the 2D-CD 4AR and 2DW 4AR (Table 11). The 2D-CD 8AR film cooled Scheme 3 was so close to the same ΔTOGW as Scheme 2 that it should be considered equal (1.36 kg or 3.0 lbs).
- For IR considerations, the best cooling scheme for all three concepts was the one that used film-impingement cooling on the highly visible nozzle parts only. This was Scheme 4 for each concept. Using film-impingement cooling for all nozzle parts (e.g., 2D-CD 4AR Scheme 2) produced higher ΔTOGW rankings.

Of the recommended schemes, the following were approved by NASA for continued analysis and conceptual design in Task III.

- 2D-CD 4AR Cooling Scheme 1 (Figure 14)
- 2D-CD 8AR Cooling Scheme 3 (Figure 20)
- 2DW 4AR Cooling Scheme 4 (Figure 25)

5.0 CONCEPTUAL DESIGN AND COOLING ANALYSIS

5.1 OBJECTIVE

The objective of this phase of the program (Task III) was to prepare preliminary conceptual layout drawings and perform more detailed cooling analysis for the three designs approved in Task II - Trade Study.

5.2 DESIGN APPROACH AND TECHNICAL REDIRECTION

Each preliminary conceptual layout was based on the flowpaths generated in Section 3.4 "Preliminary Flowpath Design." The criteria and assumptions previously discussed in Section 4.2 "Study Criteria" were used in this more detailed phase for the 2D-CD 4AR exhaust nozzle. The design would be based on structural integrity design temperatures disregarding IR goals. However, prior to initiating work for the remaining two exhaust nozzles, a technical redirection suspended further effort on the 2DW concept. Besides cooling the 2D-CD 4AR nozzle with an assumed fan air source, it was required to establish designs for cooling the 2D-CD 8AR and another 2D-CD 4AR exhaust system utilizing only air available from the J85-21 engine. Due to the high temperature of the turbine discharge air, the following approach was used for these last two configurations.

- The amount of turbine discharge air bleed behind the liner for cooling would be limited to that presently used in the J85-21 conventional round nozzle to eliminate screech section development problems.

- Due to the increased wetted area of 2-D nozzles, it was apparent more cooling air would be needed. This additional cooling air would be compressor bleed air up to a maximum of 3% of engine inlet flow (W_2) which is within customer bleed limits for the J85-21 engine.

- Higher design metal temperatures would be set for these last two designs as compared to the original 2D-CD 4AR cooled with typical turbofan air.

Within these ground rules, conceptual layouts were designed for three 2D-CD exhaust systems shown in Figures 30, 31, and 32.

5.3 DISCUSSION OF 2D-CD 4AR (FAN AIR COOLED)

5.3.1 Overall Description

One of the final products for this study program is presented in Figure 30. As shown in this preliminary conceptual layout, the 2D-CD 4AR exhaust

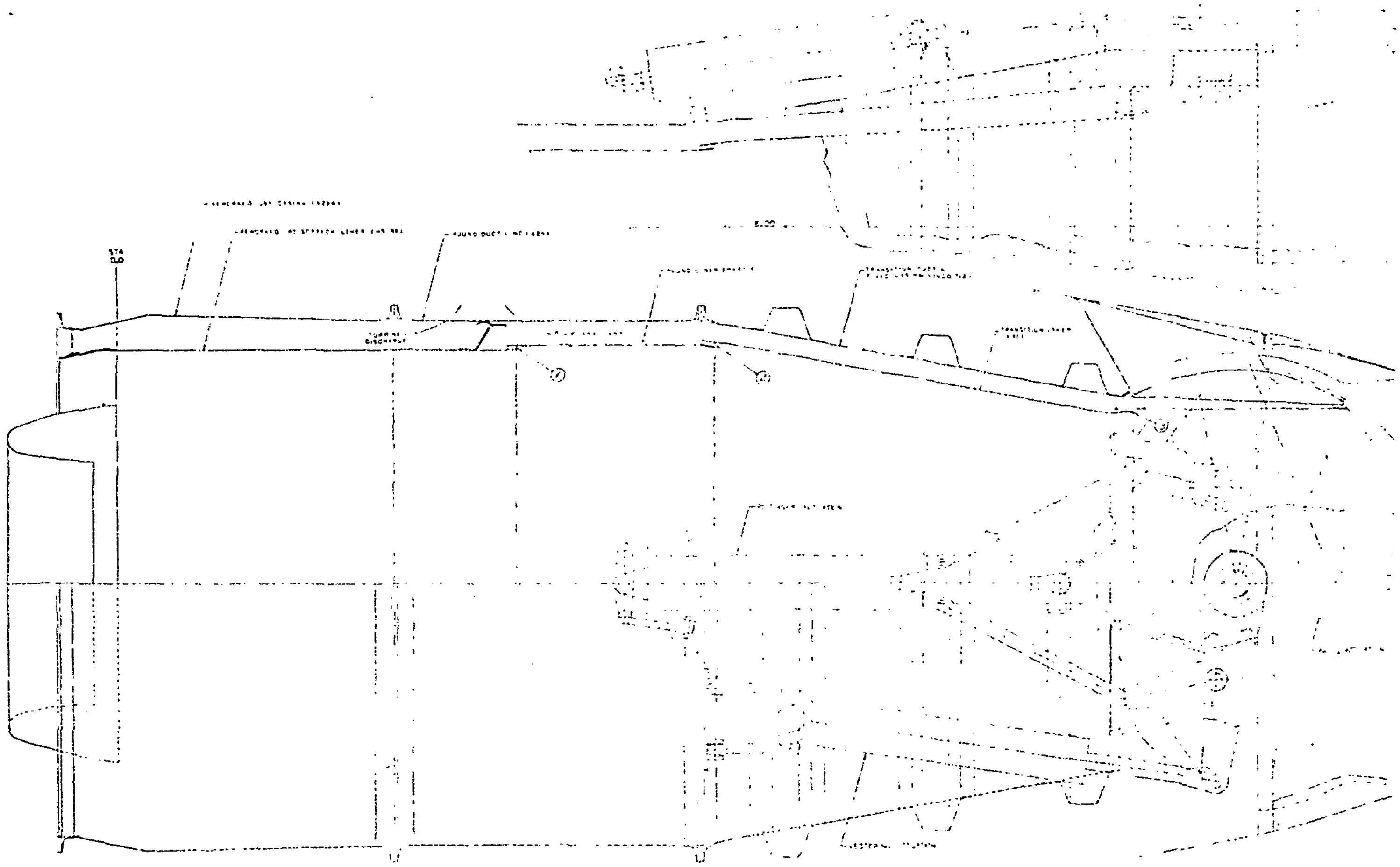

SEGMENT	FLOW	PSG	PC
(1) ROUND	.48	33.6	1.
(2) TRANSITION	.83	32.0	1
(3) GIMBAL SECTION	.5	31.2	1.
(4) CONVERGENT & SIDEWALLS	2.6	28.[illegible]	1.
(5) DIVERGENT FLAP	2.7	[illegible]0	1.

NOTE: FLOW
PSG
PC/PSG

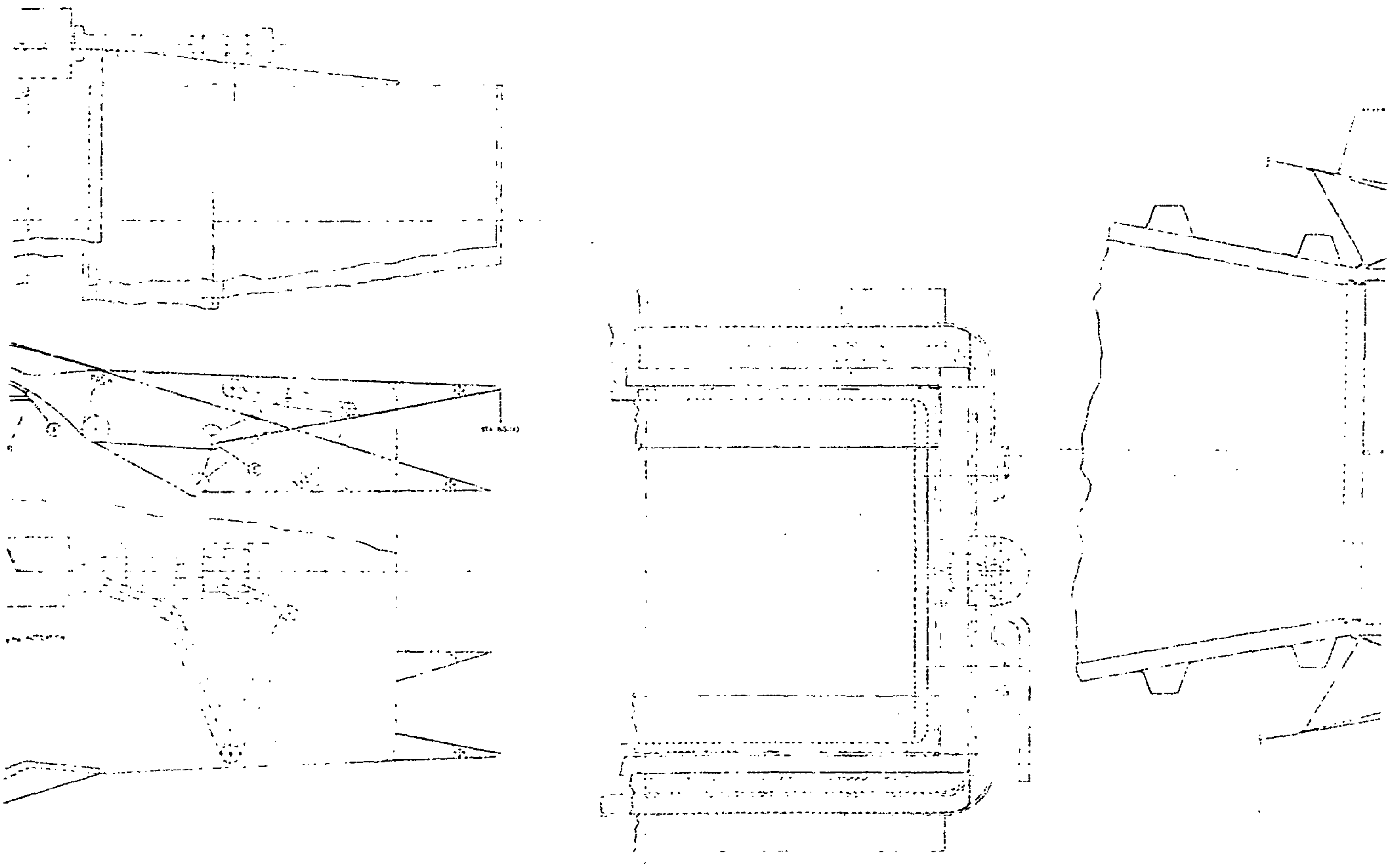

B

TABLE 2 COOLING FLOWS & PRESSURES

SLOT IDENT	MAX A/B SLS FLOW	PSG	PC/PSG	M=.90 36 (DRY) FLOW	PSG	PC/PSG	M=1.50 20K (A/B) FLOW	PSG	PC/PSG	M=2.00 35K (A/B) FLOW	PSG	PC/PSG	M=2.60 35K A/B FLOW	PSG	PC/PSG
(1) ROUND	.48	33.6	1.029	1.31	36.3	1.179	.16	39.2	1.21	.17	14.5	1.020	.80	25.3	1.105
(2) TRANSITION	.85	32.8	1.061	1.6	26.1	.231	1.47	31.2	[illegible]	.22	13.6	1.055	2.01	24.5	1.148
(3) C WALL ...	.5	36.2	1.16	.77	36.3	1.223	.6	31.6	1.225	.25	13.5	1.105	.61	23.3	1.233
(4) CONVERGENT & SIDEWALLS	2.6	20.7	1.168	3.2	36.3	1.175	1.77	25.5	1.280	1.07	12.2	1.175	2.31	21.5	1.267
(5) DIVERGENT FLAP	2.7	8.8	1.140	3.49	23.4	1.435	3.51	26.0	1.424	1.16	7.7	1.537	2.20	13.5	1.407

NOTE: FLOWS = LBS/SEC
PSG = PSIA (GAS STREAM STATIC PRESSURE)
PC/PSG = LOCAL COOLING PRESSURE/PSG (SLOT PRESSURE RATIO)

TABLE 1

DATA POINT	AXIAL STATION	T-METAL °F SLS MAX A/B	M=.90 (DRY)	M=1.50 20K (A/B)	M=2.00 35K (A/B)	M=2.60 35K (A/B)
1	0	835.	556	775.	719.	782.
2	2.00	1222	935	1175.	1170.	1153.
3	4.00	1265.	903.	1215	1190.	1188.
4	6.00	1319	886	1260	1175	1220
5	8.00	1352	955.	1299.	1225.	1278.
6	10.00	1410	925	1358.	1246.	1319.
7	12.00	1455.	903	1403	1259.	1356
8	14.00	1495	890	444	1267.	1389.
9	16.00	880	394.	641	685.	655.
10	18.00	1242.	505	909	1143.	937.
11	20.00	1373	583.	1.05	1209.	1124.
12	22.00	1452	641	1227	1249	1232
13	24.00	660.	394	629	623.	687.
14	26.00	872.	486	694.	641.	705.
15	28.00	1033	441.	981	652.	818.
16	30.00	1172	474	797.	661	919.
17	32.00	1280	504.	936	668	1010
18	34.00	1358	531	1070	673	1046.
19	36.00	1417	557	1151.	678.	1170.
20	38.00	675	425	595	548.	594.
21	40.00	1149	477.	872.	621.	910.
22	42.00	1492.	565.	1147.	690.	1150.
23	44.00	1661.	589	1274	720.	1226.
24	46.00	[illegible]	445	659	600	679
25	48.00	850 (1222)	461 (677)	718 [illegible]	675 (1024)	750 [illegible]
26	50.00	1150 (1037)	52? (664)	9?? (1129)	622 (629)	977. (711)
27	52.00	1408 (966)	6?8 (695)	1169 (1010)	758 (668)	1176 (83?)
28	54.00	9?5 (1087)	4?5 (49?)	876 (925)	549 (682)	993 (92?)
29	56.00	770 (1134)	473 (525)	707 (1133)	637 (744)	703 [illegible]
30	58.00	965 (1579)	525. (561)	856 (1120)	676 (883)	858 [illegible]
31	60.00	1149	558	1001.	747.	1012.
32	62.00	1327	610	1154	822.	1161.
33	64.00	1402	645	1293.	893.	1300

NOTE: TEMPERATURES IN PARENTHESIS ( ) ARE FOR SIDEWALLS

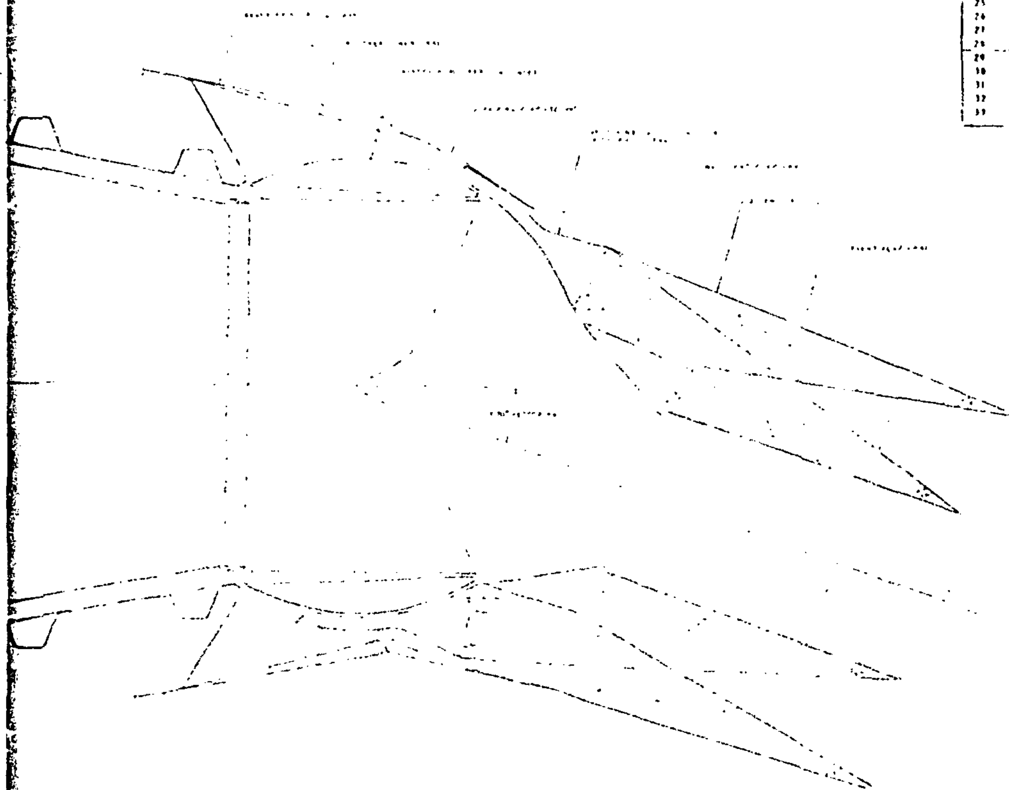

1 in. = 2.54 cm
1 psi = 36.89 Pa
1 lb/sec = 14.54 kg/sec
K = 5/9° R

Figure 36. [illegible] 4AR Fan Air Cooled.

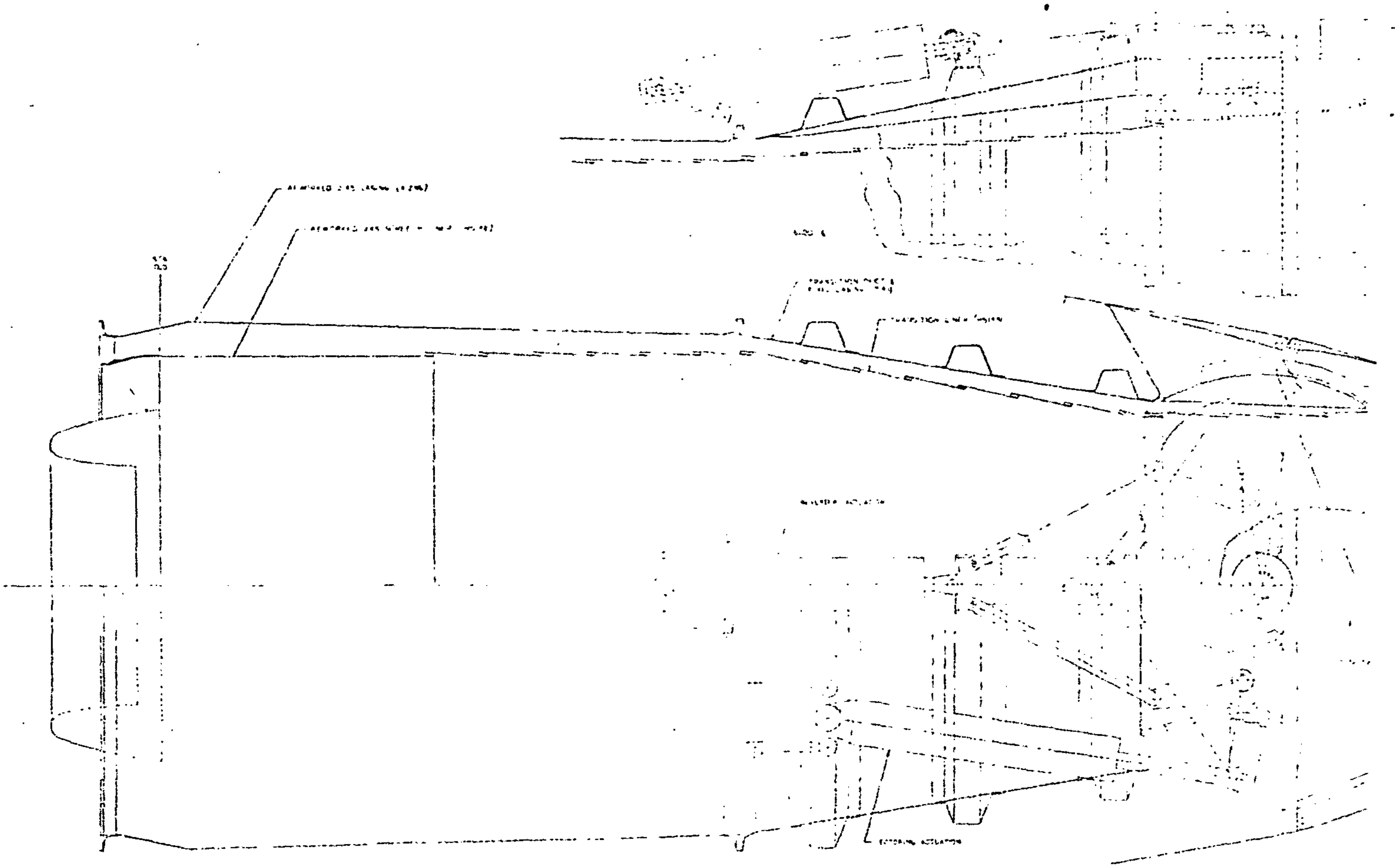

	[illegible]			[illegible]
	FLOW	PC/PSG	TC	FLOW
LINER SLOTS (TURB. DISCH.)	12.36	1.379	50.6	[illegible]
DIVERGENT FLAP (COMP. BLEED)	1.72	6.4	967.0	[illegible]

NOTE: FLOWS - Lbs/Sec
PC - PTSI FOR LINER, PSI FOR FLAP
PSG - GAS STREAM STATIC PRESSURE AT LI[illegible]
FOR LINER OR AT THROAT FOR FLAP.

1 in. = 2.
1 psi = 3(
1 lb/sec =
K = 5/9(

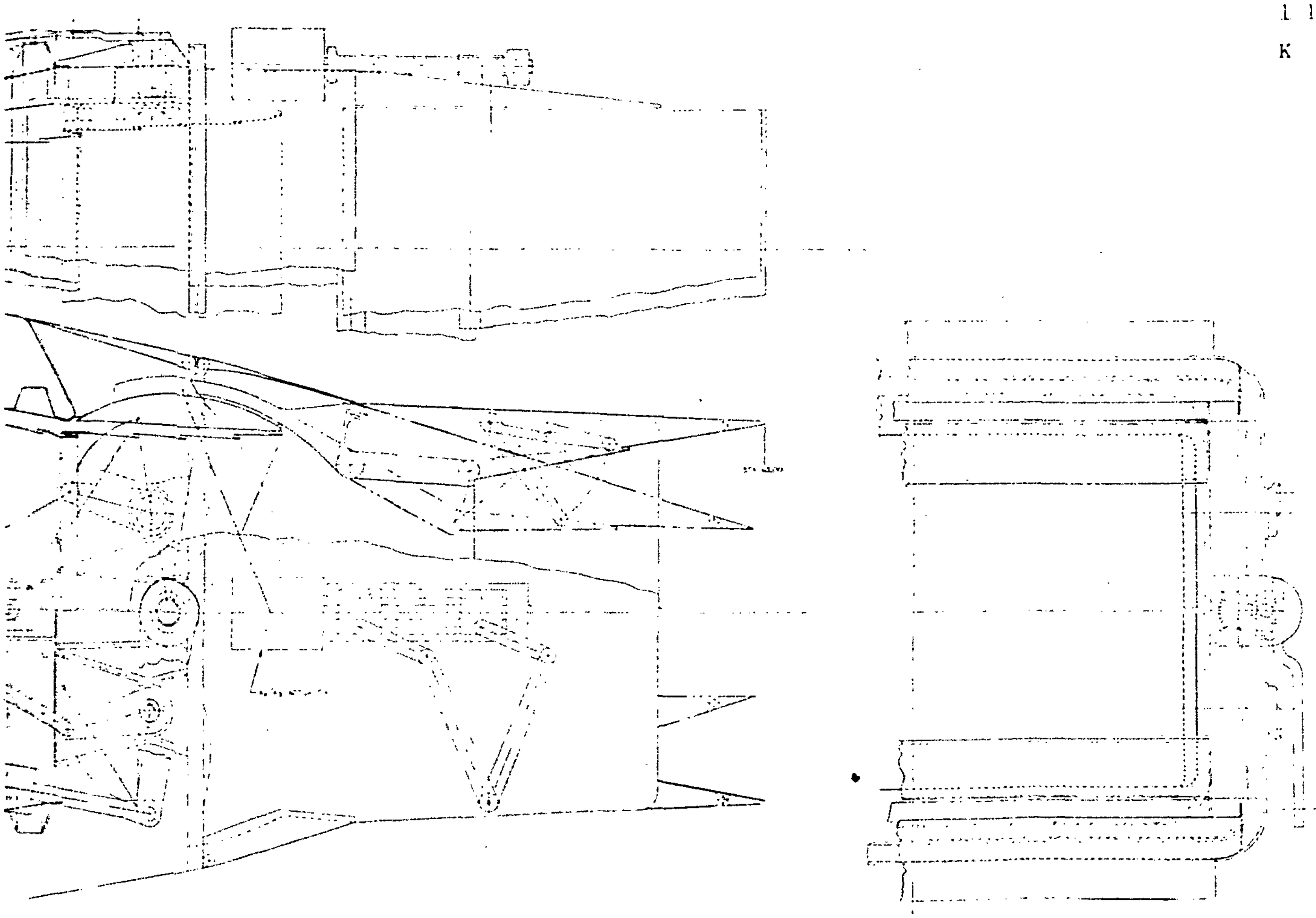

C..NG FLOWS & PRESSURES

LS (A/B)			M 0.9 @ 10K (DRY)			M=1.5 @ 20K (A/B)			M=1.6 @ 35K (A/B)			M=.8 @ 35K		
.OW	PC PSI	PC	FLOW	PC PSI	PC	FLOW	PC PSI	PC	FLOW	PC PSI	PC	FLOW	PC PSI	PC
32	1.160	39.5	0.75	[illegible]	4.8	0.6	1.37	65.7	[illegible]	1.350	[illegible]	0.16	1.160	29.7
20	6.1	112.1	1.78	5.8	121.1	1.31	6.0	128.1	.12	5.8	45.5	09	6.2	85.3

.MID EXIT

1.54 cm

36.89 Pa

= 14.54 kg/sec

1° R

TABLE I							
		T-METAL °F					
DATA POINT	AXIAL STATION	M=1.3 @SL (A/B)	SLS MAX A/B	M=.9 @10K (DRY)	M=1.5 @22K (A/B)	M=.8 @35K (A/B)	M=1.6 @35K (A/B)
1	0.	1523	1348.	1345.	1402	870.	124..
2	2.0	1589	1581	1345.	1591.	1535.	1563.
3	4.0	1652	1635	1345	1649.	1554.	1610.
4	6.0	1700	1661	1545	1695	1586.	1651.
5	8.0	1707	1689	1345	1703.	1595.	1640
6	10.0	1706	1686	1345.	1701	1588	1652.
7	12.0	1702	1684	1345.	1698	1597.	1650.
8	14.0	1708	1691	1345	1703	1602	1663.
9	16.0	1708.	1690	1345.	1705	1601	1665.
10	18.0	1711.	1694.	1345	1708.	1604.	1668.
11	20.0	1702	1687.	1345.	1700.	1607	1663.
12	22.0	1703	1687	1345	1701	1604	1664.
13	24.0	1700.	1677	1345.	1699.	1609	1665.
14	26.0	1702.	1688	1345.	1700.	1609.	1667.
15	28.0	1702.	1688	1325.	1699.	1610	1666.
16	30.0	1707	1689	1345	1699.	1609	1665
17	32.0	1702.	1688	1345.	1708.	1610	1666
18	34.0	1704.	1691.	1345.	1702.	1610.	1668
19	36.0	1705.	1691	1345	1702.	1612.	1668.
20	38.0	617	16.6	1345	1629	1587	1694.
21	40.0	1708	1697	1345	1738	1625.	1675.
22	42.0	1698.	1697	1345.	1701.	1637.	1677
23	44.0	1704.	1690.	1345	1733.	1641.	1680.
24	46.0	1445	1385	1140	1475	1710	1329.
25	48.0	1540	1492.	1199	1527.	1301.	1458
26	50.0	1611	1543.	1195.	1583.	1310.	1501.
27	52.0	1655.	1580.	1194	1623.	1325.	1532
28	54.0	1181	1474	1055	1477	1265	1421.
29	56.0	1577	1509	1090.	1559.	1322	1492
30	58.0	1016.	1548.	1098	1599.	1338.	1523
31	60.0	232	1126	801.	1242.	1006	1180.
32	62.0	587	1520.	976	1621.	1417	1540.
33	64.0	799	1760.	1069	1834.	1653	1775.

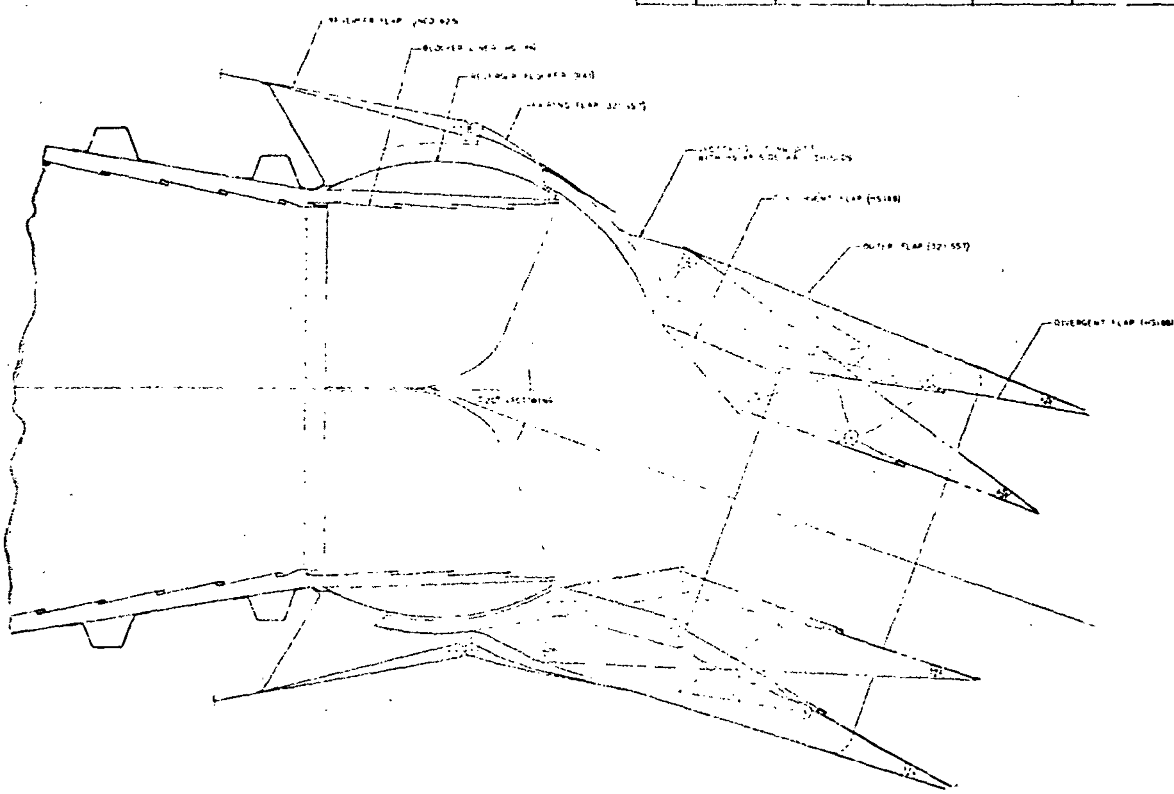

Figure 31. 385 2D-CD -AR Turbine Discharge and Compressor Bleed Cooled.

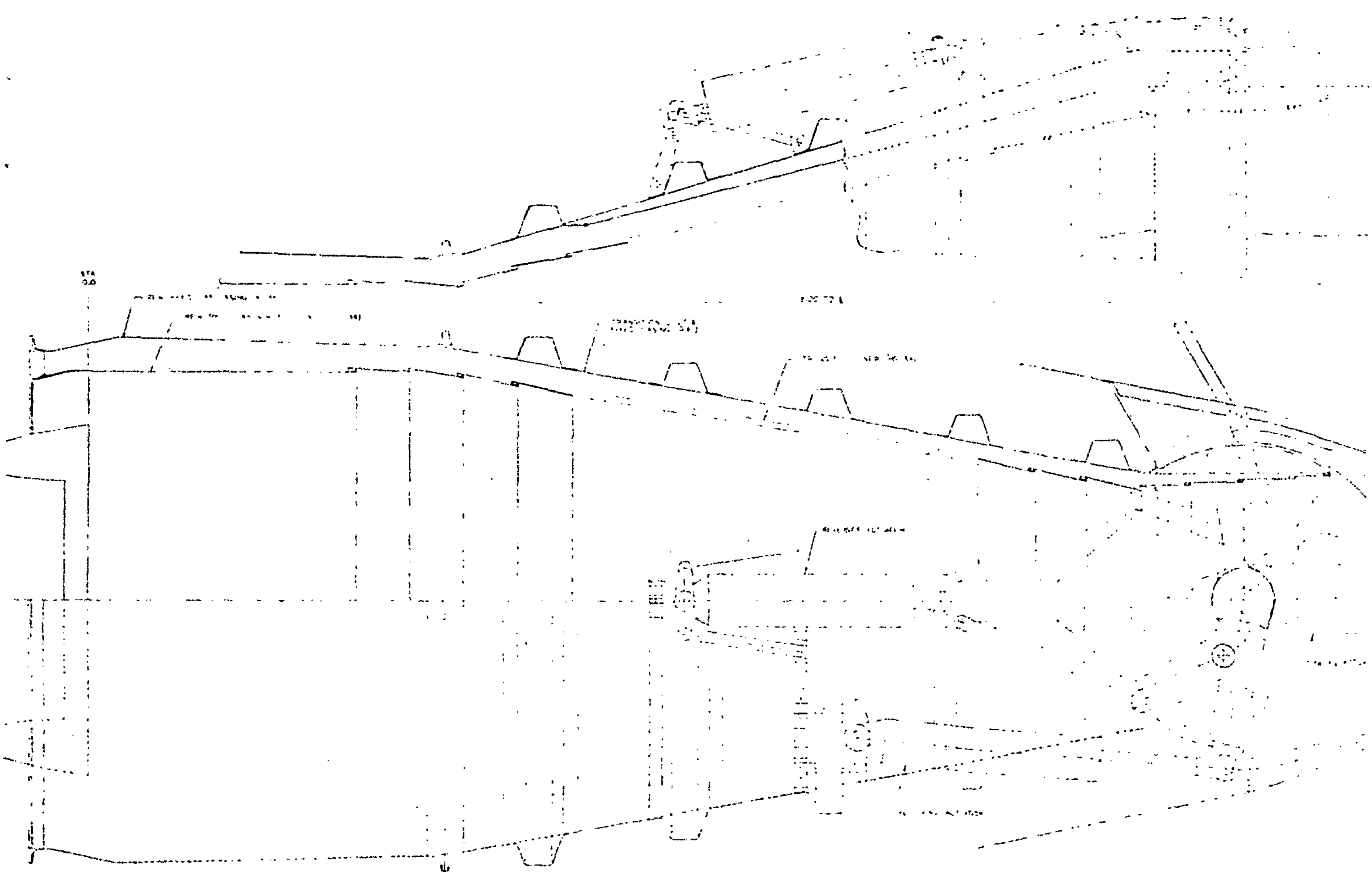

TABLE 2 COOLING FLOWS & PRESSURES	M=1.9 @ 5K (A/B)			5.5 A B			M= [illegible] 30 [illegible]			M=1.5 @ 20K (A/B)			M= 0.8 @ 35K (A/B)			M= 1.6 @ 35K		
	FLOW	PC/PSG	PC	FLOW	PC/PSG	PC	FLOW	PC/PSG	PC	FLOW	PC/PSG	PC	FLOW	PC/PSG	PC	FLOW	PC/PSG	PC
LINER SLOTS (TURB. DISCH.)	12.38	1.374	58.6	6.95	1.386	39.5	6.69	1.35	41.8	9.61	1.37	45.7	5.46	1.356	16.5	6.20	1.388	29.7
CONVERGENT & DIVERGENT FLAP (COMP. BLEED)	2.37	6.1	167.8	4.47	6.1	112.1	4.76	5.8	171.1	1.81	6.0	178.1	.71	5.8	41.3	1.22	6.2	85.[illegible]

NOTE: FLOWS = Lbs/Sec
PC = PSI FOR LINER, PS3 FOR FLAP
PSG = GAS STREAM STATIC PRESSURE AT LINER EXIT FOR LINER OR AT THROAT FOR FLAP.

1 in. = 2.54 cm

1 psi = 36.89 Pa

1 lb/sec = 14.54 kg/sec

K = 5/9° R

DATA POINT	AXIAL STATION	M=[illegible] (A.B)
1	0	1607
2	2	1567
3	4	1647
4	6	1591
5	8	1699
6	10	1700
7	12	1695
8	14	1796
9	16	1707
10	18	1703
11	20	1701
12	22	1794
13	24	1704
14	26	1702
15	28	1704
16	30	1703
17	32	1703
18	34	1704
19	36	1706
20	38	1707
21	40	1709
22	42	1700
23	44	1712
24	46	1717
25	48	1548
26	[illegible]	1532
27	[illegible]	1595
28	54	1697
29	56	[illegible]
30	58	1697
31	60	1259

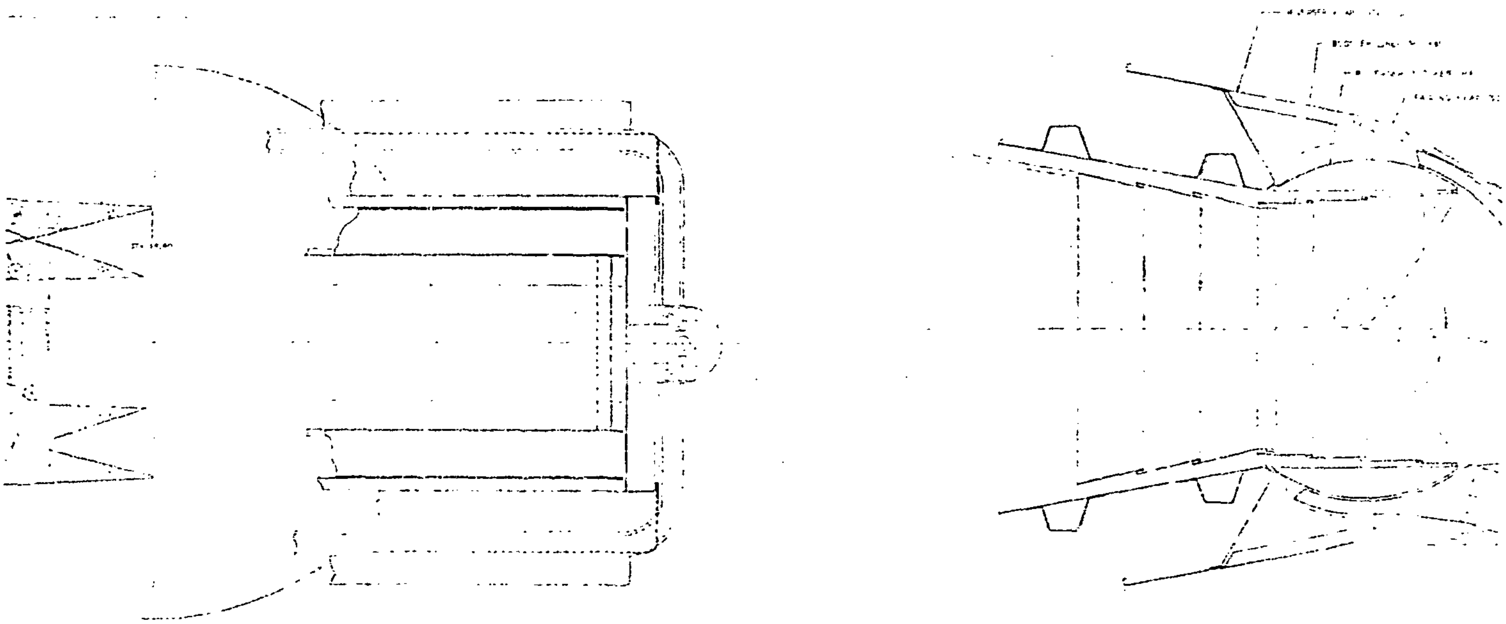

Figure 32. J85 2D-CD SAR Tu
Cooled.

? 20K (A/B)		M- 0.8 @ 35K (A/B)			M- 1.6 @ .9K		
PC/PSG	PC	FLOW	PC/PSG	PC	FLOW	PC/PSG	PC
1.37	45.7	2.40	1.336	16.3	6.20	1.388	29.7
6.0	128.1	.71	5.8	45.3	1.22	6.2	85.[illegible]

TABLE 7

DATA POINT	AXIAL STATION	T - METAL °F					
		M=1.6@5L (A/B)	SLS MAX A/B	M=.9@10K (DRY)	M=1.5@20K (A/B)	M=.8@35K (A/B)	M=1.6@35K (A/B)
1	0	1607	1508	1345	1544	1231	1433
2	2	1582	1580		1590	1536	1543
3	4	1647	1632		1665	1578	1606
4	6	1192	1674		1668	1509	1648
5	8	1699	1668		1697	1610	1664
6	10	1700	1687		1699	1612	1645
7	12	1693	1681		1693	1606	1658
8	14	1796	1690		1705	1606	1666
9	16	1767	1691		1702	1606	1668
10	18	1703	1688		1699	1605	1666
11	20	1701	1666		1698	1606	1665
12	22	1786	1691		1707	1609	1669
13	24	1724	1687		1701	1609	1668
14	26	1702	1684		1700	1609	1666
15	28	1706	1692		1705	1611	1669
16	30	1705	1619		1701	1611	1667
17	32	1705	[illegible]		1703	1613	1670
18	34	1764	1690		1701	1614	1669
19	36	1706	1691		1703	1615	1671
20	38	1797	1693		1705	1616	1673
21	40	1789	1691		1700	1719	1678
22	42	1708	1698		1709	1633	1681
23	44	1712	1791		1712	1654	1683
24	46	1717	1705	1345	1717	1725	1686
25	48	1348	1282	1061	1345	1134	1296
26	50	1552	1426	1189	1522	1309	1466
27	52	1595	1339	1197	1581	1341	1515
28	54	1047	[illegible]	777	1029	960	1039
29	56	447	[illegible]	977	1476	1269	1425
30	58	1697	1664	1093	1722	1540	1673
31	60	159	[illegible]	1153	1891	1727	1840

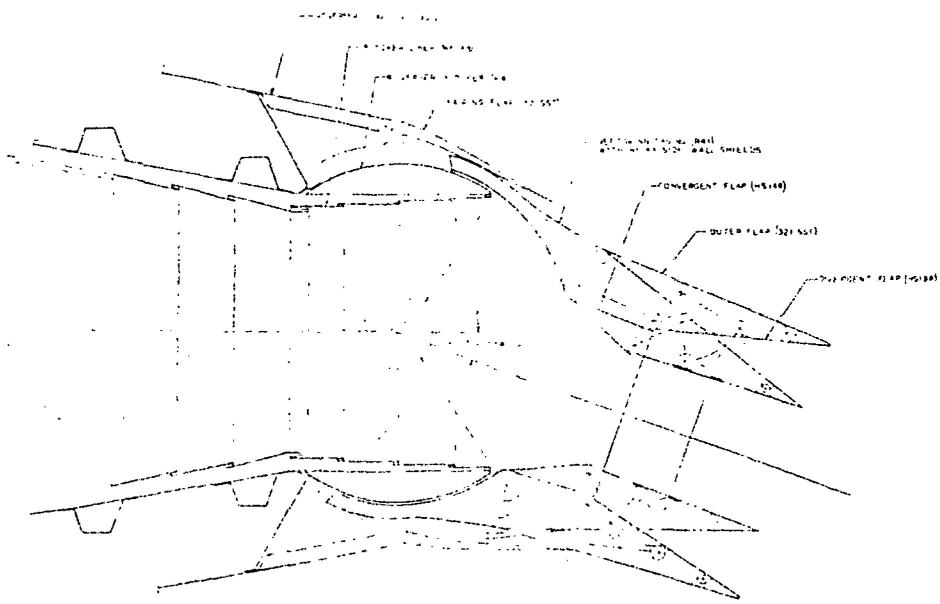

Figure 32. J85 2D-CD SAR Turbine Discharge and Compressor Bleed Cooled.

system is designed to be cooled with turbofan air. The mechanical features of this design provide the potential for meeting the future needs of highly maneuverable aircraft. Convergent and divergent flaps are interconnected and scheduled to provide the required area and expansion ratios at key mission cycle points. The flaps are driven by a pair (one on each side) of hydraulic motors and interconnecting linkage.

The entire aft casing which houses the flaps is mounted on a pair of bearings to allow ±0.349 radians (±20°) of vectoring. The vectoring is accomplished by a pair of hydraulic actuators connected to a crank mechanism. This gimbaled vectoring motion turns the flow subsonically, maintaining high performance. This 2D-CD exhaust system also features a thrust reverser located just downstream of the transition liner and upstream of the nozzle throat. The reverser is composed of two reverser blockers which are bearings mounted inside the fixed casing. The blockers are driven by a pair of hydraulic actuators and interconnecting linkage and crack mechanisms.

The transition duct and fixed casing comprise the main structural components which house the transition liner (transitions flowpath from round to rectangular) and reverser blockers. Other main components (i.e., aft vectoring casing, vectoring actuators, reverser actuators, etc.) attach to this transition duct and fixed casing. All major loading (including maneuver and thrust vectoring loads) are transmitted through this main structure to the engine mounting system.

5.3.2 Materials

The materials used in the fan air cooled 2D-CD 4AR nozzle are similar to those used in the ADEN demonstrator due to the similarity in design metal temperatures. All hot gas flowpath parts downstream of, and including, the transition liner are made of René 41. The engine interfacing round duct and screech liner are reworked existing J85-21 components. The short round duct and liner sections directly upstream of the transition are made of Inconel 625 and Hastelloy X, respectively. The round duct and liner, due to their geometric advantage over transition and rectangular sections, can effectively utilize the lower strength and less costly Inconel 625 or Hastelloy X instead of the very high strength René 41.

The two major structural casings (transition and vectoring casings) are made of Inconel 718 which has very high strength at a somewhat lower temperature capability as compared to René 41.

All low temperature exterior fairings (outer boattail flap, etc.) would use 321 Stainless Steel which is a very cost effective material.

Table 14 summarizes the hot flowpath materials and design temperatures.

Table 14. Flowpath Material Summary.

Component	Material	Design Temperature
Round Liner	Hastelloy X	1061 K (1450° F)
Transition Liner	René 41	1061 K (1450° F)
Blocker Liner	René 41	1061 K (1450° F)
Convergent Flap	René 41	1061 K (1450° F)
Divergent Flap	René 41	1061 K (1450° F)
Sidewalls	René 41	1033 K (1400° F)

5.3.3 Cooling Scheme

The cooling scheme for this fan air cooled 2D-CD 4AR exhaust system was based on the assumptions and results similar to those outlined in Section 4.0. With reference to Figure 30, the cooling analysis analytical results are shown on the layout drawing in Tables 1 and 2. This cooling system assumed that an external cooling source was available and capable of supplying air at temperature and pressure conditions similar to recent advanced turbofan engines.

For analysis of this design, the turbine discharge air for the J85-21 engine that is normally carried behind the liner for cooling would be dumped overboard aft of the screech section in order to keep the present screech liner conditions intact. The externally supplied cooling air is introduced into the liner as shown. A ring and seal separates the simulated fan air from the turbine discharge air. The liner cooling is accomplished by Film Slots 1, 2, and 3 and backside convection. The rectangular section (convergent-divergent flaps and sidewalls) is cooled by Film Slots 4 and 5. The design point (maximum metal temperature) condition for this design is sea level static Maximum A/B. The results of other off-design points are also shown on the drawing tables (Figure 30).

Table 15 summarizes these results.

Table 15. 2D-CD 4AR (Fan Air Cooled) Cooling Flow Summary.

Cycle Case	PT_c/PT_8	$W_c = \% \ W_8$
Maximum A/B SLS (Design Point)	1.039	14.5
(Dry M = 0.9 at 3048 m (10,000 ft)	1.15	21.2
(A/B M = 1.5 at 6096 m (20,000 ft)	1.14	19.8
(A/B) M = 0.8 at 10668 m (35,000 ft)	1.028	14.4
(A/B) M = 1.6 at 10668 m (34,000 ft)	1.12	18.2

PT_c/PT_8 = Coolant total pressure at inlet to liner/nozzle throat total pressure indicates overall coolant pressure ratio.

W_c = Coolant flow as a percent of total engine flow at nozzle throat.

5.4 DISCUSSION OF 2D-CD 4AR (TURBINE DISCHARGE AND COMPRESSOR BLEED COOLED)

5.4.1 Overall Description

The preliminary conceptual design layout for this exhaust system is shown on Figure 31 (GE Drawing 4013057-884). The mechanical features of this exhaust system, including thrust reverser and gimbaled vectoring, are the same as previously discussed in Section 5.3.1. The main difference is in the material used and the cooling scheme arrangement as discussed in the following sections.

5.4.2 Materials

The materials used for the majority of components in this design have high temperature capability greater than 1200 K (1700° F). It was necessary in this design to raise the metal temperatures from those of the fan air cooled 2D-CD 4AR exhaust system due to the high temperature, 1002 K (1345° F), of the turbine discharge cooling air. All hot flowpath surfaces including liners, flaps, and sidewalls are made of HS188 as indicated on the layout drawing. All structural casings including fixed transition casing, blocker, and aft vectoring casing are made of René 41 which has high strength at the temperatures needed to carry the turbine discharge cooling air.

5.4.3 Cooling Scheme

The cooling scheme for the 2D-CD 4AR exhaust nozzle cooled with turbine discharge air and compressor bleed air is similar to that of the fan air cooled design except that more afterburner liner and nozzle slots were used in Figure 31. The liner is a multislot arrangement with film slots being spaced every 5 cm (2.0 inches). The liner is cooled with turbine discharge air bled behind the liner and past the screech section as in the conventional J85-21 exhaust system.

The turbine discharge air is capable of cooling all hardware from the flameholder downstream to the aft end of the convergent flap, which is the nozzle throat station (A_8). The divergent flap was cooled with compressor bleed air with two film slots (i.e., one of the nozzle throat and one near the middle of the divergent flap). The sidewalls aft of the convergent flaps utilize a slot at the throat for film cooling.

Compressor bleed air used for cooling the aft end of the nozzle must be routed from the bleed ports back to the aft vectoring casing. The routing involved is not included on the conceptual layout drawing. Once inside the aft vectoring casing, the air is routed by baffles behind the convergent and divergent flaps to the individual film slots.

For the cooling analysis, J85-21 engine turbine discharge and compressor bleed coolant conditions were used. The principal results are tabulated as follows in Table 16, and in more detail in Figure 31.

Table 16. 2D-CD 4AR (Turbine Discharge and Compressor Bleed Cooled) Cooling Flow Summary.

Cycle Case	Turbine Discharge		Compressor Bleed	
	PT_c/P_{SG}	$W_c = \% W_8$	PS_3/P_{SG}	$W_c = \% W_2$
(A/B) M=1.0 at SL	1.379	14.88	6.1	2.18
Maximum A/B SLS	1.380	14.86	6.1	2.26
Dry M=0.9 at 3048 m (10,000 ft)	1.15	11.60	5.8	2.24
A/B M=1.5 at 6096 m (20,000 ft)	1.37	15.00	6.0	2.16
A/B M=0.8 at 10668 m (35,000 ft)	1.356	14.93	5.8	2.41
A/B M=1.6 at 10668 m (35,000 ft)	1.388	14.82	6.2	2.21

PT_c/P_{SG} = Coolant total pressure at liner inlet/gas stream static pressure at liner exit.

$Wc = \% W_8$ = Turbine discharge coolant flow as a percent of total engine flow at nozzle throat.

PS_3/P_{SG} = Compressor bleed static pressure/gas stream static pressure at throat.

$Wc = \% W_2$ = Compressor bleed coolant flow as a percent of total engine inlet flow.

5.5 DISCUSSION OF 2D-CD 8AR (TURBINE DISCHARGE AND COMPRESSOR BLEED COOLED)

5.5.1 Overall Description

The preliminary conceptual design layout (GE Drawing 4013057-883) for this exhaust system is shown in Figure 32. The mechanical features of this design are the same as the two previously discussed designs (Section 5.3.1). The external configuration appearance of this design is different due to the wider aspect ratio - 8AR vs 4AR for the other designs. This wider configuration produces a slightly shorter overall exhaust system length due to the reduced length nozzle flaps. The relative side view height is also reduced.

All nozzles have the same burning length (plane of flameholder to nozzle throat) and nozzle throat areas. This nozzle throat width is larger to produce the required area with a reduced height and resulted in a larger transition section wetted area for cooling.

5.5.2 Materials

The materials utilized for this concept are the same as those previously discussed for the 4AR turbine discharge and compressor bleed cooled exhaust system. All hot flowpath materials are HS188 as required by the high metal temperatures.

5.5.3 Cooling Scheme

The cooling scheme for this 2D-CD 8AR exhaust nozzle is similar to the 2D-CD 4AR design discussed in Section 5.4.3. The 2D-CD 8AR design shown in Figure 32 uses a multislot liner cooling arrangement. Turbine discharge cooling air is capable of cooling only the surface area from the flameholder to the liner exit. Everything downstream of the liner exit was cooled with compressor bleed air. The "Trade Study Analytical Summary" in Table 10 gives a comparison of the wetted areas for the 4AR and 8AR flowpaths.

Liner slots for this design are spaced every 5 cm (2.0 inches). Closer spacing between slots may improve cooling efficiency but optimization was considered beyond the scope of this preliminary study. This should be considered in a future demonstrator development program taking into account cooling efficiency, structural efficiency, complexity, and program cost effectiveness. The liner design temperatures were met using an amount of turbine discharge air consistent with the present J85-21 conventional exhaust system as shown in the tables of Figure 32.

Compressor bleed air was used to cool all hardware downstream of the liner exit. This is accomplished using two slots, one at the liner exit formed by the gap between the reverser blocker and the circular converging section of the vectoring casing and the other at the nozzle throat using bleed air fed down the backside of the convergent flap.

For the cooling analysis, the assumed design point was considered M = 1.0 at sea level based on the existing J85-21 design point. This design condition differs from the fan source design because the combination of turbojet supplied coolant pressures and temperatures produces maximum metal temperatures at M = 1.0 at sea level. For this design, analytical iterations resulted in using 3% compressor bleed with the maximum divergent flap temperature about 1211 K (1720° F). After arriving at the cooling flows and cooling distributions, the off-design case temperatures were determined. The results indicated that a higher maximum metal temperature of 1227 K (1750° F) was required at M = 1.5 at 6096 m (20,000 ft). In addition, the cooling flows at the off-design points very slightly exceeded the previously set 3% limit.

The material used for this divergent flap was HS188 which is capable of operating at 1227 K (1750° F). The effects of slightly exceeding the previously set design temperatures or bleed flow was not assessed.

The cooling results are summarized in Table 17.

Table 17. 2D-CD 8AR (Turbine Discharge and Compressor Bleed Cooled) Cooling Flow Summary.

Cycle Case	Turbine Discharge		Compressor Bleed	
	PT_c/P_{SG}	$W_c = \% W_8$	PS_3/P_{SG}	$W_c = \% W_2$
(A/B) M = 1.0 at SL	1.379	14.88	6.1	3.00
Maximum A/B at SLS	1.380	14.91	6.1	3.15
(Dry) M=0.9 at 3048 m (10,000 ft)	1.15	11.49	5.8	3.08
(A/B) M=1.5 at 6096 m (20,000 ft)	1.37	15.02	6.0	2.98
(A/B) M=0.8 at 10668 m (35,000 ft)	1.356	15.15	5.8	3.29
(A/B) M=1.6 at 10668 m (35,000 ft)	1.388	14.75	6.2	3.03

PT_c/P_{SG} = Coolant total pressure at liner inlet/gas stream static pressure at liner exit.

$W_c = \% W_8$ = Turbine discharge coolant flow as a percent of total engine flow at nozzle throat.

PS_3/P_{SG} = Compressor static bleed pressure/gas stream static pressure at throat.

$W_c = \% W_2$ = Compressor bleed coolant flow as a percent of total engine inlet flow.

5.6 TECHNOLOGY RISKS

During the development of the three preliminary conceptual layouts, technology areas were identified which require further investigation, evaluation, and/or special design approaches. These areas were identified as risks due to their need for special design attention or for the lack of a solid technological data base. These areas are summarized as follows.

5.6.1 Sealing

The conceptual designs utilize seals for both hot gas leakage control and coolant flow distribution control. Special design attention must be applied to sealing especially in the nozzle concepts studied in this program which have reverser blockers and gimbaled vectoring that require seals between moving parts. The preliminary nature of this program did not address the actual design details. Inadequate sealing would result in decreased engine thrust caused by leakage of heated, high pressure air.

5.6.2 2-D Structural Efficiency

Rectangular exhaust system structures are inherently less efficient than conventional round nozzles. The 2-D nozzles generally require a structural framework and interconnecting flat panels. Potential problem areas such as large deflections due to pressure, thermal gradients, and severe vibrations of the flat panels and structural frames require design approaches that are not usually associated with conventional round nozzles. Advanced exhaust systems also impose severe casing loads, moments, etc., due to combined maneuver and thrust vectoring effects. The preliminary conceptual designs of this program must address this technology when a detailed hardware design program is initiated.

5.6.3 Cooling

Advanced 2-D exhaust systems demand effective cooling flow distribution and control to ensure a successful flightweight high performance design. This critical cooling also includes the analytical methodology required in the detailed design. Previous experience in turbine cooling and exhaust system cooling has provided methods of analyses applicable to the 2-D exhaust system cooling design. This methodology was applied to the successful augmented deflector exhaust nozzle (ADEN) full-scale flightweight demonstrator design. During the ADEN tests, unanticipated hot streaks existed on the upper and lower flaps associated with secondary flow fields which produced a hot gas split plume exiting the nozzle. This indicates the need for a solid technological data base explicitly for 2-D exhaust system cooling. This base should include three-dimensional and secondary flow effects, heat transfer characteristics and mechanisms, effects of shocks, flow turning, and performance plus the applicational methodology for the future 2-D exhaust system designs.

5.6.4 Aeroelastic Instability

Most new nozzles encounter operating regimes where primary flow instability is capable of coupling with natural nozzle elasticity to yield a destructive cyclic mode. These areas have been identified in C-D nozzles for the J79, J93, GE4, and F101 nozzles. Regions where these instabilities exist are predictable through analysis of test data and are considered in all new nozzle designs. Two-dimensional geometry may result in different modes of instability and should be carefully evaluated in any new design.

6.0 SUMMARY OF RESULTS

Thirty-one nonaxisymmetric exhaust nozzle designs were categorized as belonging to one of three generic groups: two-dimensional convergent-divergent (2D-CD), two-dimensional asymmetric (2DA), or two-dimensional wedge (2DW). The gimbaled hinge 2D-CD emerged as the best study concept based on totalled rankings of static performance, weight, and design criteria. The 2DW was selected as the second study concept because of unique problem areas. The 2DA nozzle was not selected because a substantial data base existed for 2DA nozzles from the ADEN program.

Increases in cooling system complexity result in increased propulsion system weight and reduced nozzle performance. Both effects increase aircraft TOGW. In general, the simplest (predominantly film cooling) arrangement produced the smallest TOGW increase for the concepts evaluated. Consequently, film cooling was selected for application where nozzle structural integrity was the prime design criteria. When lower surface temperatures are required for reduction of infrared signatures, more complex approaches such as impingement film should be utilized.

The cooling flow source has a significant impact on cooling system design due to variations in coolant flow pressures and temperatures. As an example, cooling flow supplied by the J85 turbine discharge and compressor bleed required four times the number of liner cooling slots compared to a system designed for a typical fan air source.

Three J85-21 exhaust system layouts were completed predominantly using film cooling and the pivoting hinge flap 2D-CD nozzle concept. These include:

Aspect Ratio	Coolant Source
4.0	Fan
4.0	Turbine Discharge and Compressor Bleed
8.0	Turbine Discharge and Compressor Bleed

This study indicates that the pivoting* 2D-CD is a viable and structurally sound exhaust system. It is recommended that further design definition continue culminating in full-scale test hardware.

* "Gimbaled" is being replaced by "pivoting" which more accurately represents the vectoring motion.

7.0 APPENDIX

7.1 COOLING METHODOLOGY

Previous cooling experience and methodology in afterburner and exhaust system cooling was utilized to analyze the three preliminary conceptual designs. This analysis required estimating cooling flows needed to meet the design point temperatures, determining off-design point coolant flows, and subsequent metal temperatures for these off-design point flows. Existing time-sharing computer programs used in other successful cooling design programs (ADEN, F101X, JTDE) were used to improve the analytical efficiency of the normally time-consuming calculations. The sections below describe the heat transfer model, flow balance computer program, and heat transfer expressions used to define nozzle cooling requirements, and reach design objectives.

7.2 HEAT TRANSFER MODEL

Each of the three conceptual designs was modeled in the time sharing program, PORTENO, for calculating metal temperatures. The exhaust system flowpath parameters, both hot gas and coolant, were modeled in this program at 5 cm (2.0 inches) axial increments starting at the plane of the flameholders downstream to the end of the exhaust system. (The last data point was actually beyond the end of the divergent flap.) The input parameters for each data point required the area and perimeter of the hot flowpath and coolant flowpath (liner gap).

The axial location of each film slot was also input so that the characteristic dimension (x) for heat transfer coefficients and film effectiveness could be calculated for each data point downstream of the film slot.

Other fixed geometry input required in the cooling model included an indicator for the type of preprogrammed cooling slot or screech hole pattern for determining film effectiveness. Figure 33 shows the two types of film effectiveness curves that were used for these conceptual designs. Any subsequent calculations for the previously located slots or holes would use the film effectiveness values for one of the two curves shown on Figure 33. All slots of these designs used the film slot curve while the screen flow near the flameholder used the screech hole curve.

The axial station location of the nozzle throat was used for calculating the sinusoidally increasing gas temperature (T_G) distribution from the flameholder to the nozzle throat.

The remaining input required to complete the cooling model involves J85-21 engine cycle data for the design point or off-design point condition being

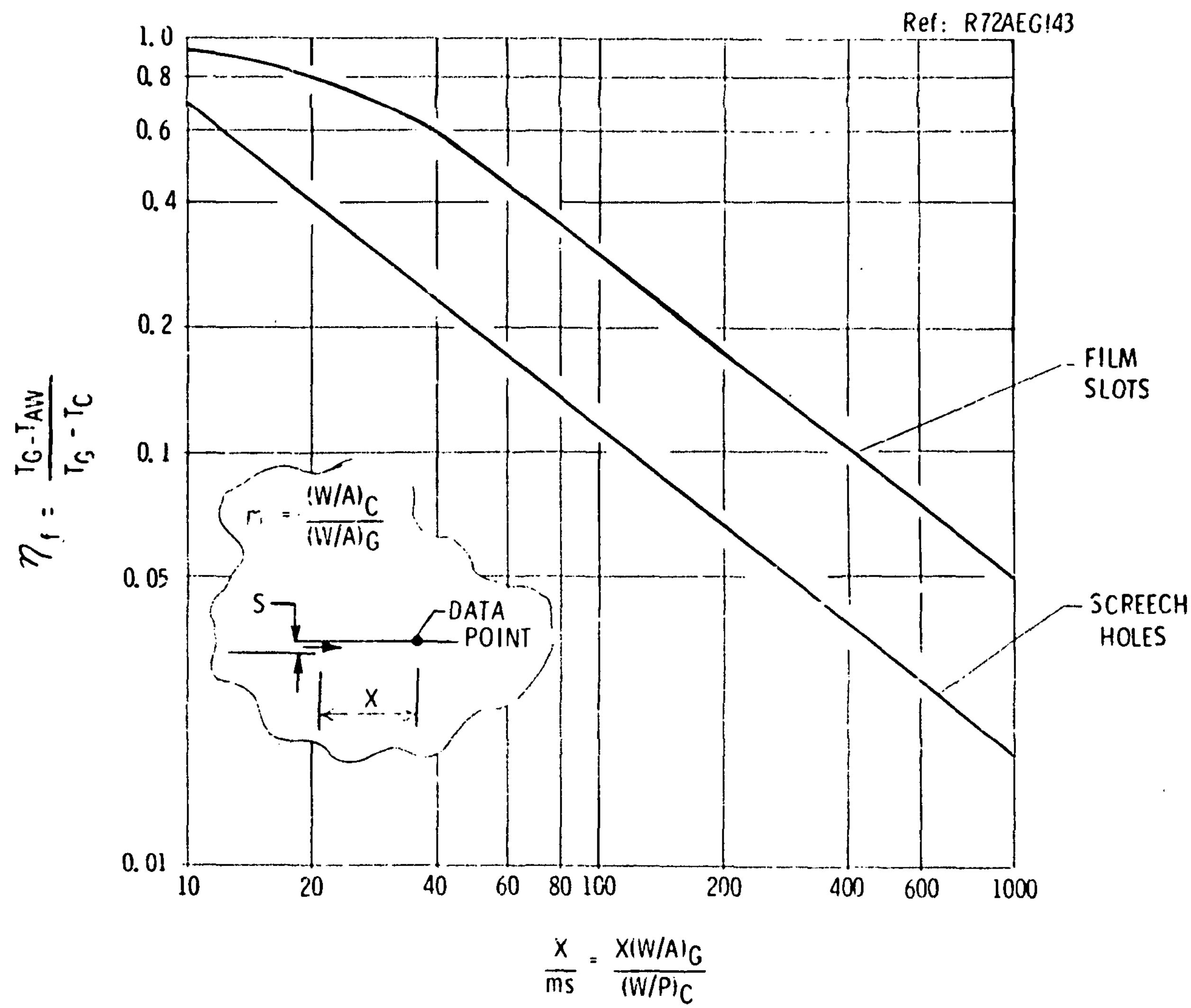

Figure 33. F101 Liner Effectiveness.

analyzed. For each conceptual design, the assumed design point was analyzed first to allow slot flow iterations to meet the design temperatures. The following coolant and gas stream cycle parameters were input:

- Estimated coolant flow entering the liner (W_{CT}).
- Gas stream flow and temperature at liner inlet station (W_{GT}), (T_0).
- Gas stream temperature and location at nozzle throat (T_8), (X_8).
- Estimated cooling flow and temperature at each slot (W_C), (T_C).
- Fuel-to-air ratio and design metal temperature for radiation calculations (FAR, (Tm).

The metal temperature output for every data point from the program must be evaluated to verify meeting design temperatures. Any large discrepancies from the calculated to the desired metal temperature required rerunning the program. This iteration for obtaining the desired metal temperature was accomplished by adjusting the coolant flows for the slot and slots affecting the data point temperature. Further iterations were completed until satisfactory metal temperatures were obtained.

7.3 FLOW BALANCE PROGRAM

The cooling flows required to meet design metal temperatures were then input into the time sharing program, FLOCAL. This flow balance program calculates the balance flows for a network of nodes and branches. Figure 34 shows the model used for the 2D-CD 4AR (fan air cooled) conceptual design. The nodes are shown from 1 through 12 along with the interconnecting branches joining the nodes and simulating cooling flowpath geometry, film slots, etc. The nodes represent discrete locations in the coolant or hot gas stream.

The initial model was set up with the branches simulating liner gaps and film slots. The node input consisted of the gas stream static pressures and design point liner inlet pressure which is representative of the typical turbofan coolant driving pressure. The program then calculates the total coolant flow entering the liner and the distribution of this coolant flow through the film slots, out the end of the liner, or to the A_8 throat slot. These flows, which did not exactly equal the flows required from the heat transfer analysis, were iterated by adjusting the liner branch areas.

The final configuration of branch areas would be designed into the exhaust system during a detailed hardware design phase. During a detail design phase, liner hangers, dams, restrictions, and other coolant flowpath parameters are accounted for and put into this analysis.

The cooling flows for the off-design conditions were determined by inputting the coolant inlet pressure and hot gas stream pressures into the flow

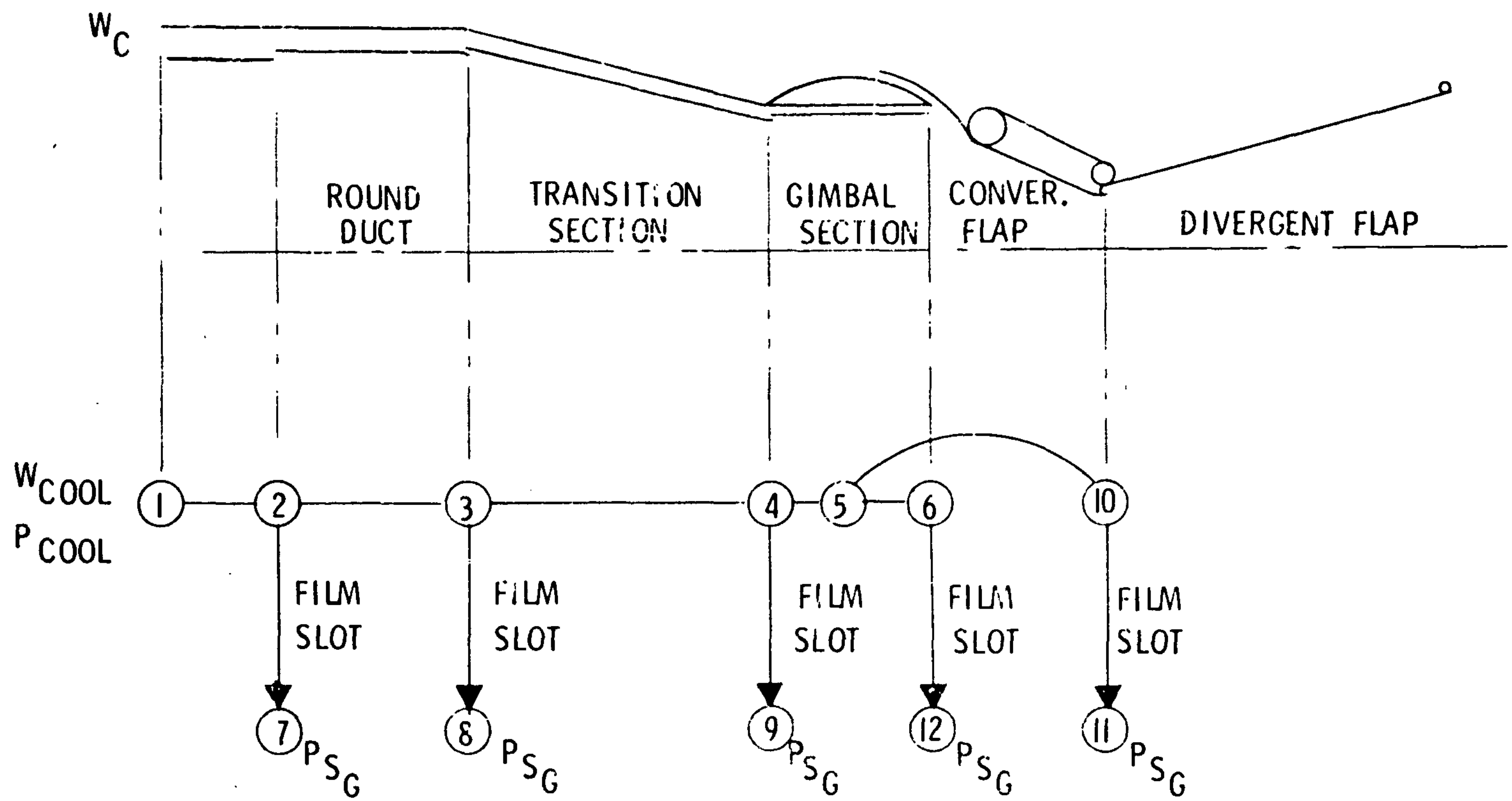

Figure 34. J85 2D-CD 4AR Flow Model.

balance program. The coolant inlet pressure was based on typical turbofan pressure and the hot gas stream pressures were based on the J85-21 cycle conditions. (See Section 5.3.3 for pressure ratios used.) Once the flows for these off-design points were determined, they were put back into the heat transfer program "PORTENO" for calculating metal temperatures at these cycle conditions.

After the technical redirection, the remaining two conceptual designs utilized only air available from the engine itself for cooling. For these designs, this flow balance program was not used. The existing J85-21 engine known cooling flow (15.4% W51) at the design point (M = 1.0 at sea level) and associated coolant pressure ratio (P_{TC}/P_{SG}) were taken from the cycle data. The off-design point pressure ratios from the cycle data were ratioed to obtain the off-design flows. The design point and off-design point flows for the compressor bleed coolant were similarly ratioed and obtained. The existing J85-21 liner design is similar to these designs and, therefore, it was not necessary in this preliminary study to try to simulate unknown hanger, blockages, restrictions, etc.

The turbine discharge pressure ratios and compressor bleed pressure ratios are shown in Sections 5.4.3 and 5.5.3. The required individual slot flows obtained in the heat transfer analysis were ratioed by the overall coolant pressure ratio to obtain off-design individual slot flows. Film slots fed from the compressor bleed were obtained by ratioing the overall pressure ratios.

7.4 HEAT TRANSFER EXPRESSIONS

The following provides a brief summary of the expressions used in the heat transfer analysis by the time sharing program PROTENO.

The initial step involved obtaining the film effectiveness (η_f) for each data point downstream of a slot or screech section in order to determine adiabatic wall temperature (T_{AW}). The curves in Figure 33 were preprogrammed to provide the effectiveness (η_f) for a film slot or screech section as selected by an input option. The adiabatic wall temperature with accumulation effects of multiple slots upstream of the discrete data point was determined as follows:

$$* \quad T_{AW} = T_G \left[\prod_{i=1}^{n} \left(1 - \eta_i\right) \right] + \sum_{i=1}^{n} \left[\left(\eta_i \, T_{c_i}\right) \prod_{j=i+1}^{n} \left(1 - \eta_j\right) \right] \qquad (1)$$

The gas stream and coolant side coefficient at each data point were calculated using the turbulent correlations:

* Expression for T_{AW} based on multiple slot correlation (Reference 12).

$$H_g = 0.0296 \left(\frac{W}{A}\right)_G^{0.8} \left(\frac{1}{X}\right)^{0.2} \frac{K\, P_r^{1/3}}{\mu^{0.8}} \tag{2}$$

$$H_c = 0.023 \left(\frac{W}{A}\right)_C^{0.8} \left(\frac{1}{D_H}\right)^{0.2} \frac{K\, P_r^{0.4}}{\mu^{0.8}} \tag{3}$$

The fluid properties in the above expressions are calculated or preprogrammed as a function of the gas stream or coolant temperatures and pressures. The characteristic dimensions, flows, and areas are extracted from the input data to the program.

The radiation heat flux included hot gas stream radiation to the flowpath liner and the radiation from the liner to the outer wall of the coolant passage at coolant temperature. Also, the radiation of the hardware visible to ambient surroundings was considered downstream of the throat.

$$\text{(Upstream Throat)} \quad Q_{G/L} = \sigma\left(\frac{\varepsilon_m + 1}{2}\right) \varepsilon_p \, T_G^{4.0} \tag{4}$$

$$\text{(Downstream Throat)} \quad Q_{G/L} = \sigma\left(\frac{\varepsilon_m + 1}{2}\right) \varepsilon_p \, T_G^{1.5} \left(T_G^{2.5} - T_m^{2.5}\right) \tag{5}$$

$$Q_{L/C} = \sigma\left(\frac{\varepsilon_m + 1}{2}\right) \left(T_m^{4.0} - T_c^{4.0}\right) \tag{6}$$

Using the above relationships in the program, an initial metal temperature was calculated without the unknown Q L/C and then recalculated accounting for this radiation ($Q_{L/C}$) based on the first-time-through metal temperature. The primary gas emissivity (ε_p) is calculated in the program as a function of gas conditions, fuel-air ratio, and geometry. The liner emissivity (ε_m) was a function of material.

The following sketch summarizes the major expressions involved in solving the overall heat balance in order to determine the data point metal temperature.

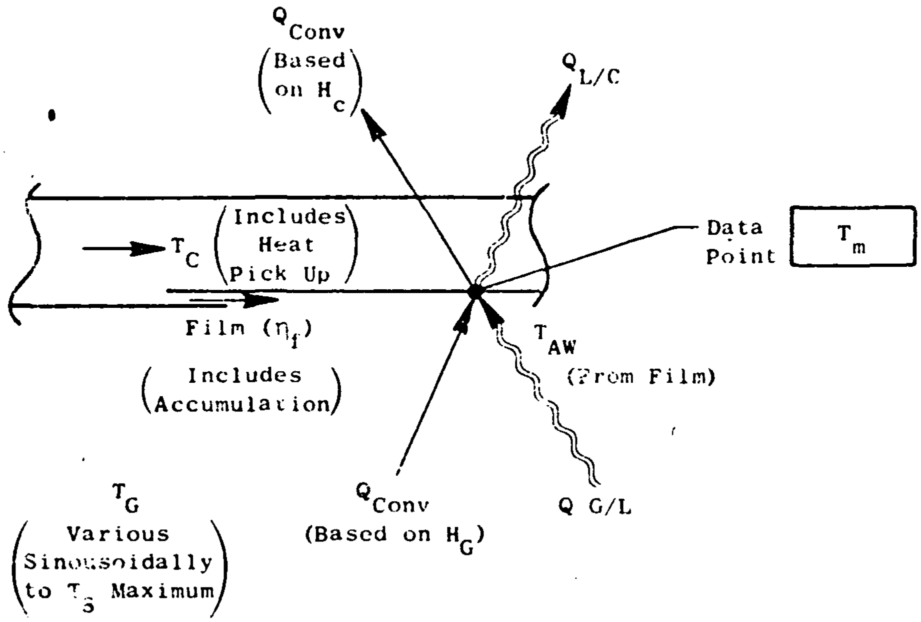
Q Conv
Based on H c
Q L/C
Includes Heat Pick Up
T C
Data Point
T m
Film (η f)
Includes Accumulation
T AW
(From Film)
T G
Various Sinousoidally to T S Maximum
Q Conv
(Based on H G)
Q G/L

8.0 REFERENCES

1. Berrier, B.L. Palcza J.L., Richey, G.K., Zakanycz, S.: "Nonaxisymmetric Nozzle Technology." Report of Ad Hoc Interagency Nonaxisymmetric Nozzle Working Group, AAF, DOD, NASA, Navy.

2. Hiley, P.E. and Wallace, H.W.: "Investigation of Augmented Deflector Exhaust Nozzles Installed in Tactical Aircraft." AFFDL-TR-75-61, U.S. Air Force, June 1975.

3. Sedgwick, Thomas A.: "Investigation of Augmented Deflector Exhaust Nozzles Installed in Tactical Aircraft." AFFDL-TR-75-42, U.S. Air Force, May 1975.

4. Maiden, Donald L.: "Performance of an Isolated Two-Dimensional Variable-Geometry Wedge Nozzle with Translating Shroud and Collapsing Wedge at Speeds Up to Mach 2.01." NASA TN D-7906, April 1975.

5. Capone, Francis J.: "A Summary of Experimental Research on Propulsive-Life Concepts in the Langley 16-Foot Transonic Tunnel." AIAA Paper No. 75-1315, 1975.

6. "Airframe Studies of V/STOL Vectorable Nozzle for Twin Engine Aircraft." Grumman Report No. PDR 623-6, September 1973.

7. "Airframe Studies of V/STOL Vectorable Nozzles for Single Engine Aircraft." Grumman Report No. PDR 623-10, May 1974.

8. McGrath, J.M. and Speir, D.W.: "Nonaxisymmetric Nozzle IR and RCS Studies (U)." GE Report R74AEG34 (Limited Rights Data), January 1975.

9. "V/STOL Exhaust System IR Studies (U)." GE Report R75AEG432, October 1975.

10. "Advanced V/STOL Propulsion Component Development - Nozzle/Deflector." GE Report R77AEG441, August 1977.

11. Willard, C.M.W. and Struble, W.T.: "Experimental Evaluation of Nonaxisymmetric Exhaust Nozzles - Phase I - Interim Report." McDonnell Douglas Corporation Report MDC A5208, February 10, 1978.

12. Sellers, J.P., Jr.: "Gaseous Film Cooling with Multiple Injection Stations." AIAA Journal, Volume I, Page 2154, 1963.

Preceding page blank

9.0 LIST OF SYMBOLS

A	Area
A_C	Cooled Surface Area
AR	Dry Throat Aspect Ratio
C_{FG}	Gross Thrust Coefficient
C_{FGR}	Resultant Gross Thrust Coefficient
C_P	Specific Heat Ratio
D_H	Hydraulic Diameter
ΔW_C	Incremental Engine Weight Related to Cooling System Components
$\Delta W_{C_{FG}}$	Incremental Engine Weight Related to ΔC_{FG}
FAR	Fuel/Air Ratio
F_G	Gross Thrust
F/H	Flame Holder
F_N	Net Thrust
H	Height
h	Heat Transfer Coefficient
IR	Infrared Radiation
K	Thermal Conductivity
$(L/H)_p$	Projected Boattail Length/Height Ratio
M	Mach Number
m	Mass Flow Ratio
P_R	Prandtl Number
P_T	Total Pressure
P	Static Pressure
PSG	Gas Stream Static Pressure
PS3	Compressor Bleed Static Pressure
$Q_{G/L}$	Gas to Liner Radiation
$Q_{L/C}$	Liner to Coolant Radiation
RCS	Radar Cross Section
S	Slot Height
T	Static Temperature
TE	Trailing Edge
TOGW	Takeoff Gross Weight
T/R	Thrust Reverser

Preceding page blank

T_T	Total Temperature °K
T/W	Thrust/Weight Ratio
W	Weight Flow
W_{CT}	Coolant Flow at Liner Exit
W_{GT}	Gas Stream Flow
W_{J85}	J85 Engine Weight
W_2	Engine Inlet Flow
X	Distance
δ	Thrust Vector Angle
ε_m	Metal Emissivity
ε_G	Gas Emissivity
η_F	Film Effectiveness
η_G	Gross Effectiveness
μ	Viscosity Coefficient
σ	Stefan - Boltzman Constant

SUBSCRIPTS

AW	Adiabatic Wall
C	Cooling Flow
CL	Liner Cooling Flow
CS	Secondary Flap Cooling Flow
i	Ideal
Max	Maximum
m	metal
S	Static
SG	Static Gage
0	Freestream
6	Liner Inlet Station
8	Nozzle Throat Station
9	Nozzle Exit Station

END

DATE

FILMED

2-25-81

NTIS